DOE/METC--92/4108

DE92 001111

METC Gasifier Advanced Simulation (MGAS) Model

Technical Note

By

M. Syamlal
EG&G Washington Analytical Services Center, Inc.

and

L. A. Bissett
U.S. Department of Energy

U.S. Department of Energy
Office of Fossil Energy
Morgantown Energy Technology Center
P.O. Box 880
Morgantown, West Virginia 26507-0880

January 1992

MASTER

DISTRIBUTION OF THIS DOCUMENT IS UNLIMITED

This document is
PUBLICLY RELEASABLE
Larry E. Williams
Authorizing Official
Date: 06/26/2007

DISCLAIMER

This report was prepared as an account of work sponsored by an agency of the United States Government. Neither the United States Government nor any agency Thereof, nor any of their employees, makes any warranty, express or implied, or assumes any legal liability or responsibility for the accuracy, completeness, or usefulness of any information, apparatus, product, or process disclosed, or represents that its use would not infringe privately owned rights. Reference herein to any specific commercial product, process, or service by trade name, trademark, manufacturer, or otherwise does not necessarily constitute or imply its endorsement, recommendation, or favoring by the United States Government or any agency thereof. The views and opinions of authors expressed herein do not necessarily state or reflect those of the United States Government or any agency thereof.

DISCLAIMER

Portions of this document may be illegible in electronic image products. Images are produced from the best available original document.

TABLE OF CONTENTS

LIST OF FIGURES

LIST OF TABLES

EXECUTIVE SUMMARY

METC is developing an advanced moving-bed gasifier, which is the centerpiece of the Integrated Gasifier Combined-Cycle (IGCC) system, with the features of good efficiency, low cost, and minimal environmental impact. A mathematical model of the gasifier, the METC-Gasifier Advanced Simulation (MGAS) model, has been developed for the analysis and design of advanced gasifiers and other moving-bed gasifiers. This report contains the technical and the user manuals of the MGAS model.

The MGAS model can describe the transient operation of coflow, counterflow, or fixed-bed gasifiers. It is a one-dimensional model and can simulate the addition and withdrawal of gas and solids at multiple locations in the bed, a feature essential for simulating beds with recycle. The model describes the reactor in terms of a gas phase and a solids (coal or char) phase. These phases may exist at different temperatures. The model considers several combustion, gasification, and initial stage reactions. The model consists of a set of mass balances for 14 gas species and three coal (pseudo-) species and energy balances for the gas and the solids phases. The resulting partial differential equations are solved using a finite difference technique.

The MGAS code is written in FORTRAN and is portable. It is written in a modular fashion so that changes, such as reaction schemes and kinetics, can be made easily. It has a user-friendly input data file that allows great flexibility in specifying the reactor geometry and flow conditions. The code was extensively debugged by conducting several simulations of varying degrees of complexity.

The product gas composition and temperature predicted by the model were compared with data from a METC gasifier run. Good agreement was obtained by adjusting certain model parameters. For a detailed validation of the model, however, its predictions need to be compared with experimental data on temperature and concentration profiles in the bed.

1.0 INTRODUCTION

METC is developing an advanced moving-bed gasifier, which is the centerpiece of the IGCC system, with the features of good efficiency, low cost, and minimal environmental impact. In such a system, the gasifier provides the fuel gas for driving the gas turbine. A successful design should address several barrier issues, such as the minimization of tar yield, the reduction of particulate carry-over, the ability to process caking coals, and the maximization of the heating value of the gas. A mathematical model of the gasifier, the MGAS model, has been developed for the analysis and design of advanced gasifiers and other moving-bed gasifiers. The MGAS model can simulate a moving-bed gasifier of given specifications and predict its performance. For example, the model can calculate the composition and temperature of the fuel gas and the flow rates of the steam and air required to achieve a desired carbon conversion while the maximum char temperature is maintained below the ash fusion temperature. Thus, the model can help designers to determine the performance of reactors of different configurations without having to build them.

Mathematical models of gasifiers exist at various levels of sophistication. For a given carbon conversion, a simple mass and energy balance model will predict the composition of the fuel gas and its temperature (Denn 1986). But to determine the carbon conversion, the location and magnitude of the maximum temperature, or the transient behavior of the bed, a detailed model, which is a set of mass and energy balances in a differential equation form, is required. The mathematical abstraction used in a detailed model is depicted in Figure 1, which shows a METC gasifier and a schematic (Denn 1986) of the chemical and physical processes in the region between the grate and the top of the coal bed. The schematic divides the reactor into four zones based on the predominance of certain types of reactions occurring in those zones. However, such zones are not specified in the MGAS model, as all the reactions are allowed to take place throughout the bed. Then, in a qualitative sense, the zones may appear as a consequence of the predictions of the model.

Several detailed gasifier models are reported in the literature. Particularly noteworthy is an advanced gasifier model currently being developed at Brigham Young University (BYU). Some of the features of the models are compared with those of the MGAS model in Table 1. MGAS can (1) compute the transient response of a gasifier during process upsets, start-up, or shut-down; (2) simulate coflow, counterflow, or fixed-bed gasifiers; and (3) track 14 gas species and 4 coal (pseudo-) species. MGAS has an empirical, initial-stage, kinetics model that enables the model to predict the tar yield and the composition of devolatilization gases. MGAS tracks the gas and solids temperatures

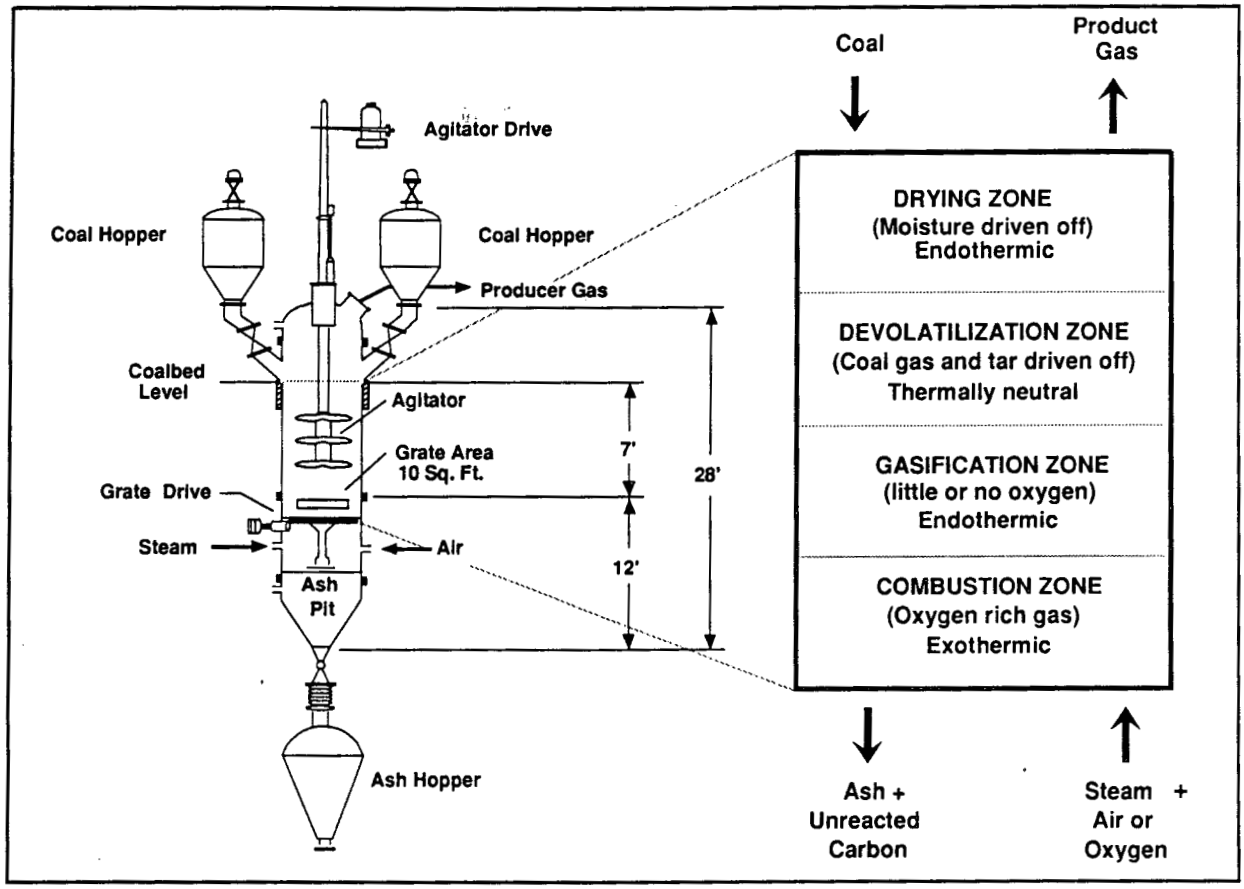

Figure 1. METC Gasifier and a Schematic of Physical and Chemical Processes

separately (two energy equations) to accurately describe the temperature changes during large particle gasification and link the devolatilization kinetics with coal heat-up.

Although MGAS has been written as a two-dimensional code, it has been validated with only one-dimensional runs. The two-dimensional feature will be validated in the future. Then MGAS will compute radial temperature profiles, a feature necessary for simulating small-diameter gasifiers or gasifiers operating under stand-by conditions.

The MGAS code is written in FORTRAN and does not use any special library packages. It is written in a modular fashion so that changes, such as reaction schemes, reaction kinetics, and physical properties can be made easily. Its user-friendly input data file allows great flexibility in specifying such parameters as the reactor geometry in two dimensions, location of the inflow and outflow ports, and composition of the gases and coal. The code has been tested on a VAX-8650 and a Silicon Graphics IRIS workstation. Because of the computational details built into

Table 1. Comparison of Gasifier Models

Model	Features	Number of Species Gas	Number of Species Solids	Initial Stage Reactions	No. of Energy Eq.
WVU	1D, Steady, Moving Bed	6	1	No	1
UD1	1D, Transient, Moving Bed	6	1	No	1
UD2	2D, Transient, Moving Bed	6	1	No	1
WU1	1D, Steady, Moving Bed	6	1	No	2
WU2	1D, Transient, Moving Bed	6	1	No	2
WU3	2D, Transient, Fixed Bed	6	1	No	1
LLNL	2D, Transient, Fixed Bed	7	2	No	1
BYU	1D, Steady, Moving Bed	14	19	Detailed Model	2
METC	1D, Transient, Moving Bed	14	4	Empirical Model	2

WVU - Wen, Chen, and Onozaki (1982)
UD1 - Yoon, Wei, and Denn (1978, 1979)
UD2 - Yu, Denn, and Wei (1983), Denn (1986)
WU1 - Cho and Joseph (1981)
WU2 - Kim and Joseph (1983)
WU3 - Bhattacharya, Salam, Dudukovic, and Joseph (1986)
LLNL - Thorsness and Kang (1986)
BYU - Hobbs, Radulovic, and Smoot (1990)
METC - This document

the code, especially the calculation of the fast reactions, (combustion at the bottom and devolatilization at the top), the computational time requirement of the code is large. For example, the simulation of 5 hours of operation of a METC gasifier, considered one-dimensional and discretized into 61 nodes, took about 35 minutes of CPU time on a VAX-8650. The code is fairly robust: although the specified number of iterations may be exceeded for several time steps during rapid changes in the bed, eventually

the code will calculate converged results as the changes become less rapid. (For example, see the log-file in Appendix H.)

The code was debugged by conducting several simulations of varying degrees of complexity. An overall elemental balance was done at the completion of every simulation and the results were printed. (For example, see the end of the output file in Appendix H.) For simulations reaching a steady-state, such a balance checks the accuracy of the species balances.

The product gas composition and temperature predicted by the model were compared with data from a METC gasifier run as shown in Appendix D: a comparison of the predicted and experimental tar yield was used to adjust the rate of the tar cracking reaction; and a comparison of the predicted and expected maximum char temperature was used to adjust the partitioning of the heat of the carbon combustion reaction. (See Section 3.2 for details.) Good agreement between the computed and the experimental product distributions does not by itself imply that the model is validated. The required detailed validation of the model through comparisons of the computed and the experimental profiles will be the subject of a future report.

The development of the MGAS model was started in March 1990. It originated from a METC desulfurization reactor model called HDR (Hot-gas Desulfurization Reactor). The fixed-bed HDR model was initiated by T.J. O'Brien, DOE, and the model was developed by V. Padhye (ORAU research trainee) in collaboration with EG&G Washington Analytical Services Center, Inc. The model was then extensively modified to develop a moving-bed HDR model (Syamlal 1989). The MGAS project was initiated by J. Boyle, DOE. End-user inputs were obtained during the course of the model development through meetings with METC engineers having expertise in gasification. Thus, many of the model specifications (including the formulation of the devolatilization model) came from L. Bissett, DOE. Except for the initial stage, the chemistry and reaction kinetics used in MGAS have been taken from Wen et al. (1982). Other items that proved useful for code development are the section on source-term linearization in Patankar (1980) and the reliable sparse matrix routine of Kapitza and Eppel (1987).

This report describes Version 1.0 of the MGAS model. The report is in two parts: a technical manual and a user manual. The technical manual (the main body of the report) gives the physical, mathematical, and numerical details of the model, intended for users who need a thorough understanding of the model. The user manual (Appendices A to C) describes the computer code and shows how to set up an input file for a given problem and to interpret the resulting output. The appendices give information on the FORTRAN subroutines and variables, input data files, and output files.

2.0 BALANCE EQUATIONS

In the MGAS model, the gas and the solids (coal or char) in the reactor are considered as two phases that flow either countercurrently, as in Figure 1, or cocurrently. The phases interact with each other by transferring mass, momentum, and energy. The behavior of the reactor can then be described by solving the balance equations for mass, momenta, and energy. In the present version of MGAS, the solids and the gas are assumed to flow in a plug-flow manner (in the z-direction), and hence only a simplified form of the momentum balance is solved to determine the pressure drop through the bed. Although the equations are written for a two-dimensional coordinate system, a true two-dimensional description is possible only when the flow fields are described in two dimensions. The present version, however, will allow the simulation of radial temperature profiles.

Gas species mass balance. MGAS tracks 14 gas species: CO, CO_2, CH_4, H_2, H_2O, H_2S, N_2, O_2, NH_3, Tar, C_2H_4, C_2H_6, C_3H_8, and C_6H_6. For each of the gas species "m", a mass balance is written as follows:

$$\frac{\partial}{\partial t}(\epsilon \rho_g y_m) + \nabla\cdot(\epsilon \rho_g y_m \vec{v}_g) = R_{gm} \quad . \tag{1}$$

Coal species mass balance. MGAS treats coal as a mixture of four pseudo-species: Fixed Carbon (FC), Volatile Matter (VM), Moisture (M), and Ash (A). For each of the pseudo species "m", a mass balance is written as follows:

$$\frac{\partial}{\partial t}[(1-\epsilon)\,\rho_s x_m] + \nabla\cdot[(1-\epsilon)\,\rho_s x_m \vec{v}_s] = R_{sm} \quad . \tag{2}$$

Void fraction is assumed to be a constant, and the solids density ρ_s is assumed to change because the consumption of solids causes the opening up of internal pores in the solids.

Overall gas mass balance. The sum of all the components of equation (1) and the condition that $\Sigma y_m = 1$ gives the overall mass balance for the gas phase:

$$\frac{\partial}{\partial t}(\epsilon \rho_g) + \nabla\cdot(\epsilon \rho_g \vec{v}_g) = \sum_m R_{gm} \quad . \tag{3}$$

Overall coal mass balance. The sum of all the components of equation (2) and the condition that $\Sigma x_m = 1$ gives the overall mass balance for the coal phase:

$$\frac{\partial}{\partial t}[(1-\epsilon)\rho_s] + \nabla\cdot[(1-\epsilon)\rho_s\vec{v}_s] = \sum_m R_{sm} \quad . \tag{4}$$

Also note that $\Sigma_m R_{gm} = -\Sigma_m R_{sm}$, since all the solids consumed in the reactions appear as gases.

Gas energy balance. The conservation of gas phase energy is written in terms of the gas temperature as follows:

$$\epsilon\rho_g C_{pg}\left(\frac{\partial T_g}{\partial t} + \vec{v}_g\cdot\nabla T_g\right) = k_g\nabla^2 T_g - (\gamma + \gamma_r\sum_m R_{gm}C_{pg})(T_g - T_s) + (-H_{rg}) \quad . \tag{5}$$

An $\epsilon\left(\frac{\partial P}{\partial t} + \vec{v}_g\cdot\nabla P\right)$ term in the energy balance has been neglected in the above equation because it is much smaller than the other terms in the equation. The solids and the gas phases may exist at different temperatures and the heat transfer between the phases is modeled with the term $\gamma(T_s - T_g)$. The partitioning of the heat of each of the gas-solids reactions is discussed in Section 3.0.

Coal energy balance. The conservation of coal phase energy is written in terms of the coal temperature as follows:

$$(1-\epsilon)\rho_s C_{ps}\left(\frac{\partial T_s}{\partial t} + \vec{v}_s\cdot\nabla T_s\right) = k_s\nabla^2 T_s + \left(\gamma + (\gamma_r - 1)\sum_m R_{gm}C_{pg}\right)(T_g - T_s) + (-H_{rs}) \quad . \tag{6}$$

Note that the heating value of coal does not appear in equation (6). It is implicitly accounted for by the heats of reactions of the combustion and gasification reactions. This approximation was verified to be reasonable by performing an overall energy balance on the gasifier based on the heating value of coal and the composition of product gas at steady-state predicted by the model.

In equations (5) and (6) the term containing γ_r accounts for the energy required to heat up the reaction products from the gas temperature to the solids temperature or vice versa. It is derived based on the assumptions that the difference between the gas and the solids temperatures is small and that the specific heat of the reaction products is approximately equal to that of the gas. γ_r is defined as

$$\gamma_r = \begin{cases} 1 & \sum_m R_{gm} \geq 0 \\ 0 & \sum_m R_{gm} < 0 \end{cases} , \qquad (7)$$

Bed pressure drop. The bed pressure drop is determined from the following simplified form of a momentum balance:

$$\epsilon \nabla P = F_{gs} (\vec{v}_s - \vec{v}_g) + \epsilon \rho_g \vec{g} \quad . \qquad (8)$$

In the above equation, inertial and transient terms and the wall friction term have been neglected. The dominant cause of pressure drop is the gas-solids friction, which is very sensitive to the void fraction distribution in the bed.

3.0 CHEMISTRY AND KINETICS

The chemical reactions in a gasifier can be divided into two parts: the initial stage reactions that occur as fresh coal is heated up and the subsequent gasification and combustion reactions.

3.1 Initial Stage Reactions

The initial stage reactions of coal are complex, and they lead to a wide variety of products, the composition of which depends upon the type of coal and, perhaps, the processing conditions. A number of devolatilization models of varying complexity exist in the literature (Saxena 1990). The work of Solomon and coworkers (1990) has led to a fairly detailed predictive model of devolatilization. In the MGAS model, a simple phenomenological model is used with the objectives of predicting the yields of tar and some major gas components and preserving a strict elemental balance. Tar is the organic condensate, including what is commonly referred to as oils. The following three initial stage reactions are postulated:

1. Drying:

$$M \xrightarrow{R_m} \text{Steam}.$$

2. Devolatilization:

$$VM \xrightarrow{R_d} \alpha^d\ \text{Tar} + \beta^d_{CO}\ CO + \beta^d_{CO2}\ CO_2 + \beta^d_{CH4}\ CH_4 + \beta^d_{C2H4}\ C_2H_4 + \beta^d_{C2H6}\ C_2H_6 + \beta^d_{C3H8}\ C_3H_8 + \beta^d_{C6H6}\ C_6H_6 + \beta^d_{H2}\ H2 + \beta^d_{H2O}\ H_2O + \beta^d_{H2S}\ H^2S + \beta^d_{NH3}\ NH_3.$$

3. Tar-cracking:

$$\text{Tar} \xrightarrow{R_c} \alpha^c\ FC + \beta^c_{CO}\ CO + \beta^c_{CO2}\ CO_2 + \beta^c_{CH4}\ CH_4 + \beta^c_{C2H4}\ C_2H_4 + \beta^c_{C2H6}\ C_2H_6 + \beta^c_{C3H8}\ C_3H_8 + \beta^c_{C6H6}\ C_6H_6 + \beta^c_{H2}\ H2 + \beta^c_{H2O}\ H_2O + \beta^c_{H2S}\ H_2S + \beta^c_{NH3}\ NH_3.$$

The stoichiometric coefficients in the above reaction scheme are determined by assuming certain phenomenological rules, which are discussed later. Note that α's and β's are on a mass basis and hence $\alpha^d + \Sigma\beta_m{}^d = 1$ and $\alpha^c + \Sigma\beta_m{}^c = 1$.

Table 2. Kinetic Constants

Coal --->	1	2	3	4
k_2 (1/atm.s)	930	600	2250	70
E_2 (cal/mol)	45000	45000	42000	30000
k_5 (1/atm.s)	930	600	2250	70
E_5 (cal/mol)	45000	45000	42000	3000
k_d (1/s)	$1.1\ 10^5$	$1.1\ 10^5$	$1.1\ 10^5$	$5.1\ 10^4$
E_d (cal/mol)	21200	21200	21200	18700
k_c (1/s)	$2.5\ 10^7$	$2.5\ 10^7$	$2.5\ 10^7$	$9.0\ 10^7$
E_c (cal/mol)	29000	29000	29000	27750
w_{g3}	0.0068	0.0068	0.0155	0.014

1 - Pittsburgh No. 8 2 - Arkwright/Pittsburgh
3 - Illinois No. 6 4 - Rosebud Subbituminous

Reaction kinetics: The rate of the above three reactions is determined from information provided by Wen et al. (1982). The drying rate expression is assumed to be similar to the devolatilization rate expression of Wen et al.:

$$R_m = k_m \exp\left(\frac{-E_m}{RT_s}\right)(1-\epsilon)\,\rho_s x_M \quad . \tag{9}$$

The kinetic constants k_m and E_m have the same values as k_d and E_d given in Table 2. The initial-stage reaction rates were limited to a maximum value equal to that at 1000 K.

The devolatilization rate expression of Wen et al. (1982) was modified to account for the fact that at any given temperature only a certain fraction of the total volatile matter is released, regardless of how long the coal is kept at that temperature. Hence, in the modified rate expression, the devolatilization rate becomes zero if the volatile fraction is less than or equal to a minimum possible volatile fraction x^*, which is a function of the solids temperature:

$$R_d = \begin{cases} k_d \exp\left(\frac{-E_d}{RT_s}\right)(1-\epsilon)\,\rho_s\,(x_{VM}-x^*) & x_{VM} \geq x^* \\ 0 & x_{VM} < x^* \end{cases} . \qquad (10)$$

x^* is determined from a correlation of Gregory and Littlejohn (1955), which gives the volatiles remaining in the residue as a function of temperature. The following formula is obtained by modifying the Gregory and Littlejohn formula such that x_0^* goes to zero when T_s is greater than or equal to 1223 K, the temperature at which the volatile matter content is determined in ASTM proximate analysis:

$$x_0^* = \begin{cases} \dfrac{\left(\dfrac{867.2}{(T_s-273)}\right)^{3.914}}{100} & T_s < 1223 \\ 0 & T_s \geq 1223 \end{cases} . \qquad (11)$$

The above correlation is based on the maximum volatiles yield obtained from experiments in which different types of coals were heated to and maintained at various temperatures. If its validity is suspect for a particular type of coal, a similar correlation can be developed by repeating the experiment with that type of coal.

x_0^* is the weight of remaining volatiles as a fraction of the original dry ash free coal and from it x^* can be obtained as follows:

$$x^* = \frac{\rho_{s0}\,(x_{FC0}+x_{VM0})\,x_0^*}{\rho_s} . \qquad (12)$$

The coal should contain ash for the above equation to be valid, since, in its derivation, the fraction of ash is an indicator of the extent of devolatilization.

The tar cracking rate is taken from Wen et al. (1982):

$$R_c = k_c \exp\left(\frac{-E_c}{RT_g}\right) \epsilon \rho_g y_T \quad . \tag{13}$$

The kinetic constants k_c and E_c are given in Table 2. The value of k_c was decreased so that the predicted tar-yield is comparable to METC data (see Appendix D).

Determination of the stoichiometric coefficients: The phenomenological model is based on data from certain lab-scale experiments that characterize the coal. In the following list of such data, the first three are from experiments routinely performed, whereas the next two are not:

1. x_{FC} and x_{VM} from proximate analysis.
2. x_C, x_H, x_O, x_N, and x_S from ultimate analysis.
3. Composition of tar (f^T_C, f^T_H, f^T_O, f^T_N, f^T_S).
4. Composition of gases formed during devolatilization.
5. Composition of gases formed during cracking.

In MGAS, the proximate and the ultimate analyses are defined on an as-received basis. Sometimes it is necessary to adjust x_{FC} so that any small discrepancies in the balance $(x_C - x_{FC}) + x_H + x_O + x_N + x_S = x_{VM}$ can be eliminated. Then, the composition of the pseudo-species VM is determined from the proximate and ultimate analyses as follows:

$$f^V_C = (x_C - x_{FC})/x_{VM},$$

$$f^V_H = x_H/x_{VM},$$

$$f^V_O = x_O/x_{VM},$$

$$f^V_N = x_N/x_{VM},$$

and $$f^V_S = x_S/x_{VM}.$$

From experimental data on the composition of the devolatilization gases, the following distribution of elemental oxygen in the species CO, CO_2, and H_2O and elemental hydrogen in the hydrocarbons can be determined:

O distribution: $dO_{CO} + dO_{CO2} + d^{O}_{H2O} = 1.$

H distribution:

$$d^{H}_{H2} + d^{H}_{CH4} + d^{H}_{C2H6} + d^{H}_{C2H4} + d^{H}_{C3H8} + d^{H}_{C6H6} = 1.$$

From experimental data on the composition of cracking gases, the following distribution of elemental oxygen in the species CO, CO_2, and H_2O and elemental hydrogen in the hydrocarbons can be determined:

O distribution: $c^{O}_{CO} + c^{O}_{CO2} + c^{O}_{H2O} = 1.$

H distribution:

$$c^{H}_{H2} + c^{H}_{CH4} + c^{H}_{C2H6} + c^{H}_{C2H4} + c^{H}_{C3H8} + c^{H}_{C6H6} = 1.$$

It is assumed that for a given coal, the above elemental distributions hold good for all processing conditions and all extents of devolatilization. It is further assumed that all the sulfur in coal becomes H_2S and that all the nitrogen in coal becomes NH_3 (Cho and Joseph 1981). From these assumptions, the stoichiometric coefficients in the devolatilization and cracking reactions are fully determined, as evident from the following paragraphs.

The stoichiometric coefficients of devolatilization are determined as follows. On the basis of 1 g of volatile matter released, the following quantities can be computed:

Hydrogen consumption:

in H_2S formation: $h1 = (f^{V}_{S} - \alpha^{d} f^{T}_{S})\ (2/32)$,

in NH3 formation: $h2 = (f^{V}_{N} - \alpha^{d} f^{T}_{N})\ (3/14)$,

in H_2O formation: $h3 = (f^{V}_{O} - \alpha^{d} f^{T}_{O})\ d^{O}_{H2O}\ (2/16)$.

Hydrogen remaining (will be consumed in the formation of hydrocarbons): $h4 = f^{V}_{H} - \alpha^{d} f^{T}_{H} - h1 - h2 - h3$.

Carbon consumed by the remaining hydrogen: $c1 = h4\ (d^{H}_{CH4}\ 12/4 + d^{H}_{C2H6}\ 24/6 + d^{H}_{C2H4}\ 24/4 + d^{H}_{C3H8}\ 36/8 + d^{H}_{C6H6}\ 72/6)$.

Carbon consumed by Oxygen: $c2 = (f^{V}_{O} - \alpha^{d} f^{T}_{O})\ (\ d^{O}_{CO}\ 12/16 + d^{O}_{CO2}\ 12/32)$.

Now by solving the carbon balance, $c1 + c2 + \alpha^{d} f^{T}_{C} = f^{V}_{C}$, for α^{d} we get

$$\alpha^d = \frac{\left(\begin{array}{l}(42d^H_{CH4}+168d^H_{C6H6}+63d^H_{C3H8}+56d^H_{C2H6}+84d^H_{C2H4})\,f^V_S + \\ [(84d^H_{CH4}+336d^H_{C6H6}+126d^H_{C3H8}+112d^H_{C2H6}+168d^H_{C2H4})\,d^O_{H2O}-84d^O_{CO2}- \\ 168d^O_{CO}]\,f^V_O+(144d^H_{CH4}+576d^H_{C6H6}+216d^H_{C3H8}+192d^H_{C2H6}+288d^H_{C2H4})\,f^V_N+ \\ (-672d^H_{CH4}-2688d^H_{C6H6}-1008d^H_{C3H8}-896d^H_{C2H6}-1344d^H_{C2H4})\,f^V_H+224f^V_C\end{array}\right)}{\left(\begin{array}{l}(42d^H_{CH4}+168d^H_{C6H6}+63d^H_{C3H8}+56d^H_{C2H6}+84d^H_{C2H4})\,f^T_S + \\ [(84d^H_{CH4}+336d^H_{C6H6}+126d^H_{C3H8}+112d^H_{C2H6}+168d^H_{C2H4})\,d^O_{H2O}-84d^O_{CO2}- \\ 168d^O_{CO}]\,f^T_O+(144d^H_{CH4}+576d^H_{C6H6}+216d^H_{C3H8}+192d^H_{C2H6}+288d^H_{C2H4})\,f^T_N+ \\ (-672d^H_{CH4}-2688d^H_{C6H6}-1008d^H_{C3H8}-896d^H_{C2H6}-1344d^H_{C2H4})\,f^T_H+224f^T_C\end{array}\right)} \quad (14)$$

The above formula and its FORTRAN code were obtained using MACSYMA, a symbolic mathematics package.

The other coefficients are computed as follows:

$$\beta^d_{CO} = (f^V_O - \alpha^d\, f^T_O)\; d^O_{CO}\; 28/16,$$

$$\beta^d_{CO2} = (f^V_O - \alpha^d\, f^T_O)\; d^O_{CO2}\; 44/32,$$

$$\beta^d_{CH4} = h4\; d^H_{CH4}\; 16/4,$$

$$\beta^d_{C2H4} = h4\; d^H_{C2H4}\; 28/4,$$

$$\beta^d_{C2H6} = h4\; d^H_{C2H6}\; 30/6,$$

$$\beta^d_{C3H8} = h4\; d^H_{C3H8}\; 44/8,$$

$$\beta^d_{C6H6} = h4\; d^H_{C6H6}\; 78/6,$$

$$\beta^d_{H2} = h4\; d^H_{H2},$$

$$\beta^d_{H2O} = h3\; 18/2,$$

$$\beta^d_{H2S} = h1\; 34/2,$$

$$\beta^d_{NH3} = h2\; 17/3.$$

The stoichiometric coefficients of cracking are determined as follows. On the basis of 1 g of tar cracked, the following quantities can be computed:

Hydrogen consumption:

in H_2S formation: $h5 = f^T_S\ (2/32)$,

in NH3 formation: $h6 = f^T_N\ (3/14)$,

in H_2O formation: $h7 = f^T_O\ c^O_{H2O}\ (2/16)$.

Hydrogen remaining (will be consumed in the formation of hydrocarbons): $h8 = f^T_H - h5 - h6 - h7$.

Carbon consumed by the remaining H: $c3 = h8\ (c^H_{CH4}\ 12/4 + c^H_{C2H6}\ 24/6 + c^H_{C2H4}\ 24/4 + c^H_{C3H8}\ 36/8 + c^H_{C6H6}\ 72/6)$.

C consumed by O: $c4 = f^T_O\ (\ c^O_{CO}\ 12/16 + c^O_{CO2}\ 12/32)$.

Now by solving the carbon balance, $c3 + c4 + \alpha^C = f^T_C$, for α^C we get

$$\alpha^C = f^T_C - \left(f^T_H - f^T_S 2/32 - f^T_N 3/14 - f^T_O c^O_{H2O} 2/16\right)$$
$$\left(c^H_{CH4} 12/4 + c^H_{C2H6} 24/6 + c^H_{C2H4} 24/4 + c^H_{C3H8} 36/8 + \right. \qquad (15)$$
$$\left. c^H_{C6H6} 72/6\right) - f^T_O\left(c^O_{CO} 12/16 + c^O_{CO2} 12/32\right) \ .$$

The other coefficients are computed as follows:

$\beta^C_{CO} = f^T_O\ c^O_{CO}\ 28/16$,

$\beta^C_{CO2} = f^T_O\ c^O_{CO2}\ 44/32$,

$\beta^C_{CH4} = h8\ c^H_{CH4}\ 16/4$,

$\beta^C_{C2H4} = h8\ c^H_{C2H4}\ 28/4$,

$\beta^C_{C2H6} = h8\ c^H_{C2H6}\ 30/6$,

$\beta^C_{C3H8} = h8\ c^H_{C3H8}\ 44/8$,

$\beta^C_{C6H6} = h8\ c^H_{C6H6}\ 78/6$,

$\beta^C_{H2} = h8\ c^H_{H2}$,

$\beta^C_{H2O} = h7\ 18/2$,

$\beta^C_{H2S} = h5\ 34/2$,

$\beta^C_{NH3} = h6\ 17/3$.

3.2 Gasification and Combustion

The rate expressions for gasification and combustion reactions are taken from Wen et al. (1982). There are many differences between the rate expressions given in the Wen et al. manual and their code. In the MGAS model, the rate expressions found in Wen et al.'s code are being used and the same are also given below.

Only the fixed carbon portion of the coal is assumed to take part in these reactions. This assumption is reasonable since much of the volatiles are released right at the entrance region. The Arrhenius expression for the gasification reactions is based on the gas temperature. The results are only slightly different, if the solids temperature is used instead.

The combustion of H_2 and CO has been neglected as they are not of much importance (Cho and Joseph 1981). Because of the extremely fast nature of those reactions, retaining them in the model causes convergence problems.

Steam gasification: $C + H_2O \rightleftharpoons CO + H_2$.

This reaction is assumed to take place throughout the volume of the char particle. The rate of reaction (Wen et al. 1982) is

$$R_2 = k_2 \exp\left(\frac{-E_2}{RT_g}\right)\left(\frac{\rho_s X_{FC}}{12}\right)(p_{H2O} - p^*_{H2O}) \quad , \tag{16}$$

where

$$p^*_{H2O} = \frac{p_{H2}\, p_{CO}}{\exp(17.29 - 16326/T_g)} \quad . \tag{17}$$

The coefficients k_2 and E_2 depend upon the type of coal. The values for these coefficients for three coals are given in Table 2. The partial pressures are in atm. The heat of reaction is 31,382 cal/mol and is assigned to the solids phase.

CO_2 gasification: $C + CO_2 \rightleftharpoons 2CO$.

This reaction is assumed to take place throughout the volume of the char particle. The rate of reaction (Wen et al. 1982) is

$$R_5 = k_5 \exp\left(\frac{-E_5}{RT_g}\right)\left(\frac{\rho_s x_{FC}}{12}\right)(p_{CO2} - p^*_{CO2}) \quad , \tag{18}$$

where

$$p^*_{CO2} = \frac{p^2_{CO}}{\exp(20.92 - 20282/T_g)} \quad . \tag{19}$$

The coefficients k_5 and E_5 depend upon the type of coal. The values for these coefficients for three coals are given in Table 2. The partial pressures are in atm. The heat of reaction is 41,220 cal/mol and is assigned to the solids phase.

Methanation: $(1/2)C + H_2 \rightleftharpoons (1/2)CH_4$.

This is a slow reaction (as opposed to a rapid reaction that occurs during devolatilization and described by the phenomenological model for initial stage reactions), assumed to take place throughout the volume of the char particle. The rate of reaction (Wen et al. 1982) is

$$R_6 = \exp(-7.087 - 8078/T_g)\left(\frac{\rho_s x_{FC}}{12}\right)(p_{H2} - p^*_{H2}) \quad , \tag{20}$$

where

$$p^*_{H2} = \sqrt{\frac{p_{CH4}}{\exp(-13.43 + 10999/T_g)}} \quad . \tag{21}$$

The partial pressures are in atm. The heat of reaction is -8,944.5 cal/mol and is assigned to the solids phase.

Water gas - shift reaction: $CO + H_2O \rightleftharpoons CO_2 + H_2$.

This is a fast reaction catalyzed by coal minerals. The rate of reaction (Wen et al. 1982) is

$$R_3 = 2.877\,10^5 w_{g3} f_3 P^{(0.5 - P/250)} \exp\left(\frac{-27760}{RT_g}\right)(y_{CO} y_{H2O} - y_{CO2} y_{H2}/K_3) \quad , \tag{22}$$

where

$$f_3 = \epsilon(1-\epsilon) x_{A0} \rho_{s0} \exp(-8.91+5553/T_g) \quad , \tag{23}$$

and

$$K_3 = \exp(-3.63061+3.955.71/T_g) \quad . \tag{24}$$

The factor w_{g3} depends upon the type of coal and is given in Table 2. P is in atm. The heat of reaction is -9,838 cal/mol and is assigned to the solids phase since the reaction is surface catalyzed.

Carbon combustion: $C + O_2 \rightarrow CO_2$.

Char combustion is a very fast reaction, and a shrinking core model is used to determine the rate of reaction.

$$R_1 = \frac{f_1 p_{O2}}{1/k_{film}+1/k_{ash}} \quad , \tag{25}$$

where

$$k_{film} = \frac{0.292(1-\epsilon)D}{2d_p^2 T_g} \quad , \tag{26}$$

$$D = 4.26(T_g/1800)^{1.75} \quad , \tag{27}$$

$$k_{ash} = k_{film} \epsilon_A^{2.5} \frac{d_c}{1-d_c} \quad , \tag{28}$$

and

$$d_c = \left(\frac{x_{FC} x_{A0}}{(1-x_{FC}) x_{FC0}} \right)^{1/3} \quad . \tag{29}$$

The partial pressures are in atm.

The carbon balance became inaccurate when there was a steep gradient in the carbon mass fraction profile as a result of combustion. The problem was traced to a quirk in the numerical

technique, an inability to handle fractional order kinetics as the mass fractions of the reactants approach zero. Such a problem is eliminated in the above rate expression by f_1, which makes the rate expression linear in x_{FC} at small values of x_{FC}. In doing so, f_1 introduces, for example, only less than a 1 percent error in the rate of combustion at a carbon mass fraction of 10^{-4}. At higher carbon mass fractions, the error decreases, and at lower carbon mass fractions, the error increases, which, however, is of no concern. The factor is calculated by

$$f_1 = \frac{x_{FC}}{x_{FC}+10^{-6}} \quad . \tag{30}$$

For partitioning the heat of reaction, the reaction is assumed to take place in two steps: the heat of reaction for the step $C + (1/2)O_2 \rightarrow CO$ (-26,416 cal/mol) is assigned to the solids phase and the heat of reaction for the step $CO + (1/2)O_2 \rightarrow CO_2$ (-67,636 cal/mol) is assigned to the gas phase. Although there is physical motivation for partitioning in this manner, it was done so that the predicted maximum char temperature is comparable to the expected maximum char temperature for a METC gasifier experiment (see Appendix D).

4.0 CONSTITUTIVE RELATIONS

Other information required to complete the model is described in this section.

4.1 Equation of State

The gas phase is assumed to obey the ideal gas law:

$$P = \rho_g R T_g \quad . \tag{31}$$

4.2 Interphase Heat Transfer

The interphase heat transfer coefficient γ_0 was calculated from a set of correlations taken from Zabrodsky (1966).

$$\gamma_0 = \frac{Nu k_g}{d_p} \quad , \tag{32}$$

where

$$Nu = \begin{cases} \underline{\text{for } \epsilon \le 0.8:} & \\ 0.106\,Re\,S_p & Re < 200 \\ 0.123\,(4Re/d_p)^{0.83} S_p^{0.17} & 200 \le Re \le 2000 \\ 0.61\,Re^{0.61} S_p & Re > 2000 \\ \underline{\text{for } \epsilon > 0.8:} & \\ (2.0 + 0.16\,Re^{0.67})\,S_p & Re < 200 \\ 8.2\,Re^{0.6} S_p & 200 \le Re \le 1000 \\ 1.06\,Re^{0.457} S_p & Re > 1000 \end{cases} \quad . \tag{33}$$

$Re = d_p \rho_g |v_g - v_s| / \mu_g$, and $S_p = 6(1-\epsilon)/d_p$. γ_0 was then corrected for the effect of transpiration (Bird et al. 1960) to get γ:

$$\gamma = \frac{C_{pg}\sum_m R_{gm}}{\exp\left(C_{pg}\sum_m R_{gm}/\gamma_0\right) - 1} \quad . \tag{34}$$

4.3 Bed-to-Wall Heat Transfer

The bed-to-wall heat transfer coefficient is taken from Leva et al. (1948):

$$h_w = 3.5 k_g \exp\left(\frac{-4.6 d_p}{D_{bed}}\right) Re^{0.7}/D_{bed} \quad , \tag{35}$$

where $Re = d_p \rho_g |v_g| / \mu_g$. It is often necessary to multiply h_w by a factor to match the experimental value for heat loss because of the inadequacy of the correlation. Thus, heat loss should be considered as a model input rather than a predicted quantity.

4.4 Specific Heats and Conductivities

The specific heats of the different components of the gas are calculated as a function of temperature and are averaged to get the average gas specific heat. The correlations are from Perry and Chilton (1973). The correlation for coal specific heat is from Johnson (1979).

The gas conductivity was taken as a constant. The solids conductivity was computed using the following correlation given by Bauer and Schlunder (1978):

$$k_s = k_g \sqrt{(1-\epsilon)}\,(\theta/\kappa_r + (1-\theta)\lambda) \quad , \tag{36}$$

where

$$\lambda = -\frac{2}{1-B\kappa_r}\left[\frac{B(1-\kappa_r)}{(1-B\kappa_r)^2}\ln(B\kappa_r) + \frac{B-1}{1-B\kappa_r} + \frac{B+1}{2}\right] \quad , \tag{37}$$

$$B = 1.25\left(\frac{1-\epsilon}{\epsilon}\right)^{1.11} \quad , \tag{38}$$

$\kappa_r = k_g/k_p$, and the parameter $\theta = 7.26\ 10^{-3}$.

4.5 Gas-Solids Drag

The gas-solids drag term for the pressure drop computation in equation (8) is taken from Ergun (1952).

$$F_{gs} = \frac{150\,(1-\epsilon)^2\mu_g}{\epsilon d_p^2} + \frac{1.75\,(1-\epsilon)\,\rho_g|\vec{v}_g-\vec{v}_s|}{d_p} \quad . \tag{39}$$

5.0 INITIAL AND BOUNDARY CONDITIONS

The bed void fraction, mass fractions of the gas species, and solids species in the bed and the bed temperature are the required initial conditions. The void fraction may be specified as a function of the height of the reactor to simulate the changes in the void fraction as a result of the reactions. The initial conditions should be such that there are no regions in the reactor where the species that react rapidly, such as oxygen and coal, are together in large concentrations.

The flow boundary conditions are those of the mass fluxes of the gas and solids at the different inflow ports. Each inflow stream is fully specified by the mass flow rate, void fraction, mass fractions of the gas and solids species, and the stream temperature. At the outflow ports, only the pressure needs to be specified. Heat transfer to the walls is specified by the condition

$$-k_g \nabla T_g = h_w (T_w - T_g) \quad . \tag{40}$$

An adiabatic reactor can be modeled by setting h_w to zero.

6.0 THE NUMERICAL TECHNIQUE

The partial differential equations given in Section 2.0 are finite-differenced, and the resulting set of coupled nonlinear algebraic equations is solved iteratively. At each time step, the specific heats, conductivities, gas viscosity, gas-solids and wall heat transfer coefficients, rates of reactions, heats of reactions, and the pressure drop through the bed are first calculated. Then the algebraic equations are solved simultaneously for all the numerical cells in the following order:

1. Calculate the gas density.
2. Calculate the gas velocity.
3. Solve the gas species balance equations for gas species mass fractions.
4. Correct the gas species mass fractions using Newton's method and check for convergence.
5. Calculate the solids velocity, if the solids density is held constant.
6. Solve the solids species balance equations for solids species mass fractions.
7. Correct the solids species mass fractions using Newton's method and check for convergence.
8. Calculate the solids density, if not held constant.
9. Solve the gas energy equation for gas temperature.
10. Correct the gas temperature using Newton's method and check for convergence.
11. Solve the solids energy equation for solids temperature.
12. Correct the solids temperature using Newton's method and check for convergence.
13. If any of the solutions is not converged, update the reaction rates and heats of reactions and go to step 1.

Following are details of the implementation of the above computational steps.

6.1 Finite Difference Cells

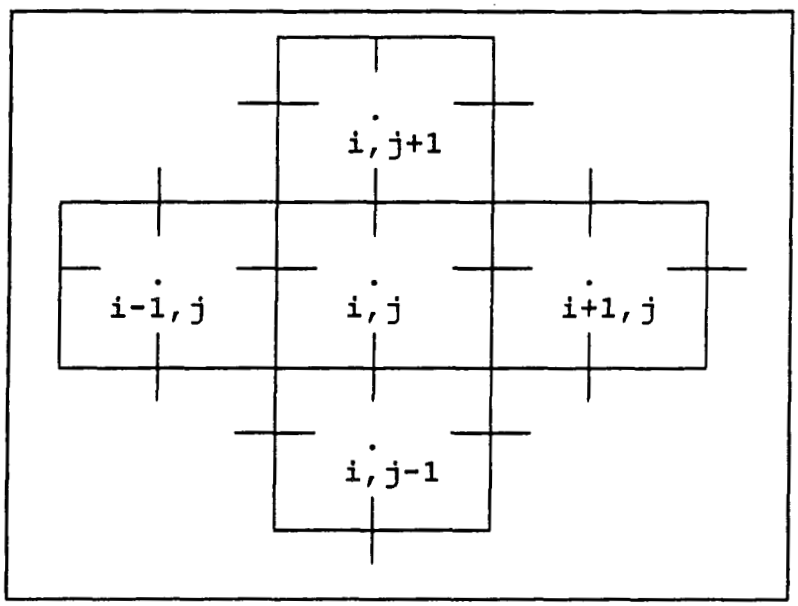

Figure 2. Finite Difference Cell Indices

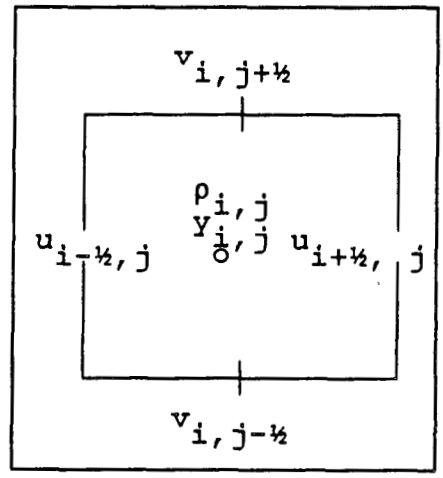

Figure 3. Storage of Scalars and Vectors

The computational domain is divided into a two-dimensional grid. The i-indices identify the cells in the r-direction and the j-indices identify the cells in the z-direction as shown in Figure 2. The scalars, such as mass fractions and densities, are stored at the cell centers, and the components of vectors, such as velocities, are stored at the cell boundaries.

6.2 Calculation of Velocity Fields

The velocity fields are assumed to be rectilinear, i.e., the r-component of the velocities are set to zero. The gas is always assumed to be flowing from the bottom to the top. The z-component of the gas velocity is calculated by solving the overall gas balance (equation [3]). In the following equations, the terms with subscript "bdry" account for the radial flows from the side-boundaries.

$$(v_g)_{i,j+\frac{1}{2}} = \sum_i \left(-\delta t \sum_m R_{gm} - [(\epsilon\rho_g)^n_{i,j} - (\epsilon\rho_g)_{i,j}] \right.$$

$$+ \frac{\delta t}{\delta z} (\epsilon\rho_g)^n_{i,j-1} (v_g)_{i,j-\frac{1}{2}} + \qquad (41)$$

$$\left. \frac{\delta t}{r_i \delta r} (r\epsilon\rho_g u_g)_{bdry} \right) / \left(\frac{\delta t}{\delta z} \sum_i (\epsilon\rho_g)_{i,j} \right) .$$

Quantities with the superscript "n" are at the new time step and all others are at the previous time step.

If the solids density is held constant, the solids velocity is calculated from the overall solids balance (equation [4]). In the coflow case, the solids flow from the bottom to the top like the gas, and the z-component of the solids velocity is calculated from

$$(v_s)_{i,j+\frac{1}{2}} = \sum_i \left(-\delta t \sum_m R_{sm} - [((1-\epsilon)\rho_s)^n_{i,j} - ((1-\epsilon)\rho_s)_{i,j}] + \right.$$

$$\frac{\delta t}{\delta z} ((1-\epsilon)\rho_s)^n_{i,j-1} (v_s)_{i,j-\frac{1}{2}} + \qquad (42)$$

$$\left. \frac{\delta t}{r_i \delta r} (r(1-\epsilon)\rho_s u_s)_{bdry} \right) / \left(\frac{\delta t}{\delta z} \sum_i ((1-\epsilon)\rho_s)_{i,j} \right) .$$

In the counterflow case, the solids flow from the top to the bottom and then the z-component of the solids velocity is calculated from

$$(v_s)_{i,j-\frac{1}{2}} = \sum_i \left(-\delta t \sum_m R_{sm} - [((1-\epsilon)\rho_s)^n_{i,j} - ((1-\epsilon)\rho_s)_{i,j}] - \right.$$

$$\frac{\delta t}{\delta z} ((1-\epsilon)\rho_s)^n_{i,j+1} (v_s)_{i,j+\frac{1}{2}} + \qquad (43)$$

$$\left. \frac{\delta t}{r_i \delta r} (r(1-\epsilon)\rho_s u_s)_{bdry} \right) / \left(-\frac{\delta t}{\delta z} \sum_i ((1-\epsilon)\rho_s)_{i,j} \right) .$$

6.3 Solution of Species Equations

The species balance equations are written in a general sparse matrix form without applying the simplifying assumption of plug-flow. This will enable the easy installation of general flow-field calculations in the code in the future.

The gas species balance equation (1) is discretized as

$$
\begin{aligned}
&\left((\epsilon\rho_g y_m)^n_{i,j} - (\epsilon\rho_g y_m)_{i,j}\right)/\delta t + \\
&\Big((u_g)_{i+\frac{1}{2},j} r_{i+\frac{1}{2}} [\xi_{i+\frac{1}{2},j} (\epsilon\rho_g y_m)^n_{i,j} + \overline{\xi}_{i+\frac{1}{2},j} (\epsilon\rho_g y_m)^n_{i+1,j}] - \\
&\quad (u_g)_{i-\frac{1}{2},j} r_{i-\frac{1}{2}} [\xi_{i-\frac{1}{2},j} (\epsilon\rho_g y_m)^n_{i-1,j} + \overline{\xi}_{i-\frac{1}{2},j} (\epsilon\rho_g y_m)^n_{i,j}]\Big)/(r_i \delta r) + \\
&\Big((v_g)_{i,j+\frac{1}{2}} [\xi_{i,j+\frac{1}{2}} (\epsilon\rho_g y_m)^n_{i,j} + \overline{\xi}_{i,j+\frac{1}{2}} (\epsilon\rho_g y_m)^n_{i,j+1}] - \\
&\quad (v_g)_{i,j-\frac{1}{2}} [\xi_{i,j-\frac{1}{2}} (\epsilon\rho_g y_m)^n_{i,j-1} + \overline{\xi}_{i,j-\frac{1}{2}} (\epsilon\rho_g y_m)^n_{i,j}]\Big)/\delta z \\
&\qquad = (R^p_{gm})^n_{i,j} - (R^c_{gm})_{i,j} (y_m)^n_{i,j} \quad .
\end{aligned}
\tag{44}
$$

The indicator functions ξ used to represent donor cell differencing are defined as

$$
\xi_{i+\frac{1}{2},j} = \begin{cases} 0 & (u_g)_{i+\frac{1}{2},j} < 0 \\ 1 & (u_g)_{i+\frac{1}{2},j} \geq 0 \end{cases} , \tag{45}
$$

$$
\xi_{i,j+\frac{1}{2}} = \begin{cases} 0 & (v_g)_{i,j+\frac{1}{2}} < 0 \\ 1 & (v_g)_{i,j+\frac{1}{2}} \geq 0 \end{cases} , \tag{46}
$$

and

$$
\overline{\xi} = 1 - \xi \quad . \tag{47}
$$

A similar set of ξ functions can be defined based on the solids velocities also. Here, for convenience, no subscripts have been given to distinguish between ξ's based on gas or solids velocities.

Note that in equation (44) the rate of formation term has been linearized as

$$
R_{gm} = R^p_{gm} - R^c_{gm} y_m \quad , \tag{48}
$$

where the first term is the rate production of species m and the second term is the rate of consumption. Reversible reactions will contribute to both the terms, whereas irreversible reactions will contribute only to one of the terms. Such a linearization of R_{gm} will accelerate the convergence of the iterations while ensuring that y_ms are always positive (Patankar 1980).

Equation (44) can be rearranged to get the sparse matrix equation.

$$
\begin{aligned}
&-\left((u_g)_{i-\frac{1}{2},j} r_{i-\frac{1}{2}} \xi_{i-\frac{1}{2},j} \frac{\delta t}{r_i \delta r}\right)(\epsilon\rho_g)_{i-1,j} && (y_m)^n_{i-1,j} - \\
&\left((v_g)_{i,j-\frac{1}{2}} \xi_{i,j-\frac{1}{2}} \frac{\delta t}{\delta z}\right)(\epsilon\rho_g)_{i,j-1} && (y_m)^n_{i,j-1} + \\
&\Bigg[\Bigg(1+\left[(u_g)_{i+\frac{1}{2},j} r_{i+\frac{1}{2}} \xi_{i+\frac{1}{2},j} - (u_g)_{i-\frac{1}{2},j} r_{i-\frac{1}{2}} \overline{\xi}_{i-\frac{1}{2},j}\right] \frac{\delta t}{r_i \delta r} + \\
&\quad \left[(v_g)_{i,j+\frac{1}{2}} \xi_{i,j+\frac{1}{2}} - (v_g)_{i,j-\frac{1}{2}} \overline{\xi}_{i,j-\frac{1}{2}}\right] \frac{\delta t}{\delta z}\Bigg)(\epsilon\rho_g)_{i,j} \\
&\qquad\qquad + (R^c_{gm})^n_{i,j} \delta t\Bigg](y_m)^n_{i,j} + \\
&\left((v_g)_{i,j+\frac{1}{2}} \overline{\xi}_{i,j+\frac{1}{2}} \frac{\delta t}{\delta z}\right)(\epsilon\rho_g)_{i,j+1} && (y_m)^n_{i,j+1} + \\
&\left((u_g)_{i+\frac{1}{2},j} r_{i+\frac{1}{2}} \overline{\xi}_{i+\frac{1}{2},j} \frac{\delta t}{r_i \delta r}\right)(\epsilon\rho_g)_{i+1,j} && (y_m)^n_{i+1,j} \\
& && = (R^p_{gm})^n_{i,j} \delta t + \\
& && \quad (\epsilon\rho_g)_{i,j} (y_m)_{i,j} \quad .
\end{aligned}
\tag{49}
$$

In the above equation, the right-hand side has the form Ay_m, where **A** is a sparse matrix. The sets of algebraic equations for y_m and x_m, however, are nonlinearly coupled through the rate of formation terms, R_{gm}. They are also nonlinearly coupled to the energy equations since R_{gm} is a function of temperature. The strategy used in MGAS is to compute the values of R_{gm} from the previous iteration values of y_m, x_m, and temperatures of gas and solids, thereby decoupling the equations into sets of linear equations. The coupling between the equations is then accounted for through the iterative technique described at the beginning of Section 6.0. The sparse matrix equations are solved using a routine developed by Kapitza and Eppel (1987) based on a conjugate gradient method. The solution given by the sparse matrix solver is termed $(y_m)^*$. Then the values of y_m are updated on a cell-by-cell basis using Newton's method. Thus,

$$(y_m)^{k+1}_{i,j} = (y_m)^{k}_{i,j} - \frac{E^k_{ym}\left((y_m)^k_{i,j} - (y_m)^{k-1}_{i,j}\right)}{E^k_{ym} - E^{k-1}_{ym}} \quad , \tag{50}$$

where

$$E^k_{ym} = (y_m)^*_{i,j} - (y_m)^k_{i,j} \tag{51}$$

is the error in y_m and the superscripts k indicate the iteration level.

A small variation of the above solution scheme is used for solving x_m when solids velocity is held constant and solids density is varied: instead of solving for x_m^*, the sparse matrix equations are solved for

$$(\bar{x}_m)_{i,j} = [(1-\epsilon)\rho_s]_{i,j}(x_m)_{i,j} \quad . \tag{52}$$

The solids density is obtained from

$$[(1-\epsilon)\rho_s]_{i,j} = (1-\epsilon)_{i,j}\rho_{s0}x_{A0} + \sum_m (\bar{x}_m)_{i,j} \quad , \tag{53}$$

where the fact that $\rho_s x_A = \rho_{s0} x_{A0}$, i.e., the ash being inert is used to avoid solving the equations for x_A. x_m^* is then obtained as

$$(x_m)^*_{i,j} = \frac{(\bar{x}_m)_{i,j}}{[(1-\epsilon)\rho_s]_{i,j}} \quad . \tag{54}$$

As in the case of y_m, Newton's method is then used to update the values of x_m.

6.4 Solution of Energy Equations

The energy equations are finite-differenced in a slightly different form, since they are written in a non-conservative form in terms of the temperatures. For example, the gas energy equation is discretized as

$$
\begin{aligned}
&(\epsilon\rho_g C_{pg})_{i,j}\left[(T_g)^n_{i,j}-(T_g)_{i,j}\right]/\delta t + \\
&\Big((u_g)_{i+\frac{1}{2},j} r_{i+\frac{1}{2}} \overline{\xi}_{i+\frac{1}{2},j} (\epsilon\rho_g C_{pg})_{i+\frac{1}{2},j}\left[(T_g)^n_{i+1,j}-(T_g)^n_{i,j}\right] - \\
&\quad (u_g)_{i-\frac{1}{2},j} r_{i-\frac{1}{2}} \xi_{i-\frac{1}{2},j} (\epsilon\rho_g C_{pg})_{i-\frac{1}{2},j}\left[(T_g)^n_{i-1,j}-(T_g)^n_{i,j}\right]\Big)/r_i\delta r \\
&+\Big((v_g)_{i,j+\frac{1}{2}} \overline{\xi}_{i,j+\frac{1}{2}} (\epsilon\rho_g C_{pg})_{i,j+\frac{1}{2}}\left[(T_g)^n_{i,j+1}-(T_g)^n_{i,j}\right] - \\
&\quad (v_g)_{i,j-\frac{1}{2}} \xi_{i,j-\frac{1}{2}} (\epsilon\rho_g C_{pg})_{i,j-\frac{1}{2}}\left[(T_g)^n_{i,j-1}-(T_g)^n_{i,j}\right]\Big)/\delta z \\
&\quad = -\gamma_g\left((T_g)^n_{i,j}-(T_s)^n_{i,j}\right) + \text{Other R.H.S. terms} \ ,
\end{aligned}
\tag{55}
$$

where

$$
\begin{aligned}
&(\epsilon\rho_g C_{pg})_{i+\frac{1}{2},j} = \\
&0.5\left((\epsilon\rho_g)_{i+1,j}(C_{pg})_{i+1,j} + (\epsilon\rho_g)_{i,j}(C_{pg})_{i,j}\right), \text{ etc.}
\end{aligned}
\tag{56}
$$

Equation (55) and the finite-differenced solids energy equation can be written in a sparse matrix form and solved iteratively, by determining the heat of reaction from the values of x_m and y_m at the previous iteration level.

The two energy equations are coupled by the interphase heat transfer term, in addition to the heat of reaction term. To remove this coupling, a special technique is needed, as illustrated in the following example: Consider the following two equations for T_g and T_s.

$$aT_g = -\gamma_g(T_g - T_s) + b \tag{57}$$

and

$$cT_s = \gamma_s(T_g - T_s) + d \ . \tag{58}$$

The solutions for these equations are

$$T_g = \frac{b(c+\gamma_s) + d\gamma_g}{ac + a\gamma_s + c\gamma_g} \tag{59}$$

and

$$T_s = \frac{d(a+\gamma_g) + b\gamma_s}{ac + a\gamma_s + c\gamma_g} \ . \tag{60}$$

The above solutions have the following limiting forms:

$$\lim_{\gamma_g,\,\gamma_s \to 0} \; T_g = b/a \text{ and } T_s = d/c \tag{61}$$

and

$$\lim_{\gamma_g,\,\gamma_s \to \infty} \; T_g = T_s = \frac{b+d}{a+c} \quad . \tag{62}$$

Now consider the following seemingly consistent iterative scheme for solving the above equation set

$$T_g^{k+1} = \left(-\gamma_g (T_g^k - T_s^k) + b\right)/a \tag{63}$$

and

$$T_s^{k+1} = \left(\gamma_s (T_g^k - T_s^k) + d\right)/c \quad , \tag{64}$$

where the superscript k indicates the iteration level. For γ's $\to$ 0, the above iteration scheme will yield the correct limiting solution, equation (61), and hence for small values of γ's, the iteration scheme will converge. For γ's $\to \infty$, the above scheme does not yield the correct limiting solution, equation (62), and hence for large values of γ's, the scheme will not converge.

An iteration scheme similar to the one in the above example will fail also when applied to the two energy equations, at large values of γ's. However, a robust iteration scheme can be derived by rearranging the terms of the energy equations, as motivated by the solutions in equations (59) and (60). The discretized energy equations have a form similar to equations (57) and (58) and may be written in the following symbolic form:

$$\begin{aligned} &a_{i-1,j}(T_g)_{i-1,j} + a_{i,j-1}(T_g)_{i,j-1} + a_{i,j}(T_g)_{i,j} + \\ &a_{i,j+1}(T_g)_{i,j+1} + a_{i+1,j}(T_g)_{i+1,j} = -\delta t\,(\gamma_g)_{i,j}\left[(T_g)_{i,j} - (T_s)_{i,j}\right] + b_{i,j} \end{aligned} \tag{65}$$

and

$$\begin{aligned} &c_{i-1,j}(T_s)_{i-1,j} + c_{i,j-1}(T_s)_{i,j-1} + c_{i,j}(T_s)_{i,j} + \\ &c_{i,j+1}(T_s)_{i,j+1} + c_{i+1,j}(T_s)_{i+1,j} = \delta t\,(\gamma_s)_{i,j}\left[(T_g)_{i,j} - (T_s)_{i,j}\right] + d_{i,j} \quad , \end{aligned} \tag{66}$$

where a's and c's represent the elements of the sparse matrices and b and d represent the elements of the right-hand-side vector. (For example, see equation [55].) Just as in the example, these equations can be solved (in terms of the off-diagonal components) to obtain

$$(T_g)_{i,j} = \frac{\begin{array}{l}(b_{i,j}-a_{i-1,j}(T_g)_{i-1,j}-a_{i,j-1}(T_g)_{i,j-1}-a_{i,j+1}(T_g)_{i,j+1}- \\ a_{i+1,j}(T_g)_{i+1,j})(c_{i,j}+\delta t(\gamma_s)_{i,j}) + (d_{i,j}-c_{i-1,j}(T_s)_{i-1,j} \\ -c_{i,j-1}(T_s)_{i,j-1}-c_{i,j+1}(T_s)_{i,j+1}-c_{i+1,j}(T_s)_{i+1,j})\,\delta t\,(\gamma_g)_{i,j}\end{array}}{a_{i,j}c_{i,j}+a_{i,j}\,\delta t\,(\gamma_s)_{i,j}+c_{i,j}\,\delta t\,(\gamma_g)_{i,j}} \quad (67)$$

and a similar formula for $(T_s)_{i,j}$. The above solution motivates the following rearrangement of equations (65) and (66), suitable for an iterative solution:

$$\begin{array}{l}(a_{i,j}c_{i,j}+a_{i,j}\,\delta t\,(\gamma_s)_{i,j}+c_{i,j}\,\delta t\,(\gamma_g)_{i,j})(T_g)^{k+1}_{i,j}+ \\ c_{i,j}\big(a_{i-1,j}(T_g)^{k+1}_{i-1,j}+a_{i,j-1}(T_g)^{k+1}_{i,j-1}+ \\ a_{i,j+1}(T_g)^{k+1}_{i,j+1}+a_{i+1,j}(T_g)^{k+1}_{i+1,j}\big) = \\ b_{i,j}c_{i,j}+\delta t\,(\gamma_s)_{i,j}\big(b_{i,j}-a_{i-1,j}(T_g)^{k}_{i-1,j}-a_{i,j-1}(T_g)^{k}_{i,j-1}- \\ a_{i,j+1}(T_g)^{k}_{i,j+1}-a_{i+1,j}(T_g)^{k}_{i+1,j}\big)+\delta t\,(\gamma_g)_{i,j}\big(d_{i,j}-c_{i-1,j}(T_s)^{k}_{i-1,j}- \\ c_{i,j-1}(T_s)^{k}_{i,j-1}-c_{i,j+1}(T_s)^{k}_{i,j+1}-c_{i+1,j}(T_s)^{k}_{i+1,j}\big)\ ,\end{array} \quad (68)$$

and

$$\begin{array}{l}(a_{i,j}c_{i,j}+a_{i,j}\,\delta t\,(\gamma_s)_{i,j}+c_{i,j}\,\delta t\,(\gamma_g)_{i,j})(T_s)^{k+1}_{i,j}+ \\ a_{i,j}\big(c_{i-1,j}(T_s)^{k+1}_{i-1,j}+c_{i,j-1}(T_s)^{k+1}_{i,j-1}+ \\ c_{i,j+1}(T_s)^{k+1}_{i,j+1}+c_{i+1,j}(T_s)^{k+1}_{i+1,j}\big) = \\ d_{i,j}a_{i,j}+\delta t\,(\gamma_s)_{i,j}\big(b_{i,j}-a_{i-1,j}(T_g)^{k}_{i-1,j}-a_{i,j-1}(T_g)^{k}_{i,j-1}- \\ a_{i,j+1}(T_g)^{k}_{i,j+1}-a_{i+1,j}(T_g)^{k}_{i+1,j}\big)+\delta t\,(\gamma_g)_{i,j}\big(d_{i,j}-c_{i-1,j}(T_s)^{k}_{i-1,j}- \\ c_{i,j-1}(T_s)^{k}_{i,j-1}-c_{i,j+1}(T_s)^{k}_{i,j+1}-c_{i+1,j}(T_s)^{k}_{i+1,j}\big)\ ,\end{array} \quad (69)$$

where the superscript k indicates the iteration level. It can be verified that the above iteration scheme will converge to the correct limits for γ's $\to$ 0 as well as for γ's $\to \infty$. The sparse matrix system of equations (68) and (69) are solved using the equation solver developed by Kapitza and Eppel (1987) to get the solutions T_g^* and T_s^*. The values of T_g and T_s are updated using Newton's method applied on a cell-by-cell basis: for example,

$$(T_g)^{k+1}_{i,j} = (T_g)^{k}_{i,j} - \frac{E^{k}_{Tg}\left((T_g)^{k}_{i,j} - (T_g)^{k-1}_{i,j}\right)}{E^{k}_{Tg} - E^{k-1}_{Tg}} \quad , \tag{70}$$

where

$$E^{k}_{Tg} = (T_g)^{*}_{i,j} - (T_g)^{k}_{i,j} \tag{71}$$

is the error in T_g and superscript k indicates the iteration level.

6.5 Convergence Criteria

The convergence of the iterations at any time step is tested by checking each of the E's (see equations [51] and [71]) on a cell-by-cell basis. Four tolerance values, one each for gas species mass fraction, solids species mass fraction, gas temperature, and solids temperature, are specified. Convergence is said to be achieved only when the absolute values of all the E's in all the cells simultaneously become smaller than the tolerance values. In addition, the code also displays the convergence of various equations in a symbolic representation used in PCGC-3 (Smith and Smoot 1991). First, the residue of the equations is summed over all the cells; for example, for the gas energy equation

$$R^{0}_{Tg} = \sum_{i,j} \{-b_{i,j} + a_{i-1,j}(T_g)_{i-1,j} + a_{i,j-1}(T_g)_{i,j-1} + a_{i,j}(T_g)_{i,j} + a_{i,j+1}(T_g)_{i,j+1} + a_{i+1,j}(T_g)_{i+1,j}\} \quad . \tag{72}$$

To scale the residue, the diagonal elements of the sparse matrix are summed over all the cells,

$$\Psi_{Tg} = \sum_{i,j} a_{i,j}(T_g)_{i,j} \quad . \tag{73}$$

A dimensionless residual is obtained from equations (72) and (73) as

$$R_{Tg} = \frac{R^{0}_{Tg}}{\Psi_{Tg}} \quad , \tag{74}$$

and then a number of non-significant digits is defined as

$$N_{Tg} = \text{Max}(0, [N_{max} + \text{Log}_{10}(R_{Tg})]) \ , \qquad (75)$$

where N_{max} is the maximum number of significant digits, which is 15 for double precision calculations on a VAX computer. For no convergence, N_{Tg} is 15 or greater and for perfect convergence, N_{Tg} is 0. Such N values for each of the equations is printed out at every time step and, if necessary, at every iteration. They are defined in this manner to enable one to quickly determine how well the various equations are converging. (For example, see the sample log-file in Appendix H.)

7.0 CONCLUDING REMARKS

The MGAS model can describe the transient operation of coflow, counterflow, or fixed-bed gasifiers. It is a one-dimensional model and can simulate the addition and withdrawal of gas and solids at multiple locations in the bed, a feature essential for simulating beds with recycle. The model describes the reactor in terms of a gas phase and a solids (coal or char) phase. These phases may exist at different temperatures. The model considers several combustion, gasification, and initial stage reactions. The model consists of a set of mass balances for 14 gas species and three coal (pseudo-) species and energy balances for the gas and the solids phases. The resulting partial differential equations are solved using a finite difference technique.

Future work includes the following:

- Conducting simulations of various operating conditions and reactor configurations and comparing the results with experimental data, if available;
- Optimizing the numerical technique used in the code;
- Accounting for diffusional limitations in the gas-solids reaction rate expressions;
- Validating the two-dimensional feature;
- Including realistic flow-field computations to make the code truly two-dimensional;
- Including pollutant formation and capture reactions.

8.0 LIST OF SYMBOLS

a	Matrix coefficients of the discretized gas energy equation (65)
b	Right-hand side element of the discretized gas energy equation (65)
c	Matrix coefficients of the discretized solids energy equation (66)
c^H_m	Fraction of hydrogen that appears in species m in the products of the cracking reaction
c^O_m	Fraction of oxygen that appears in species m in the products of the cracking reaction
C_{pg}	Average gas specific heat
C_{ps}	Average solids specific heat
d	Right-hand side element of the discretized solids energy equation (66)
d^H_m	Fraction of hydrogen that appears in species m in the products of the devolatilization reaction
d^O_m	Fraction of oxygen that appears in species m in the products of the devolatilization reaction
d_p	Particle diameter
D	Effective diffusivity
D_{bed}	Vessel diameter
E_x	Activation energy for reaction "x"
f^T_m	Mass fraction of element m in the pseudo-species Tar
f^V_m	Mass fraction of element m in the pseudo-species Volatile Matter
F_{gs}	Gas-solids drag
H_{rg}	Heat of reaction in the gas phase
H_{rs}	Heat of reaction in the solids phase
h_w	Bed-to-wall heat transfer coefficient
k_{ash}	Mass transfer resistance of the ash layer

k_{film} Mass transfer resistance of the film layer

k_g Thermal conductivity of the gas

k_p Thermal conductivity of the solid particles

k_s Effective thermal conductivity of a bed of particles

k_x Pre-exponential factor for reaction "x"

K_x Equilibrium constant for reaction "x"

p_m Partial pressure of gas species m

P Total pressure

r Radial coordinate

R Universal gas constant

R_{gm} Rate of formation of gas species m

R_{gm}^{c} Rate of consumption of gas species m divided by y_m; See equation (48).

R_{gm}^{p} Rate of production of gas species m; See equation (48).

R_{sm} Rate of formation of solids species m

R_x Rate of reaction "x"

t Time

T_g Gas temperature

T_s Solids temperature

T_w Wall temperature

u_g Radial component of the gas velocity

u_s Radial component of the solids velocity

v_g Axial component of the gas velocity

$\vec{v}_g$ Gas velocity vector

v_s Axial component of the solids velocity

$\vec{v}_s$ Solids velocity vector

w_{g3} Shift reaction catalytic activity of ash

x_m Mass fraction of solids species m

x^* Minimum x_{VM} for a given solids temperature

y_m Mass fraction of gas species m

z Axial coordinate

GREEK SYMBOLS

α^c Fraction of Fixed Carbon in the products of the cracking reaction

α^d Fraction of Tar in the products of the devolatilization reaction

β^c_m Fraction of gas species m in the products of the cracking reaction

β^d_m Fraction of gas species m in the products of the devolatilization reaction

δr Radial dimension of computational cells

δt Time step

δz Axial dimension of computational cells

ϵ Void fraction

γ Interphase heat transfer coefficient

γ_g Equal to $\gamma + \gamma_r \Sigma_m R_{gm}$

γ_r Equal to 0 if $\Sigma_m R_{gm} < 0$; 1 if $\Sigma_m R_{gm} > 0$

γ_s Equal to $\gamma + (\gamma_r - 1) \Sigma_m R_{gm}$

μ_g Gas viscosity

ρ_g Gas density

ρ_s Solids density

ξ An indicator function for donor cell differencing; (See equations [45] and [46] for definition.)

SUPERSCRIPTS AND SUBSCRIPTS

A Ash

bdry Boundary

c	Tar-cracking reaction
d	Devolatilization reaction
FC	Fixed Carbon
g	Gas
H	Hydrogen
i	Computing mesh column index -- r-direction
j	Computing mesh row index -- z-direction
k	Superscript to identify iteration level
m	Species m
M	Moisture
n	Superscript to indicate the variables are at an advanced time level
O	Oxygen
s	Solids
T	Tar
V, VM	Volatile Matter
0	Subscript 0 indicates the initial value

9.0 REFERENCES

Bauer, R., and E.U. Schlunder. 1978. Effective radial thermal conductivity of packings in gas flow: Part II: Thermal conductivity of the packing fraction without gas flow. *Int. Chem. Eng.* 18: 189-204.

Bhattacharya, A., L. Salam, M.P. Dudukovic, and B. Joseph. 1986. Experimental and modeling studies in fixed-bed char gasification. *Ind. Eng. Chem. Process Des. Dev.* 25: 988-996.

Bird, R.B., W.E. Stewart, and E.N. Lightfoot. 1960. Transport Phenomena, 658-663, New York: John Wiley & Sons.

Cho, Y.S., and B. Joseph. 1981. Heterogeneous model for moving-bed coal gasification reactors. *Ind. Eng. Chem. Process Des. Dev.* 20: 314-318.

Denn, M.M. 1986. Process Modeling, New York: Longman.

Ergun, S. 1952. Fluid flow through packed columns. *Chem. Eng. Progress* 48(2): 89-93.

Gregory, D.R., and R.F. Littlejohn. 1955. A survey of numerical data on the thermal decomposition of coal. *Br. Coal Util. Res. Assoc. Mon. Bull.* 29(6): 173-180.

Hobbs, M.L., P.T. Radulovic, and L.D. Smoot. 1990. Fixed-bed coal gasification modeling. Paper presented at the Twenty-third symposium (international) on combustion, The Combustion Institute, Pittsburgh, Pennsylvania.

Johnson, J.L. 1979. Kinetics of Coal Gasification, New York: John Wiley & Sons.

Kapitza, H., and D. Eppel. 1987. A three-dimensional Poisson solver based on conjugate gradients compared to standard iterative methods and its performance on vector computers. *J. Comp. Physics* 68: 474-484.

Kim, M., and B. Joseph. 1983. Dynamic behavior of moving-bed coal gasifiers. *Ind. Eng Chem. Process Des. Dev.* 22: 212-217.

Leva, M., M. Weintraub, M. Grummer, and E.L. Clark. 1948. Cooling of gases through packed tubes. *Ind. & Eng. Chem.* 40: 747-752.

Patankar, S.V. 1980. Numerical Heat Transfer and Fluid Flow, 143-146. New York: Hemisphere Publishing Corporation.

Perry, R.H., and C.H. Chilton. 1973. Chemical Engineers Handbook, New York: McGraw-Hill.

Saxena, S.C. 1990. Devolatilization and combustion characteristics of coal particles. *Prog. Energy Combust. Sci.* 16: 55-94.

Smith, P.J., and L.D. Smoot. 1991. Detailed model for practical pulverized coal furnaces and gasifiers. Volume II. User manual for 1990 version pulverized coal gasification and combustion 3-dimensional (90-PCGC-3), Brigham Young University, Provo, Utah.

Solomon, P.R., D.G. Hamblen, R.M. Carangelo, M.A. Serio, and G.V. Deshpande. 1990. A general model of coal devolatilization. *J. Energy Fuels*, in press.

Syamlal, M. 1989. Hot-Gas Desulfurization Reactor (HDR) Model. Unpublished EG&G report.

Thorsness, C.B., and S. Kang. 1986. A general-purpose, packed-bed model for analysis of underground coal gasification processes. Lawrence Livermore National Laboratory Report No. UCID-20731.

Wen, C.Y., H. Chen, and M. Onozaki. 1982. DOE/MC/16474-1390. *User's manual for computer simulation and design of the moving bed coal gasifier.* NTIS/DE83009533. Springfield, Virginia: National Technical Information Service.

Yoon, H., J. Wei, and M.M. Denn. 1978. A model for moving-bed coal gasification reactors. *AIChE J.* 24: 885-903.

Yoon, H., J. Wei, and M.M. Denn. 1979. Transient behavior of moving-bed coal gasification reactors. *AIChE J.* 25: 429-439.

Yu, W.C., M.M. Denn, and J. Wei. 1983. Radial effects in moving bed coal gasifiers. *Chem. Eng. Sci.* 38: 1467-1481.

Zabrodsky, S.S. 1966. Hydrodynamics and Heat Transfer in Fluidized Beds, Cambridge, Massachusetts: The MIT Press.

Appendix A: Description of the Computer Program

The MGAS model is written in FORTRAN. It has a modular form that enables easy modification of subroutines, such as the rate of reaction module, that needs to be modified frequently to accommodate various kinetic models. Appendix E gives a list of the subroutines that constitute the MGAS model and their calling sequence. To use the program, however, it is only necessary to know the function of a few of the subroutines described in this section and the next two sections.

The main control flow is as follows: The main program (MGAS) opens data files, reads the input file, and passes control to subroutine MARCH. MARCH controls the marching in time, setting up boundary conditions after each time step and generating the various outputs at appropriate intervals. It transfers control to subroutine ITER, which controls the iterative solution of the various equations as described in Section 6.0.

The main FORTRAN variables defined in the code are listed in Appendix F. These variables are transferred between subroutines by storing them in common blocks. All the common blocks are collected in the file COMMON.INC, which is included in all subroutines. The array dimensions are specified through the file PARAM.INC as described in Appendix B. The correspondence between FORTRAN indices and the finite difference indices is as follows:

	FORTRAN	Finite Difference
Scalar:	ROG(IJ)	$(\rho_g)_{i,j}$
Vector:	UG(IJ)	$(u_g)_{i+\frac{1}{2},j}$
	VG(IJ)	$(v_g)_{i,j+\frac{1}{2}}$

The indices for neighboring cells (Appendix F) are obtained by calling subroutine INDEXA. For cell-centered quantities, scalars such as densities, the values at the boundary cells are obtained by reflection; i.e., the value at the boundary cell is assigned the same as that at the neighboring interior cell. For vectors, the values to be specified at the boundaries are determined by the boundary condition. To do the two types of assignments at the boundary, two types of indices are in use: for example, the index IJM is everywhere equivalent to (i,j-1) but the index IJB is equivalent to (i,j-1) everywhere except when the (i,j-1) cell is a boundary cell. Then IJB is set equal to (i,j) so that the values of the cell-centered quantities at the boundary cell (i,j-1) are the same as those at the interior cell (i,j).

Appendix B: Setting Up the Program

Several command files, which have been written to aid the running of the code on the METC VAX cluster, are portable only to other VAX computers. Hence the following instructions are specific to the METC installation of the MGAS model. The VAX commands to be issued are shown in bold letters.

1. Create a directory for the MGAS model. This is an optional step but is useful since the MGAS code is composed of a number of files: **CR/DIR <directory name>.**

2. Set default to the MGAS directory: **SET DEF <directory name>.**

3. Copy MGAS model files: **@DISK20:[MSYAML.MGAS.VER1]GET_MGAS.**

4. Modify FORTRAN files, if necessary (Appendix A).

5. Change the dimensions in the file PARAM.INC to specify the number of axial (JNX) and radial (INX) divisions desired.

6. Create an executable version: **@CR_MGAS.**

   The above command will activate FO_MGAS.COM for compiling all the FORTRAN files and LI_MGAS.COM for linking the object modules generated during the compilation step. At this stage there is an option to create either a single (default) or a double precision version of the code.

7. Create or modify the data file as needed. A description of all the input data entries is given in Appendix G. A sample input file is given in Appendix H.

8. Interactive execution of the code: **R MGAS.**

   The code will search for the default data file MGAS.DAT. If the file is not found, the code will prompt the user for the data file name. Enter the name of the data file.

   Batch execution of the code: Change the project code, directory path name, and data file name in the file MGAS.COM. Then submit the file MGAS.COM. If the data file name is not MGAS.DAT, make sure that no file by that name exists in the current directory, since the code will first attempt to use MGAS.DAT, if found, as the data file.

9. The standard output will be in the file MGAS.OUT (or the name specified as OUTFILE in the input file). The special outputs, if specified, will be in the files MGAS01.OUT, etc. (or the names specified as the SAMFILE in the input file). A sample standard output is given in Appendix H.

10. After step 6 is completed, if a file, say RRATES.FOR, is modified and JNX and INX are not changed, the executable version of the code can be generated with the following commands:

    FOR RRATES.FOR
    @LI_MGAS.

11. During a batch execution, check for error messages and the progress of the job by reading the log file. At every time step, the code prints out the number of iterations in the previous time step and the extent of convergence of various equations. A sample of the log file is given in Appendix H.

12. All the FORTRAN modules may be collected in the file MGAS.ALL with the command **@ALL_MGAS**.

Appendix C: Setting Up a Simulation

Setting up a problem using the MGAS model may involve two tasks: the frequent task is that the data file needs to be modified, and occasionally a few subroutines need to be modified, for example, to incorporate a new rate of reaction model, to change certain physical properties, or to create special outputs.

INPUT FILE

While modifying the input file, keep in mind that the default units used in the code are grams, centimeters, seconds, calories, and degrees Kelvin. All the dimensional quantities appear in files PVARS.FOR, PCONS.FOR, and the default values specified in INPUT.FOR. Hence, if a different set of units need to be used, the dimensional quantities in those three subroutines should be modified.

The input file uses a NAMELIST format, which makes the writing of a data file convenient. A NAMELIST input has the form "Variable name = Value". The variable names and descriptions are given in Appendix G and a sample input file in Appendix H. The variable names may appear in any order, but for ease of reading a data file, a particular grouping of the variables is suggested in Appendix G. The input data should begin only after a line that contains the key word "$DATA" beginning in column 2, and data entry ends with the key word "$END". The lines above $DATA and those below $END may be used for writing comments about the data file.

Default values are specified for several input variables, such as tolerances and composition of tar in subroutine INPUT. Some default values, such as heating value of coal and tar and coal density, are calculated using empirical formulas.

RUN TIME

On some computers, such as the VAX, the progress of a simulation can be determined from the LOG file (see Appendix H). At every time step, the code prints out the time, the number of iterations, and the extent of convergence of gas species, solids species, gas energy, and solids energy equations (Section 6.5). Non-convergence is indicated by the symbol '>'. When the combustion zone is moving, usually the convergence is poor. It is conjectured that non-convergence occurs when the combustion zone moves at a velocity greater than $\delta z/\delta t$.

OUTPUT FILE

The first section of the OUTPUT file echoes all the input data (Appendix H) and some of the quantities derived from the input data. In the echo, the variable names as well as a brief description of the variable are given. The echo section also gives a picture of the reactor configuration, in which the location of the fluid cells (regions where the gas and solids phases are present) are marked by a ".", obstacle and boundary cells are marked by a "B", and the inflow/outflow ports are marked by the respective port number. This section of the output is useful for ensuring that the input data was correctly entered.

The second section of the OUTPUT file contains data on the conditions at various locations in the bed and various times at intervals of TOUT. The accuracy of the initial conditions can be ascertained by checking the data for the start time.

The third section of the OUTPUT file gives a summary report for the simulation. It contains an echo of the input data in a brief, NAMELIST-like format, the flow rates, composition, and temperature of the various inflow and outflow streams, the maximum char temperature, percent carbon conversion, the heating value of the product gas, and the heat loss from the gasifier.

The fourth section of the OUTPUT file contains an overall elemental balance for time equal to TSTOP. The inflow and outflow of carbon, hydrogen, oxygen, nitrogen, and sulfur through various species are written out. If steady-state conditions exist at TSTOP, then the difference between the total inflow and outflow for any element should be small (see Appendix H).

RESTART

Occasionally, it is necessary to restart a run so that the run can be continued further in time. It is possible to do so, since the code writes a restart file called MGAS.RES (or the name specified as RESFILE in the input). To restart a run, set the variable RUN to 1 in the input file. The code will then read the initial conditions for the run from the file MGAS.RES and continue the run. The boundary conditions (flow rates, etc.) and other data will be as specified in the input file. To get all the data (including the boundary conditions) from the file MGAS.RES, set the variable RUN to 2.

To change certain physical parameters and the constitutive relations, it is necessary to modify the appropriate subroutines. The following is a list of the frequently modified subroutines:

EOSG The subroutine EOSG computes the density of the gas using an equation of state; e.g., $\rho_g = P/RT$.

PCONS The subroutine PCONS computes or sets physical properties that do not change, e.g., molecular weights of different species, heat of reaction. While changing molecular weights, bear in mind that several molecular weights are written into the code of subroutines DEVOL and EBAL.

PVARS The subroutine PVARS computes physical properties that need to be updated every time step, e.g., the specific heat of gas needs to be updated every time step because it is a function of temperature, which varies with time.

RHEATS The subroutine RHEATS computes the interphase heat transfer term γ.

RRATES The subroutine RRATES computes the rates of reaction and the heats of reaction.

SAMPLE The subroutine SAMPLE can create up to five special outputs, if an output format or contents different from the standard output is desired; e.g., sample gas temperatures at a location in the bed at time intervals of 120 seconds and create a table of time in hours versus temperature in °F.

To get the CPU time taken by a run, check the end of the OUTPUT file.

Appendix D: Results of a Simulation

METC gasifier experiment R106-Baseline was simulated using the MGAS model. The input and output data files for the simulation are given in Appendix H. The simulation reached steady-state conditions in less than 5 hours of reactor operation. The predicted yields, composition, and temperatures at steady-state are compared with experimental data in Table D-1.

Table D-1. Comparison of Simulation Results with METC Data

		R106-Baseline Experiment	MGAS Simulation
Dry Product Gas (lb/h)		6841	6972
Steam (lb/h)		1362	1282
Tar (lb/h)		344	351
Total (lb/h)		8547	8605
Composition of Product Gas (mole %)	CO	13.85	17.07
	CO2	9.57	7.67
	CH4	2.77	1.85
	C2H4	0.13	0.11
	C2H6	0.35	0.26
	C3H8	0.06	0.11
	C6H6	-	0.04
	H2	15.54	15.63
	H2O	21.20	19.81
	H2S	0.33	0.39
	N2	35.55	35.55
	NH3	-	0.57
Exit Gas Temperature (°F)		1082	1044
Max. Char Temp. (°F)		< 2300	2212
Heat Loss (Btu/h)		$1.22\ 10^6$	$1.25\ 10^6$
Carbon Conversion (%)		89.9	89.2

The predicted gas and solids temperature profiles at steady-state are shown in Figure D-1.

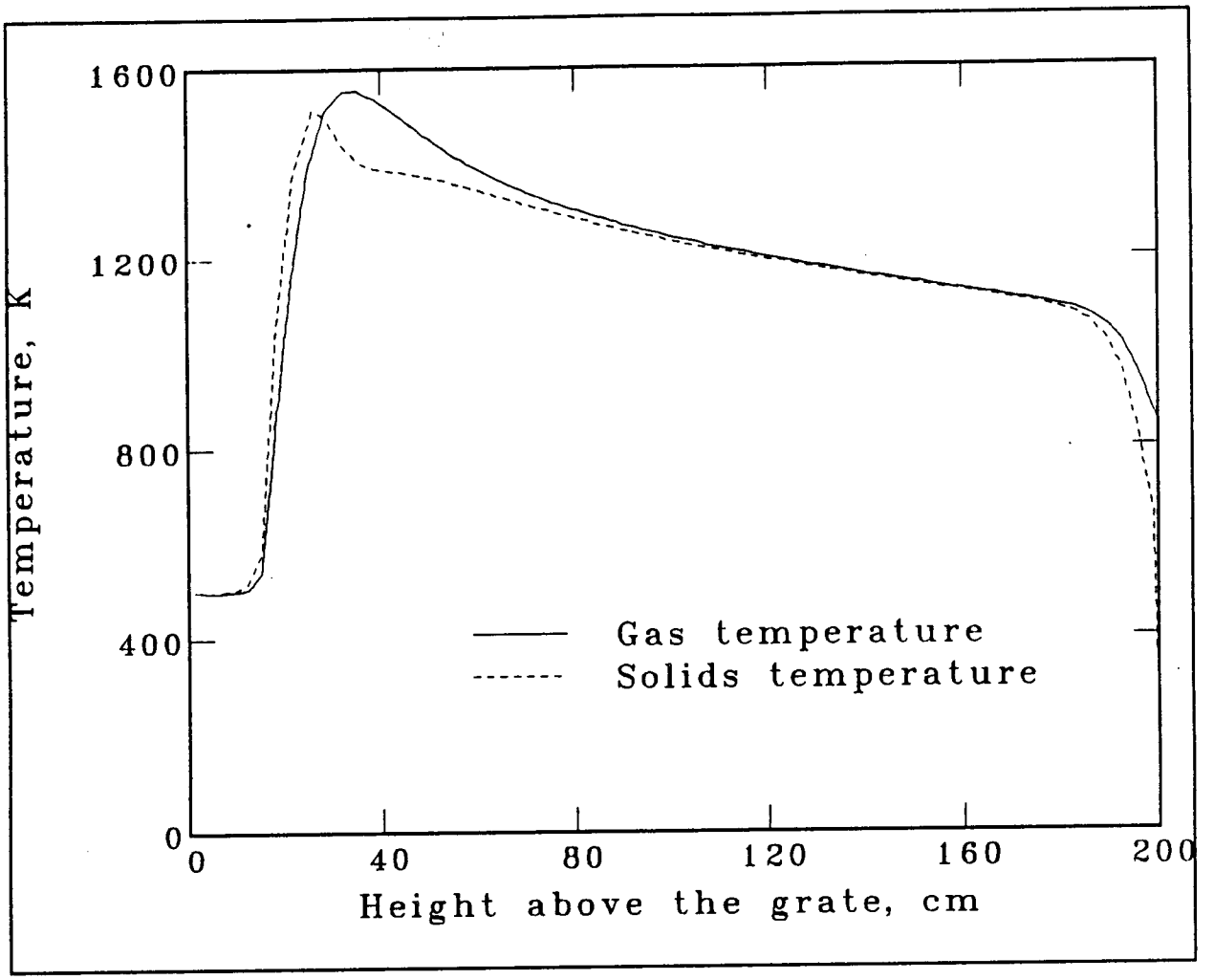

Figure D-1. Gas and Solids Temperature Profiles

Appendix E: List of Subroutines

The following are the files that constitute the MGAS code. Each file with the extension .FOR contains one or more FORTRAN subroutines.

File Name	Function
AVGFLOW.FOR	Compute average flow through ports.
COMMON.INC	A file that contains all the common blocks.
CPUTIME.FOR	Determines the CPU time required.
DEVOL.FOR	Calculates the parameters of the devolatilization model.
DRAGS.FOR	Calculates the gas-solids drag.
EBAL.FOR	Computes an overall elemental balance at the end of a simulation.
ECHO.FOR	Echoes the input data and default values in the standard output file.
EOSG.FOR	Calculates the gas density from the equation of state.
FLAGS.FOR	Sets up cell flags to identify boundaries, inlet and outlet ports, and obstacles.
HFGS.FOR	Calculates the heat flux due to conduction in the gas.
HFSS.FOR	Calculates the heat flux due to conduction in the solids.
IDONOR.INC	Calculates ξ, a function of the velocity used for donor cell differencing. Returns a value of 1 for the velocity component greater than or equal to zero and 0 for less than zero. Defined in equations (45) and (46).
IGCGD.FOR	Contains subroutines LUZERO, ILU, IGCG, LIMUL, UIMUL, and BMUL that constitute a sparse matrix inversion routine based on the conjugate gradient method (Kapitza and Eppel 1987). Double precision version.
IGCGS.FOR	Single precision version of IGCGD.

INDEX.FOR	Computes the indices of neighboring cells.
INPUT.FOR	Reads the input data file. Sets default values.
ITER.FOR	Controls the iterative solution of the finite difference equations at every time step.
LOCS.FOR	Computes the r and z components for given i and j indices or vice versa.
MGAS.FOR	The main program. Gets input and calls MARCH to get the time dependent solution.
MARCH.FOR	Controls the marching in time and calls the output routines as required.
OUTPUT.FOR	Generates the standard output at intervals of TOUT.
PARAM.INC	Defines the dimensions of the arrays. Define the number of radial (INX) and axial (JNX) cells in the finite difference mesh in this file.
PCONS.FOR	Sets all the physical constants (e.g., molecular weights). This routine is called only once at the beginning of a run.
PVARS.FOR	Sets all the properties that need to be updated every time step (e.g., specific heats as function of temperature). This routine is called once every time step.
REPORT.FOR	Generates a summary report at the end of a run.
RHEATS.FOR	Calculates the interphase heat transfer coefficient.
RRATES.FOR	Calculates the rates of reactions and the heats of reactions.
SAMPLE.FOR	Generates user specified outputs at intervals of TSAM. The quantities to be sampled and the output format are specified by modifying the subroutine.
SETACR.FOR	Sets the quantities a's and c's and the right-hand side required for the solution of the energy equations.

SETDRS.FOR	Sets discretization parameters such as DT/DR, DT/R(I)DR, R(I), etc.
SETFLOW.FOR	Converts the specified flow rates to velocity boundary conditions.
SETUP.FOR	Sets up the initial conditions.
SOLVETG.FOR	Solves the sparse matrix equation for the gas temperatures. Contains ENTRY points INITTG and GETTG.
SOLVETS.FOR	Solves the sparse matrix equations for the solids temperatures. Contains ENTRY points INITTS and GETTS.
SOLVEVG.FOR	Updates the gas velocities in the bed.
SOLVEVS.FOR	Updates the solids velocities in the bed, if required.
SOLVEXM.FOR	Solves the sparse matrix equation for coal species mass fractions. Contains ENTRY points INITXM and GETXM.
SOLVEYM.FOR	Solves the sparse matrix equation for gas species mass fractions. Contains ENTRY points INITYM and GETYM.
TAPERD.FOR	Reads the restart file.
TAPEWR.FOR	Writes the time dependent records of the restart file at intervals of TRES.
TAPEWRI.FOR	Writes the initial records of the restart file.
UPDATEO.FOR	Updates the old time level values.

The calling sequence of the above subroutines is as follows:

This is a primary tree starting at the program 'MGAS'.

```
MGAS-+-INPUT--(EXIT)
     |
     +-TAPERD--ABORT--(EXIT)
     |
     +-TAPEWRI
     |
     +-FLAGS--LOCRZ
     |
     +-INDEX
     |
```

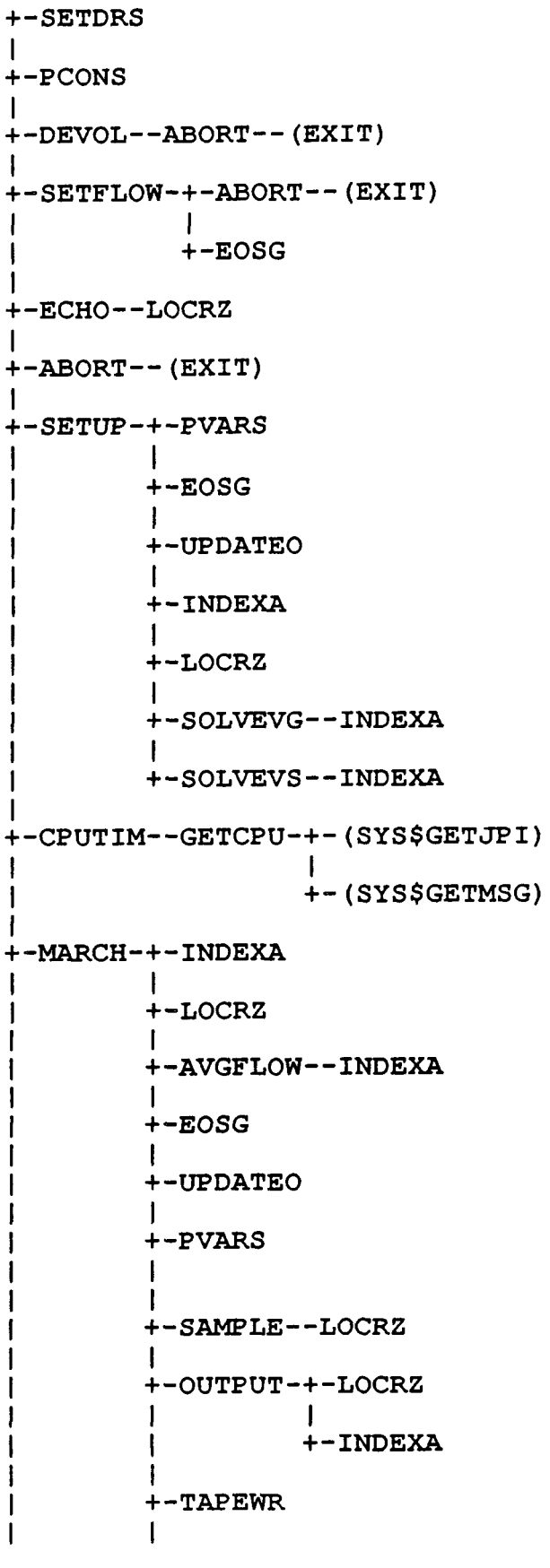
+-SETDRS
+-PCONS
+-DEVOL--ABORT--(EXIT)
+-SETFLOW-+-ABORT--(EXIT)
+-EOSG
+-ECHO--LOCRZ
+-ABORT--(EXIT)
+-SETUP-+-PVARS
+-EOSG
+-UPDATEO
+-INDEXA
+-LOCRZ
+-SOLVEVG--INDEXA
+-SOLVEVS--INDEXA
+-CPUTIM--GETCPU-+-(SYS$GETJPI)
+-(SYS$GETMSG)
+-MARCH-+-INDEXA
+-LOCRZ
+-AVGFLOW--INDEXA
+-EOSG
+-UPDATEO
+-PVARS
+-SAMPLE--LOCRZ
+-OUTPUT-+-LOCRZ
+-INDEXA
+-TAPEWR

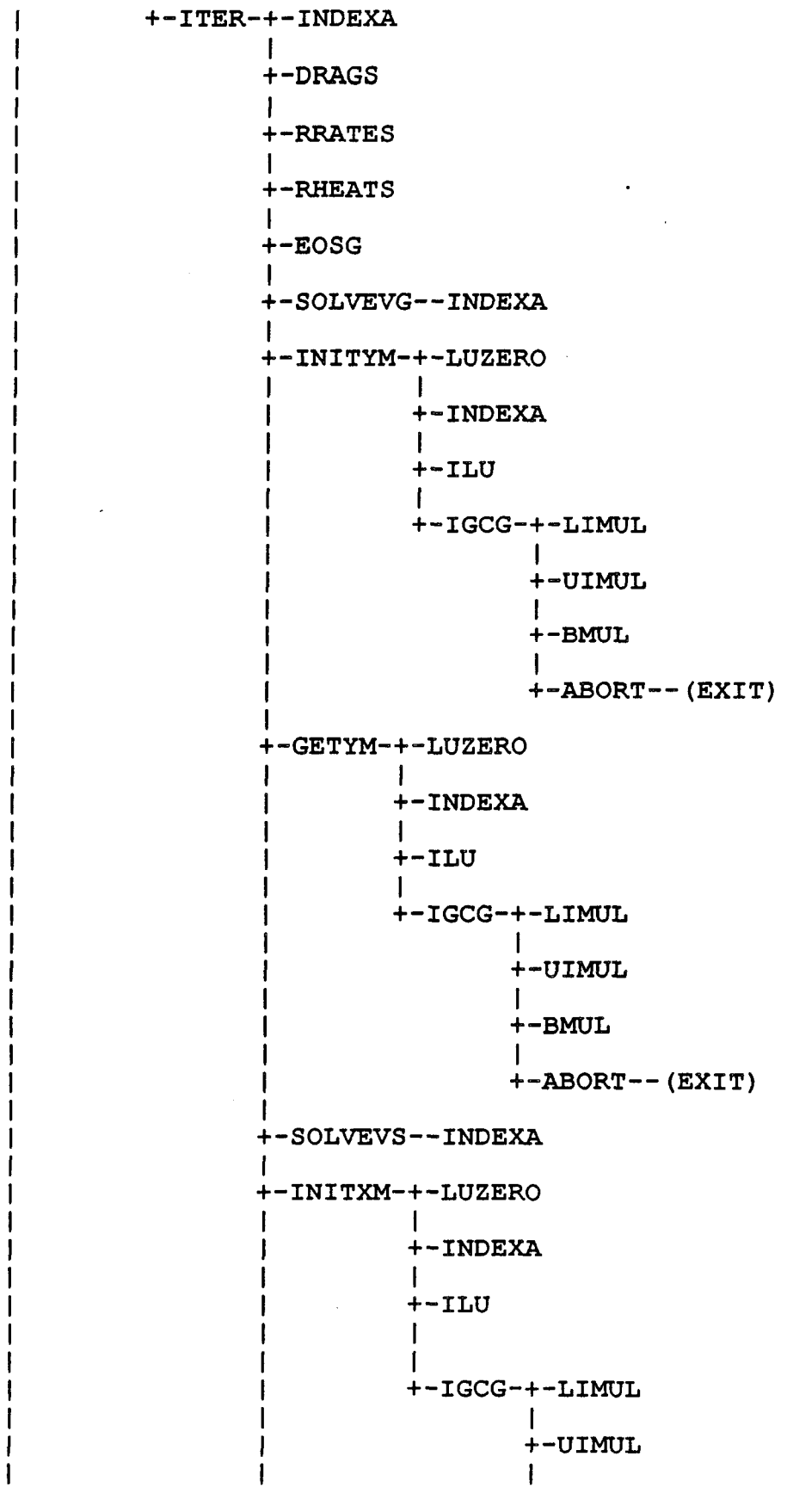
+-ITER-+-INDEXA
+-DRAGS
+-RRATES
+-RHEATS
+-EOSG
+-SOLVEVG--INDEXA
+-INITYM-+-LUZERO
+-INDEXA
+-ILU
+-IGCG-+-LIMUL
+-UIMUL
+-BMUL
+-ABORT--(EXIT)
+-GETYM-+-LUZERO
+-INDEXA
+-ILU
+-IGCG-+-LIMUL
+-UIMUL
+-BMUL
+-ABORT--(EXIT)
+-SOLVEVS--INDEXA
+-INITXM-+-LUZERO
+-INDEXA
+-ILU
+-IGCG-+-LIMUL
+-UIMUL

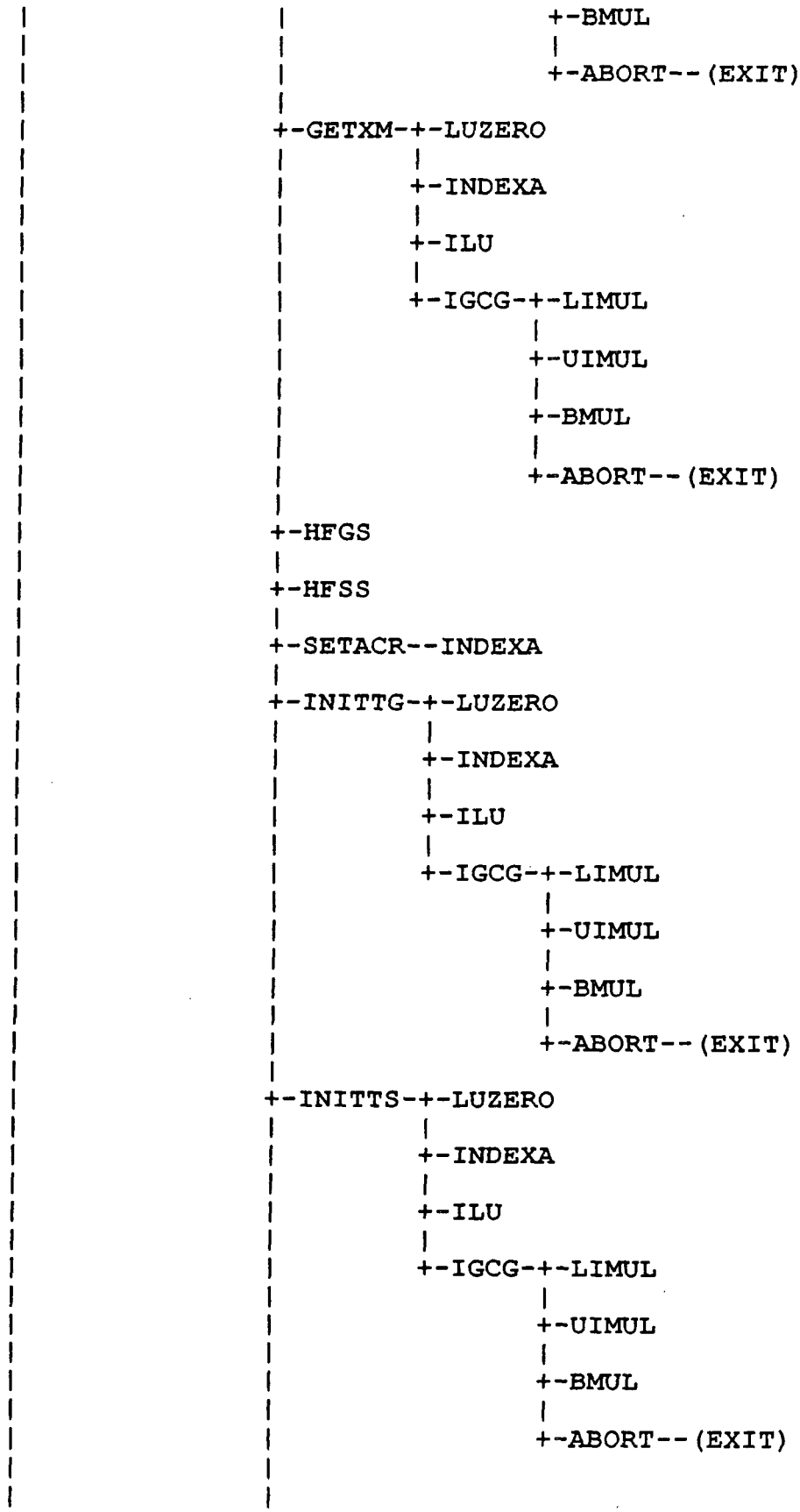
+-BMUL
+-ABORT--(EXIT)
+-GETXM-+-LUZERO
+-INDEXA
+-ILU
+-IGCG-+-LIMUL
+-UIMUL
+-BMUL
+-ABORT--(EXIT)
+-HFGS
+-HFSS
+-SETACR--INDEXA
+-INITTG-+-LUZERO
+-INDEXA
+-ILU
+-IGCG-+-LIMUL
+-UIMUL
+-BMUL
+-ABORT--(EXIT)
+-INITTS-+-LUZERO
+-INDEXA
+-ILU
+-IGCG-+-LIMUL
+-UIMUL
+-BMUL
+-ABORT--(EXIT)

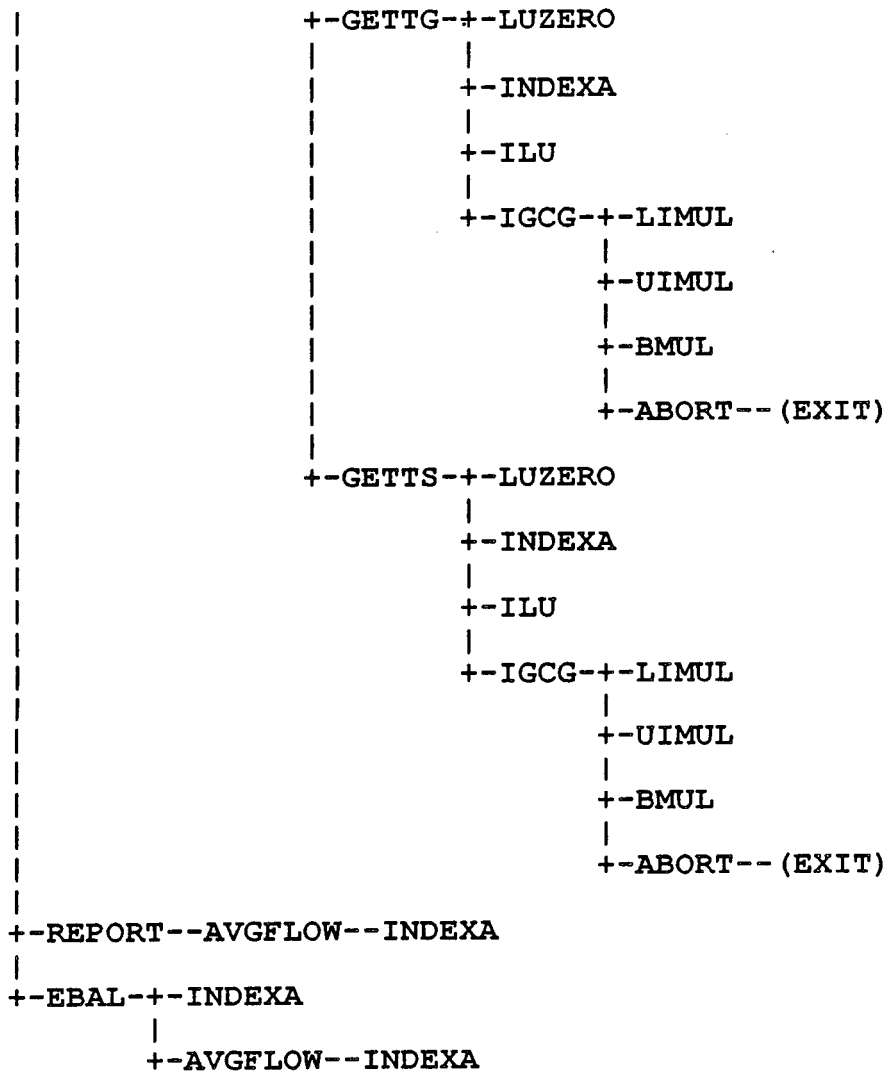
+-GETTG-+-LUZERO
+-INDEXA
+-ILU
+-IGCG-+-LIMUL
+-UIMUL
+-BMUL
+-ABORT--(EXIT)
+-GETTS-+-LUZERO
+-INDEXA
+-ILU
+-IGCG-+-LIMUL
+-UIMUL
+-BMUL
+-ABORT--(EXIT)
+-REPORT--AVGFLOW--INDEXA
+-EBAL-+-INDEXA
+-AVGFLOW--INDEXA

Appendix F: List of Variables

The following is a description of the FORTRAN variables used in the code. For a description of the variables in the input data file, refer to Appendix G.

Variable	Description
AEx	Activation energy of reaction "x".
AKx	Pre-exponential factor of reaction "x".
ALPHAC	Fraction of Fixed Carbon in the products of the cracking reaction -- α_c.
ALPHAD	Fraction of Tar in the products of the devolatilization reaction -- α_d.
BETAC	Fraction of gas species m in the products of the cracking reaction -- β^c_m.
BETAD	Fraction of gas species m in the products of the devolatilization reaction -- β^d_m.
CG	Average specific heat of gases -- C_{pg}.
COFLOW	Logical variable that is set true when the gas and solids are flowing in the same direction.
CS	The specific heat of solids -- C_{ps}.
CYCLE	The calculation cycle, i.e., the number of time steps.
DAFC	Density of dry, ash-free coal.
DEB_NIT	Logical variable that determines whether the convergence data is printed for every iteration.
DEB_SIDE	Logical variable that determines whether the printout includes values in the fictitious cells on the sides.
DR	Width of computational cells -- δr.
DRXNGC	Rate of consumption of gas species divided by the mass fraction of the gas species -- R^c_{gm}.
DRXNSC	Rate of consumption of solids species divided by the mass fraction of the solids species.

DT	Time step -- δt.
DTOBDR	$\delta t/(r_{i+\frac{1}{2}}\delta r)$.
DTODR	$\delta t/\delta r$.
DTODZ	$\delta t/\delta z$.
DTORDR	$\delta t/(r_i \delta r)$.
DZ	Height of computational cells -- δz.
EP	Void fraction -- ϵ.
EPA	Void fraction of the ash layer surrounding a burning char particle.
EPO	The void fraction at the previous time step.
FL	Cell flags: 1 => fluid cell, 2 => boundary or obstacle cell, 5 => inflow cell.
FLP	Flags the port number associated with an inflow or outflow cell: -1 => boundary or obstacle cell, 0 => fluid cell, # => port number.
FVC	Fraction of carbon in Volatile Matter -- f^V_C.
FVH	Fraction of hydrogen in Volatile Matter -- f^V_H.
FVN	Fraction of nitrogen in Volatile Matter -- f^V_N.
FVO	Fraction of oxygen in Volatile Matter -- f^V_O.
FVS	Fraction of sulfur in Volatile Matter -- f^V_S.
HEATC	Heat of cracking reaction.
HEATD	Heat of devolatilization reaction.
HFGR	Conductive heat flux through the gas in the radial (r) direction.
HFGZ	Conductive heat flux through the gas in the axial (z) direction.
HFSR	Conductive heat flux through the solids in the radial (r) direction.
HFSZ	Conductive heat flux through the solids in the axial (z) direction.

HGSG	Gas-solids heat transfer coefficient -- ($\gamma + \gamma_r \Sigma_m R_{gm}$)
HGSS	Solids-gas heat transfer coefficient -- ($\gamma + (\gamma_r - 1) \Sigma_m R_{gm}$)
HORG	Heat of gas phase reactions.
HORS	Heat of solids phase reactions.
HWALL	Bed-to-wall heat transfer coefficient.
I	Computational mesh column (r-direction) index -- i.
IB	Number of discretizations in the radial direction.
IB1	IB + 1.
IB2JB2	IB2 * JB2.
IB2	IB + 2.
IJ	Index of computational cell (i,j): IJ = I + (J-1)*IB2.
IJB	Index of cell centered quantities for the cell (i, j-1).
IJBR	Index of cell centered quantities for the cell (i+1, j-1).
IJL	Index of cell centered quantities for the cell (i-1, j).
IJM	Index of the cell (i, j-1).
IJP	Index of the cell (i, j+1).
IJR	Index of cell centered quantities for the cell (i+1, j).
IJRR	Index of cell centered quantities for the cell (i+2, j).
IJT	Index of cell centered quantities for the cell (i, j+1).
IJTL	Index of cell centered quantities for the cell (i-1, j+1).
IJTR	Index of cell centered quantities for the cell (i+1, j+1).

IJTT	Index of cell centered quantities for the cell (i, j+2).
IMJ	Index of cell (i-1, j).
IMJM	Index of cell (i-1, j-1).
IMJP	Index of cell (i-1, j+1).
INDS	An array for storing the IJ values of the neighboring cells.
IPJ	Index of cell (i+1, j).
IPJM	Index of cell (i+1, j-1).
IPJP	Index of cell (i+1, j+1).
J	Computational mesh row (z-direction) index -- j.
JB	Number of axial discretizations.
JB1	JB1 = JB + 1.
JB2	JB2 = JB + 2.
KAPG	Thermal conductivity of the gas -- k_g.
KAPS	Thermal conductivity of the solids -- k_s.
LARGENO	10^{32}.
MUG	Viscosity of the gas -- μ_g.
MWm	Molecular weight of the species "m"; e.g., H2O, H2, CO, C2H4, etc.
MWAVG	Average molecular weight of the gas.
NIT	Number of iterations.
NO	Number of obstacles.
P	Pressure.
R	Radial coordinate of the center of the cell (i, j) -- r_i.
RB	Radial coordinate of the right boundary of cell (i, j) -- $r_{i+1/2}$.
RDR	$1/\delta r$.

RDR2	$1/\delta r^2$.
RDZ	$1/\delta z$.
RDZ2	$1/\delta z^2$.
RGASP	Rate of net gas production from gas-solids reactions -- $\Sigma_m R_{gm}$.
RGP	Gas density * void fraction -- $\rho_g \epsilon$.
RGPO	Gas density * void fraction at the previous time step.
ROG	Gas density -- ρ_g.
RRB	$1/r_{i+1/2}$.
RRIDR	$1/r_i \delta r$.
RRXNGP	The rate of production of gas species -- R^p_{gm}.
RRXNSP	The rate of production of solids species.
RSP	Solids density * volume fraction -- $\rho_s(1-\epsilon)$.
RSPO	Solids density * volume fraction at the previous time step.
SMALLNO	10^{-15}.
SXG	$\xi_{i+\frac{1}{2},j}$, gas: 1 if UG > 0; 0 if UG < 0
SXS	$\xi_{i+\frac{1}{2},j}$, solids: 1 if US > 0; 0 if US < 0
SYG	$\xi_{i,j+\frac{1}{2}}$, gas: 1 if VG > 0; 0 if VG < 0
SYS	$\xi_{i,j+\frac{1}{2}}$, solids: 1 if VS > 0; 0 if VS < 0
TG	Gas temperature -- T_g.
TGO	Gas temperature at previous time step.
TS	Solids temperature -- T_s.
TSO	Solids temperature at previous time step.
UG	Radial component of the gas velocity -- u_g.

US	Radial component of the solids velocity -- u_s.
VG	Axial component of the gas velocity -- v_g.
VMSTAR	Maximum possible volatile matter density at a location -- $x^*(1-\epsilon)\rho_s$.
VS	Axial component of the solids velocity -- v_s.
WG3	Activity of the ash in catalyzing the water-gas shift reaction -- w_{g3}.
XM	Mass fraction of the solids species -- x_m.
XMO	Mass fraction of the solids species at the previous time step.
YM	Mass fraction of the gas species -- y_m.
YMO	Mass fraction of the gas species at the previous time step.

Appendix G: The Input File

The following is a description of the variables in the input data file:

Variable		Description
1) Run Control		
NAME		Run identification.
RUN	0	New run;
	1	Restart run - Only initial conditions from *.RES file. All other data from *.DAT file;
	2	Restart run - All data from *.RES file. The inputs from the *.DAT file are only RUN, TIME, and TSTOP.
		In a restart run, the record corresponding to TIME will be read from the file *.RES and used as the initial condition. If TIME is not specified, the last record will be read.
TIME		Starting time of the simulation.
TSTOP		Stopping time.
DT		Time step.
2) Output Control		
OUTFILE		Name of the standard output file.
RESFILE		Name of the restart file.
SAMFILE(N)		Name of the "N"th sample file (N < 6).
TOUT		Interval at which the standard output is written.
TRES		Interval at which restart file is written.
TSAM(N)		Interval at which the "N"th sample file is written.
IRES	0	Keep only the latest record in the restart file;
	1	Keep all the records in the restart file.

3) Physical and Numerical Data

COAL	This parameter determines the constants in the reaction rate expression based on the type of coal (1 - Pittsburgh No. 8, 2 - Arkwright/ Pittsburgh, 3 - Illinois No. 8, and 4 - Rosebud).
PAm	Proximate analysis: mass fraction of pseudo-species m (FC - fixed carbon, VM - volatile matter, M - moisture, and A - ash). Note that PAFC + PAVM + PAM + PAA = 1.
UAm	Ultimate analysis: mass fraction of element or pseudo-species m (C - carbon, H - hydrogen, O - oxygen, N - nitrogen, S - sulfur, M - moisture, and A - ash). Note that UAC + UAH + UAO + UAN + UAS + PAM + PAA = 1.
HHVC	Higher heating value of coal. This parameter and HHVT are used to compute the heats of devolatilization and cracking reactions. However, non-zero values of those heats of reactions may cause convergence problems. Those heats of reactions are set to zero if HHVC = 0.
DP	Diameter of the coal particles at the inlet.
ROS	Density of the coal particles at the inlet.
ROSMIN	Minimum possible density of the coal particles. If ROSMIN is equal to ROS, the density is held constant, and the solids axial velocity is varied.
FTm	Mass fraction of element m in the pseudo-species tar.
HHVT	Higher heating value of tar.
CHm	Fraction of hydrogen that appears in species m in the products of the cracking reaction.
COm	Fraction of oxygen that appears in species m in the products of the cracking reaction.
dHm	Fraction of hydrogen that appears in species m in the products of the devolatilization reaction.
dOm	Fraction of oxygen that appears in species m in the products of the devolatilization reaction.

GRAV		Gravitational acceleration.
GASCON		Universal gas constant.
C(N)		'Nth' user defined constant (N < 21).
TOLTG		Convergence tolerance for gas energy equation.
TOLTS		Convergence tolerance for solids energy equation.
TOLXM		Convergence tolerance for solids species equations.
TOLYM		Convergence tolerance for gas species equations.

4) Geometry and Discretization

RLEN		Reactor length.
RDIA		Reactor diameter.
CORD	0	Cartesian coordinate system;
	1	Axisymmetric cylindrical coordinate system.
OB(N,M)		Coordinates of the 'N'th obstacle: OB(N,1) Distance to the right of the obstacle; OB(N,2) Distance to the left of the obstacle; OB(N,3) Distance to the bottom of the obstacle; OB(N,4) Distance to the top of the obstacle. In two-dimensional simulations, obstacles may be specified to block off parts of the reactor.

5) Initial Conditions

BHEIGHT	Bed height. This is used to specify a partially filled reactor. The default is a full reactor.
HXZONE	Height of the ash layer at the bottom. This specifies a region at the bottom of the bed where all reaction rates are set to zero. It is often necessary to specify three or four numerical cells at the bottom of the bed as HXZONE to allow heat transfer between the incoming gas and the outgoing ash. The recommended value is the height of 2 or 3 numerical cells.

EPx — EPMIN and EPMAX are the minimum and the maximum void fractions. If both are given, a linear variation in the void fraction is specified in the bed with EPMAX at the top of the bed and EPMIN at the bottom of the bed. If only one is given, a uniform void fraction equal to that quantity is specified throughout the bed.

PI — Initial pressure. Also the pressure at the top of the bed.

TI — Initial bed temperature.

XMI — Mass fractions of various solids species initially in the bed. The default value is XMI(1) = $x_{FC02}/(1-x_{VM0})$.

YMI — Mass fractions of various gas species initially in the bed. The default value is YMI(7) = 1.0.

6) Boundary Conditions

Up to 99 ports may be specified for inflow and outflow boundary conditions. The parameter NPOR in PARAM.INC should be greater than or equal to the number of ports.

TWALL — Temperature of the wall.

HLFAC — Correction factor for the wall heat transfer coefficient. HLFAC should be equal to zero for adiabatic conditions.

HLOSS — If a value is specified for HLOSS the code will try to adjust the HLFAC so that the computed heat loss is equal to HLOSS. When this option is activated, the rate of convergence becomes poor.

RPORT(N,M) — R Coordinates of the "N"th inlet port: RPORT(N,1) - Distance to the right of the port; RPORT(N,2) - Distance to the left of the port. If both are equal or only one of them is given, then the inlet is assumed to be from the side. If both are not specified and ZPORT is specified then the port is assumed to be fully open radially.

ZPORT(N,M) — Z Coordinates of the "N"th inlet port: ZPORT(N,1) - Distance to the bottom of port; ZPORT(N,2) - Distance to the top of the port. If both are equal or only one of them is given, then the inlet is assumed to be from the top or the bottom.

FROMPORT(N)	Identifies the port as a recycle port with the flow coming from port number "FROMPORT".
EPORT(N)	Void fraction at the "N"th port.
PPORT(N)	Pressure at the "N"th port.
RECYCFR(N)	The fraction of the flow from "FROMPORT" recycled to port number "N".
FAIR(N)	Flow rate of air through the "N"th port. The mass fractions of the gas species in air are assumed to be O_2 - 0.233 and N_2 - 0.767.
TAIR(N)	Temperature of air.
FSTEAM(N)	Flow rate of steam through the "N"th port.
TSTEAM(N)	Temperature of steam.
FH2O(N)	Flow rate of steam through the "N"th port.
TH2O(N)	Temperature of steam.
FN2(N)	Flow rate of nitrogen through the "N"th port.
TN2(N)	Temperature of nitrogen.
FO2(N)	Flow rate of oxygen through the "N"th port.
TO2(N)	Temperature of oxygen.
FGMIX(N)	Flow rate of a gas mixture through the "N"th port. It is useful for specifying the inflow of special gas mixtures; for example, if one of the inlet streams is air mixed with CO_2. With a negative sign, it specifies an outflow from the port. It specifies the flow in a recycle stream when used in conjunction with FROMPORT.
TGMIX(N)	Temperature of the gas mixture.
YGMIX(N,M)	Mass fractions of the various gas species in the gas mixture.
FCOAL(N)	Flow rate of coal through the "N"th port.
TCOAL(N)	Temperature of coal.

The following is an alternate way of specifying boundary conditions at inlet ports, if flow rates and temperatures are not specified as above.

TPORT(N)	Temperature of gas and solids at the "N"th port.
VGPORT(N)	Gas velocity at the "N"th port.
VSPORT(N)	Solids velocity at the "N"th port.
XMPORT(N,M)	Mass fractions of the various solids species at the "N"th port.
YMPORT(N,M)	Mass fractions of various gas species at the "N"th port.

Appendix H: Sample Data Files

INPUT DATA FILE

The following is a data file for the simulation of METC gasification experiment R-106 Baseline. The LOG-file and OUTPUT-file are also given in this appendix. A comparison of the simulation results with METC experimental data is given in Appendix D.

```
 $DATA
     NAME = 'METC experiment R-106 Baseline'

     TSTOP = 18000.    RUN = 1
     OUTFILE = 'METC1.OUT'
     RESFILE = 'METC1.RES'

     COAL = 1    HHVC = 0.0
     PAFC  = 0.5162  PAVM = 0.372  PAM = 0.0364  PAA = 0.0754
     UAC = 0.7493  UAH = 0.048  UAO = 0.0555  UAN = 0.0142
     UAS = 0.0212
     DP(1) = 2.0

     RLEN = 200.66    RDIA = 106.68    HXZONE = 10.0

     PI = 1.47E7  EPMIN = 0.4      TI = 644.26

     TWALL = 355.0  HLFAC = 2.6306

     ZPORT(1,1) = 0.0
     FSTEAM(1) = 240.28     TSTEAM(1) = 667.59
     FAIR(1)    = 603.53     TAIR(1)    = 372.04

     ZPORT(2,1) = 200.66
     FCOAL(2) = 284.75  TCOAL(2) = 310.93

   $END
```

920765

LOG FILE

```
$ R/NODEBUG MGAS
TIME =  0.0000000E+00 OUTPUT TO METC1.OUT
TIME =  0.0000000E+00 OUTPUT TO METC1.RES
   Time  NIT y1 y2 y3 y4 y5 y6 y7 y8 y9 y0 y1 y2 y3 y4 x1 x2 x3 Tg Ts
     60. 184  0  0  0  0  0  0  0  0  0  0  0  0  0  0  0  1  0  0  0
    120. 154  0  0  0  0  0 39  0  0 39 39 39 39 39  0  0  0  0  0  0
    180. 154  0  0  0  0  0 39  0  0 39 39 39 39 39  0  0  0  0  0  0
    240. 146  0  0  0  0  0 39  0  0 39 39 39 39 39  0  0  0  0  0  0
    300. 143  0  0  0  0  0 39  0  0 39 39 39 39 39  0  0  0  0  0  0
    360. 125  0  0  0  0  0  6  0  0  6  6 39  6 39  6  0  0  0  0  0
    420. 122  0  0  0  0  0  3  0  0  3  8  3  2  3  6  0  0  0  0  0
    480. 109  0  0  0  0  0  2  0  0  2  6  3  4  3  4  0  1  0  0  0
    540. 112  0  0  0  0  0  2  0  0  2  6  3  3  3  3  0  0  1  0  0
    600. 103  0  0  0  0  0  0  0  0  0  0  0  0  0  0  0  1  0  0  0
    660.  89  0  0  1  0  0  1  0  0  1  1  1  1  1  1  0  0  1  0  0
    720. 103  0  0  0  0  0  0  0  0  0  0  0  0  0  0  0  0  0  0  0
    780. 101  0  0  1  0  0  1  0  0  1  1  1  1  1  0  0  0  1  0  0
    840. 104  0  0  0  0  0  0  0  0  0  0  0  0  0  0  0  0  1  0  0
    900. 111  0  0  0  0  0  1  0  0  1  1  1  0  1  0  0  0  1  0  0
    960. 112  0  0  0  0  0  1  0  0  1  1  1  0  1  2  0  0  2  0  0
   1020. 149  0  0  1  0  0  1  0  0  1  1  1  1  1  1  0  0  1  0  0
   1080. 185  0  0  1  0  0  1  0  0  1  1  1  1  1  1  0  0  1  0  0
   1140.  98  0  0  1  0  0  1  0  0  1  1  1  1  1  2  0  0  1  0  0
   1200. 141  0  0  0  0  0  1  0  0  1  1  1  0  1  1  0  0  1  0  0
   1260.  80  0  0  1  0  0  1  0  0  1  1  1  1  1  2  0  0  1  0  0
   Time  NIT y1 y2 y3 y4 y5 y6 y7 y8 y9 y0 y1 y2 y3 y4 x1 x2 x3 Tg Ts
   1320.  84  0  0  1  0  0  0  0  0  0  0  0  1  0  1  0  0  1  0  0
   1380. 103  0  0  1  0  0  1  0  0  1  1  1  1  1  1  0  0  0  0  0
   1440.  69  0  0  2  0  0  2  0  0  2  2  2  2  2  1  0  0  1  0  0
   1500.  90  0  0  1  0  0  2  0  0  2  2  2  2  2  2  0  0  2  0  0
   1560.  98  0  0  1  0  0  1  0  0  1  2  2  1  2  2  0  0  2  0  0
   1620.  77  0  0  1  0  0  1  0  0  1  1  1  1  1  1  0  0  2  0  0
   1680. 122  0  0  1  0  0  2  0  0  2  2  2  1  2  1  0  0  1  0  0
   1740.  86  0  0  1  0  0  1  0  0  1  1  0  1  0  2  0  0  1  0  0
   1800.  76  0  0  1  0  0  2  0  0  2  2  2  1  2  2  0  0  2  0  0
   1860.  74  0  0  1  0  0  2  0  0  2  2  2  1  2  2  0  0  1  0  0
   1920.  74  0  0  1  0  0  1  0  0  1  1  1  1  1  2  0  0  1  0  0
   1980.  85  0  0  1  0  0  1  0  0  1  1  1  1  1  1  0  0  2  0  0
   2040.  73  0  0  1  0  0  1  0  0  1  1  1  1  1  2  0  0  0  0  0
   2100.  83  0  0  2  0  0  2  0  0  2  2  2  2  2  1  0  0  2  0  0
   2160.  89  0  0  2  0  0  2  0  0  2  2  2  2  2  2  0  0  2  0  0
   2220. 101  0  0  1  0  0  2  0  0  2  2  2  1  2  2  0  0  1  0  0
   2280.  65  0  0  1  0  0  1  0  0  1  1  1  1  1  2  0  0  1  0  0
   2340.  85  0  0  1  0  0  2  0  0  2  2  2  1  2  2  0  0  2  0  0
   2400.  59  0  0  0  0  0  1  0  0  1  2  1  1  1  2  0  0  1  0  0
   2460.  59  0  0  1  0  0  1  0  0  1  2  1  1  1  1  0  0  1  0  0
   2520.  66  0  0  1  0  0  1  0  0  1  1  1  1  1  2  0  0  1  0  0
   Time  NIT y1 y2 y3 y4 y5 y6 y7 y8 y9 y0 y1 y2 y3 y4 x1 x2 x3 Tg Ts
   2580.  59  0  0  1  0  0  1  0  0  1  1  1  1  1  1  0  0  0  0  0
   2640.  57  0  0  1  0  0  1  0  0  1  1  1  1  1  1  0  0  0  0  0
   2700.  64  0  0  1  0  0  1  0  0  1  1  1  1  1  1  0  0  0  0  0
   2760.  50  0  0  2  0  0  2  0  0  2  3  2  2  2  2  0  0  2  0  0
   2820.  69  0  0  1  0  0  1  0  0  1  2  1  1  1  1  0  0  0  0  0
```

2880.	56	0	0	1	0	0	1	0	0	1	1	1	1	1	1	0	0	0	0	0
2940.	58	0	0	0	0	0	2	0	0	2	2	2	0	2	2	0	0	1	0	0
3000.	58	0	0	2	0	0	2	0	0	2	2	2	2	2	0	0	0	2	0	0
3060.	50	0	0	1	0	0	1	0	0	1	2	1	1	1	1	0	0	0	0	0
3120.	54	0	0	1	0	0	1	0	0	1	1	1	1	1	1	0	0	1	0	0
3180.	43	0	0	1	0	0	1	0	0	1	2	1	1	1	1	0	0	1	0	0
3240.	50	0	0	0	0	0	2	0	0	1	2	2	0	2	2	0	0	1	0	0
3300.	48	0	0	1	0	0	1	0	0	1	1	1	1	1	2	0	0	1	0	0
3360.	50	0	0	2	0	0	2	0	0	2	2	2	2	2	2	0	0	2	0	0
3420.	46	0	0	2	0	0	2	0	0	2	2	2	2	2	2	0	0	1	0	0
3480.	57	0	0	2	0	0	2	0	0	2	2	2	2	2	2	0	0	2	0	0
3540.	75	0	0	1	0	0	2	0	0	2	2	2	2	2	1	0	0	2	0	0
3600.	64	0	0	1	0	0	1	0	0	1	1	0	1	1	2	0	0	2	0	0

TIME = 3600.000 OUTPUT TO METC1.OUT

TIME = 3600.000 OUTPUT TO METC1.RES

3660.	47	0	0	1	0	0	2	0	0	2	3	2	1	2	2	0	0	2	0	0
3720.	63	0	0	1	0	0	2	0	0	2	2	2	1	2	2	0	0	1	0	0
3780.	40	0	0	1	0	0	1	0	0	1	2	2	1	2	1	0	0	1	0	0
Time	NIT	y1	y2	y3	y4	y5	y6	y7	y8	y9	y0	y1	y2	y3	y4	x1	x2	x3	Tg	Ts
3840.	51	0	0	2	0	0	2	0	0	2	2	2	2	2	2	0	0	1	0	0
3900.	47	0	0	1	0	0	1	0	0	1	0	1	1	1	1	0	0	1	0	0
3960.	50	0	0	1	0	0	2	0	0	2	2	2	1	2	1	0	0	1	0	0
4020.	61	0	0	1	0	0	2	0	0	2	2	2	1	2	2	0	0	0	0	0
4080.	53	0	0	0	0	0	2	0	0	2	2	2	0	2	2	0	0	1	0	0
4140.	68	0	0	1	0	0	2	0	0	2	2	2	1	2	2	0	0	2	0	0
4200.	118	0	0	1	0	0	1	0	0	1	1	1	1	1	1	0	0	1	0	0
4260.	45	0	0	2	0	0	1	0	0	1	2	2	2	2	2	0	0	1	0	0
4320.	80	0	0	1	0	0	1	0	0	1	2	1	1	1	2	0	0	0	0	0
4380.	53	0	0	1	0	0	2	0	0	2	2	2	1	2	2	0	0	2	0	0
4440.	59	0	0	1	0	0	2	0	0	2	2	2	2	2	1	0	0	2	0	0
4500.	50	0	0	2	0	0	2	0	0	2	2	2	2	2	2	0	0	2	0	0
4560.	57	0	0	2	0	0	2	0	0	2	2	2	2	2	2	0	0	2	0	0
4620.	66	0	0	1	0	0	1	0	0	1	1	0	1	0	2	0	0	2	0	0
4680.	72	0	0	1	0	0	1	0	0	1	1	1	1	1	1	0	0	2	0	0
4740.	53	0	0	1	0	0	1	0	0	1	1	1	1	1	0	0	0	1	0	0
4800.	86	0	0	1	0	0	2	0	0	2	2	2	2	2	1	0	0	2	0	0
4860.	49	0	0	0	0	0	1	0	0	1	1	1	0	1	1	0	0	1	0	0
4920.	51	0	0	1	0	0	1	0	0	1	2	1	1	1	1	0	0	0	0	0
4980.	51	0	0	1	0	0	1	0	0	1	2	1	1	1	2	0	0	1	0	0
5040.	50	0	0	1	0	0	0	0	0	0	1	0	1	0	1	0	0	1	0	0
Time	NIT	y1	y2	y3	y4	y5	y6	y7	y8	y9	y0	y1	y2	y3	y4	x1	x2	x3	Tg	Ts
5100.	50	0	0	1	0	0	1	0	0	1	2	1	2	1	2	0	0	2	0	0
5160.	55	0	0	1	0	0	2	0	0	2	2	2	1	2	2	0	0	1	0	0
5220.	50	0	0	1	0	0	1	0	0	1	1	1	1	1	1	0	0	1	0	0
5280.	51	0	0	0	0	0	1	0	0	1	1	1	0	1	1	0	0	1	0	0
5340.	50	0	0	1	0	0	2	0	0	2	2	2	2	2	1	0	0	0	0	0
5400.	46	0	0	1	0	0	0	0	0	0	1	1	1	1	2	0	0	1	0	0
5460.	51	0	0	1	0	0	0	0	0	0	1	1	1	1	2	0	0	1	0	0
5520.	52	0	0	1	0	0	1	0	0	1	1	1	1	1	0	0	0	1	0	0
5580.	50	0	0	1	0	0	2	0	0	2	2	2	1	2	1	0	0	1	0	0
5640.	65	0	0	1	0	0	1	0	0	0	1	1	1	1	1	0	0	2	0	0
5700.	77	0	0	1	0	0	2	0	0	2	2	2	1	2	2	0	0	2	0	0
5760.	49	0	0	1	0	0	1	0	0	1	1	1	1	1	2	0	0	2	0	0

5820.	58	0	0	1	0	0	2	0	0	2	2	2	1	2	2	0	0	2	0	0
5880.	52	0	0	1	0	0	1	0	0	1	1	1	2	1	2	0	0	1	0	0
5940.	42	0	0	1	0	0	1	0	0	1	1	1	1	1	2	0	0	1	0	0
6000.	45	0	0	2	0	0	2	0	0	2	2	2	2	2	2	0	0	2	0	0
6060.	45	0	0	1	0	0	2	0	0	2	2	2	1	2	2	0	0	1	0	0
6120.	43	0	0	1	0	0	1	0	0	1	2	1	1	1	1	0	0	2	0	0
6180.	78	0	0	1	0	0	2	0	0	2	2	2	1	2	2	0	0	2	0	0
6240.	34	0	0	1	0	0	1	0	0	1	1	1	1	1	1	0	0	1	0	0
6300.	54	0	0	2	0	0	2	0	0	2	1	1	2	1	2	0	0	2	0	0
Time	NIT	y1	y2	y3	y4	y5	y6	y7	y8	y9	y0	y1	y2	y3	y4	x1	x2	x3	Tg	Ts
6360.	47	0	0	1	0	0	2	0	0	2	2	2	1	2	2	0	0	1	0	0
6420.	44	0	0	2	0	0	2	0	0	2	2	2	2	2	1	0	0	2	0	0
6480.	45	0	0	1	0	0	0	0	0	0	0	0	1	0	1	0	0	1	0	0
6540.	40	0	0	1	0	0	1	0	0	1	2	2	1	2	2	0	0	2	0	0
6600.	43	0	0	1	0	0	1	0	0	1	1	1	1	1	1	0	0	0	0	0
6660.	49	0	0	0	0	0	1	0	0	1	1	1	1	1	1	0	0	0	0	0
6720.	45	0	0	1	0	0	1	0	0	1	1	1	1	1	1	0	0	1	0	0
6780.	47	0	0	1	0	0	1	0	0	1	1	1	1	1	2	0	0	0	0	0
6840.	34	0	0	1	0	0	1	0	0	1	1	1	1	1	2	0	0	1	0	0
6900.	50	0	0	1	0	0	1	0	0	1	1	1	1	1	2	0	0	1	0	0
6960.	49	0	0	1	0	0	1	0	0	1	1	1	1	1	2	0	0	0	0	0
7020.	40	0	0	1	0	0	0	0	0	0	1	1	1	1	1	0	0	1	0	0
7080.	36	0	0	1	0	0	1	0	0	1	1	1	1	1	1	0	0	1	0	0
7140.	48	0	0	1	0	0	1	0	0	1	2	1	2	1	2	0	0	1	0	0
7200.	36	0	0	0	0	0	1	0	0	1	2	2	0	2	2	0	0	0	0	0

TIME = 7200.000 OUTPUT TO METC1.OUT

TIME = 7200.000 OUTPUT TO METC1.RES

7260.	36	0	0	0	0	0	0	0	0	0	1	0	0	0	0	0	0	1	0	0
7320.	35	0	0	1	0	0	1	0	0	1	1	1	1	1	1	0	0	1	0	0
7380.	30	0	0	1	0	0	0	0	0	0	1	1	1	1	2	0	0	1	0	0
7440.	38	0	0	2	0	0	2	0	0	2	2	2	2	2	2	0	0	1	0	0
7500.	36	0	0	0	0	0	1	0	0	1	1	1	1	1	1	0	0	1	0	0
7560.	30	0	0	0	0	0	1	0	0	1	1	1	0	1	1	0	0	0	0	0
Time	NIT	y1	y2	y3	y4	y5	y6	y7	y8	y9	y0	y1	y2	y3	y4	x1	x2	x3	Tg	Ts
7620.	35	0	0	1	0	0	1	0	0	1	2	1	1	1	2	0	0	1	0	0
7680.	38	0	0	2	0	0	1	0	0	1	0	0	2	0	2	0	0	1	0	0
7740.	31	0	0	1	0	0	2	0	0	2	2	2	1	2	1	0	0	1	0	0
7800.	34	0	0	1	0	0	1	0	0	1	1	0	1	0	2	0	0	0	0	0
7860.	29	0	0	1	0	0	2	0	0	2	2	2	1	2	2	0	0	0	0	0
7920.	35	0	0	1	0	0	1	0	0	1	2	1	1	1	1	0	0	1	0	0
7980.	28	0	0	1	0	0	1	0	0	1	2	1	1	1	1	0	0	1	0	0
8040.	24	0	0	1	0	0	1	0	0	1	1	1	1	1	2	0	0	1	0	0
8100.	24	0	0	1	0	0	1	0	0	0	1	1	1	1	2	0	0	1	0	0
8160.	24	0	0	0	0	0	0	0	0	0	1	0	1	0	1	0	0	1	0	0
8220.	30	0	0	0	0	0	1	0	0	1	1	1	0	1	1	0	0	0	0	0
8280.	30	0	0	1	0	0	0	0	0	0	1	0	1	0	1	0	0	0	0	0
8340.	26	0	0	0	0	0	1	0	0	1	2	1	1	1	2	0	0	1	0	0
8400.	30	0	0	1	0	0	0	0	0	0	1	1	1	1	2	0	0	0	0	0
8460.	22	0	0	1	0	0	1	0	0	1	1	1	1	1	1	0	0	0	0	0
8520.	22	0	0	1	0	0	1	0	0	1	1	0	1	0	2	0	0	0	0	0
8580.	30	0	0	1	0	0	1	0	0	1	1	1	1	1	2	0	0	0	0	0
8640.	22	0	0	1	0	0	2	0	0	2	2	2	2	2	2	0	0	1	0	0
8700.	26	0	0	1	0	0	1	0	0	1	1	1	1	1	1	0	0	0	0	0

```
   8760.   37  0  0  1  0  0  2  0  0  2  2  2  1  2  1  0  0  1  0  0
   8820.   24  0  0  1  0  0  1  0  0  1  1  1  2  1  2  0  0  0  0  0
    Time  NIT y1 y2 y3 y4 y5 y6 y7 y8 y9 y0 y1 y2 y3 y4 x1 x2 x3 Tg Ts
   8880.   23  0  0  1  0  0  1  0  0  1  1  1  1  1  1  0  0  0  0  0
   8940.   21  0  0  1  0  0  1  0  0  1  1  1  1  1  0  0  0  0  0  0
   9000.   22  0  0  1  0  0  0  0  0  1  0  0  1  0  1  0  0  1  0  0
   9060.   21  0  0  0  0  0  0  0  0  0  1  0  0  0  0  0  0  1  0  0
   9120.   19  0  0  1  0  0  1  0  0  1  2  1  1  1  2  0  0  1  0  0
   9180.   23  0  0  1  0  0  0  0  0  0  1  0  1  0  2  0  0  0  0  0
   9240.   22  0  0  0  0  0  1  0  0  1  2  1  0  1  2  0  0  0  0  0
   9300.   16  0  0  1  0  0  1  0  0  1  2  1  1  1  1  0  0  0  0  0
   9360.   18  0  0  1  0  0  1  0  0  1  2  1  1  1  1  0  0  1  0  0
   9420.   14  0  0  1  0  0  0  0  0  0  0  0  1  0  1  0  0  1  0  0
   9480.   17  0  0  1  0  0  1  0  0  1  1  1  1  1  0  0  0  0  0  0
   9540.   17  0  0  1  0  0  1  0  0  1  1  1  1  1  1  0  0  1  0  0
   9600.   15  0  0  1  0  0  1  0  0  1  1  1  1  1  2  0  0  1  0  0
   9660.   14  0  0  2  0  0  1  0  0  1  1  1  2  1  2  0  0  1  0  0
   9720.   13  0  0  1  0  0  1  0  0  1  1  1  1  1  2  0  0  1  0  0
   9780.   19  0  0  0  0  0  1  0  0  1  1  1  0  1  1  0  0  0  0  0
   9840.   15  0  0  1  0  0  1  0  0  1  1  1  1  1  2  0  0  0  0  0
   9900.   11  0  0  0  0  0  0  0  0  0  1  1  0  0  1  0  0  0  0  0
   9960.   10  0  0  1  0  0  1  0  0  1  1  1  1  1  2  0  0  0  0  0
  10020.    4  0  0  1  0  0  0  0  0  0  1  1  1  1  2  0  0  1  0  0
  10080.    1  0  0  2  0  0  2  0  0  2  3  2  2  2  1  0  1  0  0  0
   Time  NIT y1 y2 y3 y4 y5 y6 y7 y8 y9 y0 y1 y2 y3 y4 x1 x2 x3 Tg Ts
  10140.    4  0  0  1  0  0  2  0  0  2  2  2  1  2  2  0  0  1  0  0
  10200.    3  0  0  2  0  0  2  0  0  2  2  2  2  2  3  0  0  1  0  0
  10260.    1  0  0  2  0  0  2  0  0  2  3  2  2  2  2  1  0  1  0  0
  10320.    1  0  0  2  0  0  2  0  0  2  1  1  2  1  3  0  1  1  0  0
  10380.    1  0  0  1  0  0  2  0  0  2  2  2  0  2  2  0  1  2  0  0
  10440.    1  0  0  1  0  0  1  0  0  1  2  1  1  1  1  0  1  1  0  0
  10500.    1  0  0  2  0  0  2  0  0  2  2  2  2  2  2  0  1  1  0  0
  10560.    1  0  0  1  0  0  1  0  0  1  2  2  2  2  2  0  1  1  0  0
  10620.    2  0  0  2  0  0  2  0  0  2  3  2  2  2  2  0  0  0  0  0
  10680.    1  0  0  2  0  0  2  0  0  2  2  2  2  2  2  1  1  0  0  0
  10740.    1  0  0  2  0  0  0  0  0  1  2  1  2  1  2  0  0  1  0  0
  10800.    2  0  0  2  0  0  2  0  0  2  3  2  2  2  2  0  0  1  0  0
TIME =   10800.00        OUTPUT TO METC1.OUT
TIME =   10800.00        OUTPUT TO METC1.RES
  10860.    1  0  0  2  0  0  2  0  0  2  2  2  2  2  3  1  0  1  0  0
  10920.    9  0  0  1  0  0  1  0  0  1  2  1  1  1  2  0  0  0  0  0
  10980.    1  0  0  2  0  0  2  0  0  2  3  2  2  2  2  1  1  1  0  0
  11040.    1  0  0  2  0  0  2  0  0  2  2  2  2  2  3  0  1  0  0  0
  11100.   14  0  0  1  0  0  0  0  0  0  1  0  1  0  1  0  0  1  0  0
  11160.    3  0  0  2  0  0  2  0  0  2  2  2  3  2  3  0  0  2  0  0
  11220.    1  0  0  1  0  0  2  0  0  2  2  2  1  2  2  1  0  1  0  0
  11280.   12  0  0  1  0  0  1  0  0  1  2  2  1  2  2  0  0  0  0  0
  11340.    4  0  0  0  0  0  1  0  0  1  2  1  1  1  2  0  0  1  0  0
   Time  NIT y1 y2 y3 y4 y5 y6 y7 y8 y9 y0 y1 y2 y3 y4 x1 x2 x3 Tg Ts
  11400.    4  0  0  0  0  0  1  0  0  1  1  1  1  1  2  0  0  1  0  0
  11460.    1  0  0  2  0  0  2  0  0  2  3  2  2  2  1  0  1  0  0  0
  11520.    9  0  0  2  0  0  1  0  0  1  2  1  2  1  2  0  0  1  0  0
  11580.    3  0  0  3  0  0  2  0  0  2  1  1  3  1  3  0  0  1  0  0
```

11640.	2	0	0	2	0	0	2	0	0	2	3	2	2	2	3	0	0	1	0	0
11700.	5	0	0	0	0	0	1	0	0	1	2	1	0	1	2	0	0	0	0	0
11760.	1	0	0	2	1	0	3	0	0	3	3	3	2	3	1	0	1	0	0	0
11820.	9	0	0	1	0	0	1	0	0	1	1	1	1	1	1	0	0	0	0	0
11880.	2	0	0	2	0	0	2	0	0	2	2	2	2	2	3	0	0	1	0	0
11940.	1	0	0	2	0	0	1	0	0	1	1	1	2	1	2	0	0	0	0	0
12000.	1	0	0	2	0	0	2	0	0	2	2	2	2	2	2	0	1	0	0	0
12060.	2	0	0	2	0	0	2	0	0	2	2	2	2	2	2	0	0	1	0	0
12120.	2	0	0	2	0	0	2	0	0	2	2	2	2	2	2	0	0	1	0	0
12180.	1	0	0	2	0	0	1	0	0	0	1	1	2	1	2	0	0	0	0	0
12240.	4	0	0	1	0	0	0	0	0	1	0	0	1	0	2	0	0	1	0	0
12300.	1	0	0	2	0	0	2	0	0	2	2	2	2	2	1	0	0	0	0	0
12360.	1	0	0	2	0	0	2	0	0	2	2	2	2	2	2	0	0	0	0	0
12420.	1	0	0	2	0	0	2	0	0	2	2	2	2	2	2	0	0	0	0	0
12480.	1	0	0	2	0	0	1	0	0	1	2	1	2	1	2	0	0	1	0	0
12540.	1	0	0	1	0	0	2	0	0	2	2	2	1	2	1	0	0	1	0	0
12600.	1	0	0	1	0	0	2	0	0	2	2	2	1	2	2	0	0	0	0	0
Time	NIT	y1	y2	y3	y4	y5	y6	y7	y8	y9	y0	y1	y2	y3	y4	x1	x2	x3	Tg	Ts
12660.	1	0	0	2	0	0	1	0	0	1	1	1	2	1	2	0	0	1	0	0
12720.	1	0	0	1	0	0	0	0	0	0	1	1	1	1	2	0	0	1	0	0
12780.	1	0	0	1	0	0	1	0	0	1	2	1	1	1	2	0	0	0	0	0
12840.	1	0	0	1	0	0	1	0	0	1	2	2	1	2	2	0	0	1	0	0
12900.	1	0	0	2	0	0	2	0	0	2	2	2	2	2	2	0	0	0	0	0
12960.	1	0	0	2	0	0	2	0	0	2	2	1	2	1	2	0	0	1	0	0
13020.	1	0	0	2	0	0	2	0	0	2	2	2	2	2	1	0	0	1	0	0
13080.	1	0	0	2	0	0	2	0	0	2	2	2	2	2	2	0	0	0	0	0
13140.	1	0	0	2	0	0	2	0	0	2	2	2	2	2	2	0	0	1	0	0
13200.	1	0	0	0	0	0	1	0	0	1	2	1	0	1	1	0	0	1	0	0
13260.	1	0	0	2	0	0	2	0	0	2	2	2	2	2	2	0	0	1	0	0
13320.	1	0	0	2	0	0	2	0	0	2	2	2	2	2	2	0	0	1	0	0
13380.	1	0	0	2	0	0	2	0	0	2	2	2	2	2	2	0	0	1	0	0
13440.	1	0	0	2	0	0	1	0	0	1	1	1	2	1	2	0	0	1	0	0
13500.	1	0	0	1	0	0	2	0	0	2	2	2	1	2	1	0	0	0	0	0
13560.	1	0	0	1	0	0	2	0	0	2	2	2	1	2	2	0	0	1	0	0
13620.	1	0	0	1	0	0	2	0	0	2	2	2	1	2	2	0	0	0	0	0
13680.	1	0	0	1	0	0	1	0	0	1	2	2	2	2	2	0	0	1	0	0
13740.	1	0	0	1	0	0	2	0	0	2	2	2	1	2	2	0	0	1	0	0
13800.	1	0	0	1	0	0	2	0	0	2	2	2	1	2	2	0	0	1	0	0
13860.	1	0	0	1	0	0	2	0	0	2	2	2	1	2	2	0	0	1	0	0
Time	NIT	y1	y2	y3	y4	y5	y6	y7	y8	y9	y0	y1	y2	y3	y4	x1	x2	x3	Tg	Ts
13920.	1	0	0	2	0	0	1	0	0	1	2	1	2	1	2	0	0	1	0	0
13980.	1	0	0	2	0	0	2	0	0	2	2	2	2	2	2	0	0	1	0	0
14040.	1	0	0	2	0	0	1	0	0	1	1	0	2	0	2	0	0	1	0	0
14100.	1	0	0	2	0	0	2	0	0	2	2	2	2	2	2	0	0	1	0	0
14160.	1	0	0	2	0	0	1	0	0	0	1	1	2	1	2	0	0	0	0	0
14220.	1	0	0	2	0	0	2	0	0	2	2	2	2	2	2	0	0	1	0	0
14280.	1	0	0	2	0	0	1	0	0	1	2	2	2	2	2	0	0	1	0	0
14340.	1	0	0	0	0	0	2	0	0	2	2	2	1	2	2	0	0	0	0	0
14400.	1	0	0	1	0	0	2	0	0	2	2	2	1	2	2	0	0	1	0	0

TIME = 14400.00 OUTPUT TO METC1.OUT

TIME = 14400.00 OUTPUT TO METC1.RES

14460.	1	0	0	2	0	0	1	0	0	0	2	1	2	1	2	0	0	1	0	0
14520.	1	0	0	2	0	0	2	0	0	2	2	2	2	2	2	0	0	1	0	0

14580.	1	0	0	1	0	0	2	0	0	1	2	2	2	2	2	0	0	1	0	0
14640.	1	0	0	2	0	0	0	0	0	0	1	1	2	1	2	0	0	0	0	0
14700.	1	0	0	1	0	0	1	0	0	1	2	1	2	1	2	0	0	0	0	0
14760.	1	0	0	2	0	0	1	0	0	0	1	1	2	1	2	0	0	0	0	0
14820.	1	0	0	1	0	0	0	0	0	1	1	1	2	1	2	0	0	1	0	0
14880.	1	0	0	1	0	0	2	0	0	2	2	2	1	2	1	0	0	1	0	0
14940.	1	0	0	2	0	0	2	0	0	2	2	2	2	2	2	0	0	0	0	0
15000.	1	0	0	0	0	0	2	0	0	2	2	2	1	2	2	0	0	1	0	0
15060.	1	0	0	2	0	0	2	0	0	2	2	2	2	2	2	0	0	1	0	0
15120.	1	0	0	2	0	0	1	0	0	1	2	1	2	1	2	0	0	1	0	0
Time	NIT	y1	y2	y3	y4	y5	y6	y7	y8	y9	y0	y1	y2	y3	y4	x1	x2	x3	Tg	Ts
15180.	1	0	0	0	0	0	1	0	0	1	1	1	0	1	1	0	0	1	0	0
15240.	1	0	0	2	0	0	2	0	0	2	2	2	2	2	1	0	0	1	0	0
15300.	1	0	0	2	0	0	2	0	0	2	2	1	2	1	2	0	0	0	0	0
15360.	1	0	0	1	0	0	2	0	0	2	2	2	2	2	1	0	0	1	0	0
15420.	1	0	0	2	0	0	0	0	0	1	1	1	2	1	2	0	0	1	0	0
15480.	1	0	0	1	0	0	0	0	0	0	1	1	1	1	2	0	0	1	0	0
15540.	1	0	0	1	0	0	1	0	0	1	2	1	1	1	0	0	0	0	0	0
15600.	1	0	0	1	0	0	2	0	0	2	2	2	1	2	2	0	0	1	0	0
15660.	1	0	0	2	0	0	1	0	0	2	1	1	2	1	2	0	0	1	0	0
15720.	1	0	0	1	0	0	2	0	0	1	2	2	1	2	1	0	0	1	0	0
15780.	1	0	0	1	0	0	2	0	0	2	2	2	1	2	2	0	0	1	0	0
15840.	1	0	0	2	0	0	2	0	0	2	2	1	2	1	2	0	0	1	0	0
15900.	1	0	0	1	0	0	2	0	0	2	2	2	1	2	1	0	0	1	0	0
15960.	1	0	0	1	0	0	1	0	0	1	1	1	1	1	2	0	0	0	0	0
16020.	1	0	0	1	0	0	1	0	0	0	1	1	1	1	2	0	0	1	0	0
16080.	1	0	0	2	0	0	2	0	0	2	2	2	2	2	2	0	0	0	0	0
16140.	1	0	0	1	0	0	2	0	0	2	2	2	0	2	2	0	0	0	0	0
16200.	1	0	0	1	0	0	2	0	0	2	2	2	1	2	2	0	0	1	0	0
16260.	1	0	0	2	0	0	2	0	0	2	2	2	2	2	2	0	0	0	0	0
16320.	1	0	0	2	0	0	2	0	0	2	2	2	2	2	2	0	0	1	0	0
16380.	1	0	0	2	0	0	1	0	0	1	0	1	2	1	2	0	0	1	0	0
Time	NIT	y1	y2	y3	y4	y5	y6	y7	y8	y9	y0	y1	y2	y3	y4	x1	x2	x3	Tg	Ts
16440.	1	0	0	1	0	0	2	0	0	2	2	2	1	2	2	0	0	0	0	0
16500.	1	0	0	1	0	0	2	0	0	2	2	2	2	2	2	0	0	1	0	0
16560.	1	0	0	2	0	0	1	0	0	1	1	1	2	1	2	0	0	0	0	0
16620.	1	0	0	1	0	0	1	0	0	1	2	1	2	1	2	0	0	0	0	0
16680.	1	0	0	1	0	0	1	0	0	1	1	1	2	1	2	0	0	0	0	0
16740.	1	0	0	1	0	0	2	0	0	2	2	2	1	2	1	0	0	1	0	0
16800.	1	0	0	1	0	0	2	0	0	2	2	2	2	2	2	0	0	1	0	0
16860.	1	0	0	2	0	0	1	0	0	1	2	2	2	2	2	0	0	1	0	0
16920.	1	0	0	1	0	0	1	0	0	1	1	0	1	1	2	0	0	1	0	0
16980.	1	0	0	2	0	0	2	0	0	2	2	2	2	2	2	0	0	1	0	0
17040.	1	0	0	1	0	0	2	0	0	2	2	2	1	2	2	0	0	0	0	0
17100.	1	0	0	2	0	0	2	0	0	2	2	1	2	2	2	0	0	1	0	0
17160.	1	0	0	2	0	0	2	0	0	2	2	2	2	2	2	0	0	1	0	0
17220.	1	0	0	1	0	0	1	0	0	1	2	1	2	1	2	0	0	0	0	0
17280.	1	0	0	0	0	0	2	0	0	2	2	2	0	2	2	0	0	1	0	0
17340.	1	0	0	2	0	0	2	0	0	2	2	2	2	2	3	0	0	0	0	0
17400.	1	0	0	1	0	0	2	0	0	2	2	2	1	2	2	0	0	1	0	0
17460.	1	0	0	2	0	0	1	0	0	2	2	1	2	1	2	0	0	1	0	0
17520.	1	0	0	0	0	0	2	0	0	2	2	2	1	2	2	0	0	1	0	0
17580.	1	0	0	2	0	0	2	0	0	2	2	2	2	2	2	0	0	1	0	0

```
  17640.    1  0  0  0  0  0  2  0  0  2  2  2  0  2  2  0  0  1  0  0
   Time   NIT y1 y2 y3 y4 y5 y6 y7 y8 y9 y0 y1 y2 y3 y4 x1 x2 x3 Tg Ts
  17700.    1  0  0  2  0  0  2  0  0  2  2  2  2  2  2  0  0  1  0  0
  17760.    1  0  0  2  0  0  2  0  0  2  2  2  2  2  2  0  0  0  0  0
  17820.    1  0  0  1  0  0  2  0  0  2  2  2  1  2  1  0  0  0  0  0
  17880.    1  0  0  1  0  0  0  0  0  0  1  1  2  1  2  0  0  0  0  0
  17940.    1  0  0  1  0  0  1  0  0  1  2  1  1  1  0  0  0  0  0  0
  18000.    1  0  0  2  0  0  2  0  0  2  2  2  2  2  2  0  0  1  0  0
TIME =    18000.00      OUTPUT TO METC1.OUT
TIME =    18000.00      OUTPUT TO METC1.RES
FORTRAN STOP
$ exit
  MSYAML       job terminated at 19-FEB-1991 10:05:01.74

  Accounting information:
  Buffered I/O count:           281      Peak working set size:  1063
  Direct I/O count:             498      Peak page file size:    3293
  Page faults:                 1263      Mounted volumes:           0
  Charged CPU time:      0 00:35:14.62   Elapsed time:      0
02:18:51.20
```

OUTPUT FILE

MGAS Simulation : METC experiment R-106 Baseline

1.0 RUN CONTROL DATA

Input-file Name : METC1
RUN = 1 (Initial conditions from restart file)
Start time (TIME) = 18000.
End time (TSTOP) = 18000.
Time step (DT) = 60.000

2.0 OUTPUT CONTROL

Restart-File Name (RESFILE): METC1.RES
Time Interval for Writing Restart Data (TRES)= 3600.0
IRES = 0 (Keep only the latest restart data)

3.0 PHYSICAL AND NUMERICAL DATA

Type of Coal (COAL) = 1 (Pittsburgh No. 8)

Proximate Analysis:
Fixed Carbon (PAFC) = 0.51620
Volatile Matter (PAVM) = 0.37200
Moisture (PAM) = 0.36400E-01
Ash (PAA) = 0.75400E-01

Ultimate Analysis:
C (UAC) = 0.74930
H (UAH) = 0.48000E-01
O (UAO) = 0.55500E-01
N (UAN) = 0.14200E-01
S (UAS) = 0.21200E-01
Higher heating value of coal (HHVC) = 0.00000E+00

Composition of Pseudo-species Tar:
C = 0.88000 H = 0.80000E-01 O = 0.20000E-01
S = 0.10000E-01 N = 0.10000E-01
Higher heating value of tar (HHVT) = 9802.6

Particle (1): Diameter (DP) = 2.0000 Density (ROS) = 1.1645

Minimum Particle Density (ROSMIN) = 0.00000E+00

Universal Gas Constant (GASCON) = 0.83176E+08

User-Defined Constants:

C1 =	0.00000E+00	C2 =	0.00000E+00	C3 =	0.00000E+00	C4 =	0.00000E+00
C5 =	0.00000E+00	C6 =	0.00000E+00	C7 =	0.00000E+00	C8 =	0.00000E+00
C9 =	0.00000E+00	C10=	0.00000E+00	C11=	0.00000E+00	C12=	0.00000E+00
C13=	0.00000E+00	C14=	0.00000E+00	C15=	0.00000E+00	C16=	0.00000E+00
C17=	0.00000E+00	C18=	0.00000E+00	C19=	0.00000E+00	C20=	0.00000E+00

Tolerances: Gas mass fraction (TOLYM) = 0.10000E-04
Solids mass fraction (TOLXM) = 0.10000E-04
Gas temperature (TOLTG) = 0.10000E-02
Solids temperature (TOLTS) = 0.10000E-02

4.0 GEOMETRY AND DISCRETIZATION

Reactor Length (RLEN) = 200.66
Reactor Diameter (RDIA) = 106.68
No. of axial divisions (JB) = 61
No of radial divisions (IB) = 1
CORD =1 (Cylindrical coordinates)

5.0 INITIAL CONDITIONS

Height of Ash Layer at the Bottom (HXZONE) = 10.000
Pressure (PI) = 0.14700E+08
Void Fraction Range: EPMIN = 0.40000 EPMAX = 0.40000
Temperature (TI) = 644.26

Gas Mass Fractions (YMI):

CO =	0.00000E+00	CO2 =	0.00000E+00	CH4 =	0.00000E+00
H2 =	0.00000E+00	H2O =	0.00000E+00	H2S =	0.00000E+00
N2 =	1.0000	O2 =	0.00000E+00	NH3 =	0.00000E+00
TAR =	0.00000E+00	C2H4=	0.00000E+00	C2H6=	0.00000E+00
C3H8=	0.00000E+00	C6H6=	0.00000E+00		

Solids Mass Fractions (XMI):

Carbon =	0.87255	Volatile Matter =	0.00000E+00
Moisture =	0.00000E+00	Ash =	0.12745

6.0 BOUNDARY CONDITIONS

Wall Temperature (TWALL) = 355.00
Wall Heat Transfer Correction Factor (HLFAC) = 2.6306

Conditions at the inflow ports:

```
Port no =  1
    Radial Location:(RPORT) R1 =  0.00000E+00   R2 =   53.340
    Axial Location :(ZPORT) Z1 =  0.00000E+00   Z2 =  0.00000E+00
    Steam Flowrate (FSTEAM) =   240.28     Temperature (TSTEAM) =   667.59

    Air Flowrate (FAIR) =   603.53         Temperature (TAIR) =   372.04

    Pressure (PPORT) =  0.14700E+08
    Temperature (TPORT) =   500.92
    Void Fraction (EPORT) =   1.0000
    Gas Velocity (VGPORT) =   10.874

    Gas Mass Fractions (YMPORT):
      CO  =  0.00000E+00  CO2 =  0.00000E+00  CH4 =  0.00000E+00
      H2  =  0.00000E+00  H2O =  0.28476      H2S =  0.00000E+00
      N2  =  0.54859      O2  =  0.16665      NH3 =  0.00000E+00
      TAR =  0.00000E+00  C2H4=  0.00000E+00  C2H6=  0.00000E+00
      C3H8=  0.00000E+00  C6H6=  0.00000E+00

  Port no =  2
    Radial Location:(RPORT) R1 =  0.00000E+00   R2 =   53.340
    Axial Location :(ZPORT) Z1 =   200.66       Z2 =   200.66

    Coal Flowrate (FCOAL) =   284.75       Temperature (TCOAL) =   310.93

    Solids Velocity (VSPORT) =  0.45618E-01

    Solids Mass Fractions (XMPORT):
      Carbon   =  0.51620      Volatile Matter =  0.37200
      Moisture =  0.36400E-01             Ash =  0.75400E-01
```

7.0 REACTOR CONFIGURATION

```
      (Legend: . - Fluid cell; B - Boundary cell; # - Port no)
   Z     Cell Flags --->
 202.3   B 2 B
 199.0   B . B
 195.7   B . B
 192.4   B . B
 189.1   B . B
 185.9   B . B
 182.6   B . B
 179.3   B . B
 176.0   B . B
 172.7   B . B
 169.4   B . B
 166.1   B . B
 162.8   B . B
 159.5   B . B
 156.3   B . B
```

```
153.0  B . B
149.7  B . B
146.4  B . B
143.1  B . B
139.8  B . B
136.5  B . B
133.2  B . B
129.9  B . B
126.6  B . B
123.4  B . B
120.1  B . B
116.8  B . B
113.5  B . B
110.2  B . B
106.9  B . B
103.6  B . B
100.3  B . B
 97.0  B . B
 93.8  B . B
 90.5  B . B
 87.2  B . B
 83.9  B . B
 80.6  B . B
 77.3  B . B
 74.0  B . B
 70.7  B . B
 67.4  B . B
 64.1  B . B
 60.9  B . B
 57.6  B . B
 54.3  B . B
 51.0  B . B
 47.7  B . B
 44.4  B . B
 41.1  B . B
 37.8  B . B
 34.5  B . B
 31.3  B . B
 28.0  B . B
 24.7  B . B
 21.4  B . B
 18.1  B . B
 14.8  B . B
 11.5  B . B
  8.2  B . B
  4.9  B . B
  1.6  B . B
 -1.6  B 1 B
```

8.0 DERIVED QUANTITIES

Composition of Pseudo-species Volatile Matter (VM):

C =	0.62661	H =	0.12903	O =	0.14919
S =	0.56989E-01	N =	0.38172E-01		

Heat of devolatilization rxn (cal/g-VM) = 0.00000E+00
Heat of cracking rxn (cal/g-tar) = 0.00000E+00

TIME = 18000.00 CYCLE = 300

R = 26.670

Z (cm)	Gas Flow (g/s)	CO (mass fr)	CO2 (mass fr)	CH4 (mass fr)	H2 (mass fr)	H2O (mass fr)
Top Boundary	0.00000E+00	0.00000E+00	0.00000E+00	0.00000E+00	0.00000E+00	0.00000E+00
199.02	1084.1	0.19964	0.14094	0.12381E-01	0.13058E-01	0.14894
195.73	1061.3	0.20330	0.14349	0.10644E-01	0.12821E-01	0.14595
192.44	991.29	0.21513	0.15183	0.33661E-02	0.11761E-01	0.14272
189.15	981.21	0.21697	0.15295	0.17477E-02	0.11551E-01	0.14266
185.86	979.54	0.21736	0.15297	0.14051E-02	0.11503E-01	0.14274
182.57	978.96	0.21756	0.15284	0.12724E-02	0.11479E-01	0.14284
179.28	978.69	0.21771	0.15266	0.12055E-02	0.11462E-01	0.14295
175.99	978.53	0.21785	0.15246	0.11644E-02	0.11447E-01	0.14306
172.70	978.42	0.21797	0.15225	0.11345E-02	0.11432E-01	0.14318
169.41	978.32	0.21808	0.15203	0.11094E-02	0.11418E-01	0.14331
166.12	978.23	0.21819	0.15180	0.10867E-02	0.11403E-01	0.14345
162.83	978.15	0.21829	0.15157	0.10653E-02	0.11387E-01	0.14359
159.54	978.06	0.21839	0.15134	0.10445E-02	0.11371E-01	0.14374
156.25	977.97	0.21848	0.15111	0.10242E-02	0.11354E-01	0.14390
152.96	977.88	0.21856	0.15087	0.10040E-02	0.11336E-01	0.14407
149.67	977.79	0.21864	0.15063	0.98413E-03	0.11317E-01	0.14424
146.38	977.68	0.21870	0.15038	0.96442E-03	0.11297E-01	0.14443
143.09	977.58	0.21875	0.15014	0.94490E-03	0.11276E-01	0.14463
139.80	977.47	0.21880	0.14989	0.92550E-03	0.11255E-01	0.14484
136.51	977.35	0.21882	0.14964	0.90637E-03	0.11232E-01	0.14507
133.23	977.23	0.21883	0.14939	0.88735E-03	0.11207E-01	0.14531
129.94	977.10	0.21882	0.14914	0.86848E-03	0.11182E-01	0.14556
126.65	976.95	0.21880	0.14889	0.84971E-03	0.11154E-01	0.14583
123.36	976.80	0.21874	0.14865	0.83102E-03	0.11125E-01	0.14612
120.07	976.64	0.21866	0.14840	0.81242E-03	0.11094E-01	0.14643
116.78	976.46	0.21855	0.14816	0.79394E-03	0.11062E-01	0.14676
113.49	976.27	0.21841	0.14793	0.77558E-03	0.11026E-01	0.14712
110.20	976.06	0.21822	0.14770	0.75727E-03	0.10989E-01	0.14750
106.91	975.83	0.21799	0.14748	0.73899E-03	0.10948E-01	0.14792
103.62	975.58	0.21770	0.14727	0.72078E-03	0.10905E-01	0.14837
100.33	975.31	0.21735	0.14708	0.70259E-03	0.10858E-01	0.14885
97.040	975.01	0.21694	0.14690	0.68436E-03	0.10807E-01	0.14938
93.751	974.67	0.21644	0.14675	0.66583E-03	0.10751E-01	0.14996
90.461	974.31	0.21584	0.14662	0.64479E-03	0.10691E-01	0.15059
87.172	973.95	0.21512	0.14651	0.60333E-03	0.10624E-01	0.15127
83.882	972.21	0.21447	0.14660	0.21944E-03	0.10514E-01	0.15203
80.593	971.70	0.21346	0.14658	0.20674E-03	0.10436E-01	0.15289
77.303	971.13	0.21227	0.14661	0.19574E-03	0.10349E-01	0.15384
74.014	970.47	0.21086	0.14670	0.18445E-03	0.10252E-01	0.15491
70.724	969.70	0.20917	0.14685	0.17283E-03	0.10141E-01	0.15613
67.435	968.80	0.20714	0.14709	0.16087E-03	0.10016E-01	0.15751
64.145	967.72	0.20470	0.14743	0.14858E-03	0.98718E-02	0.15911
60.856	966.44	0.20173	0.14787	0.13594E-03	0.97045E-02	0.16098
57.566	964.88	0.19810	0.14844	0.12296E-03	0.95080E-02	0.16318
54.277	962.97	0.19363	0.14915	0.10965E-03	0.92743E-02	0.16580
50.987	960.60	0.18805	0.15002	0.96054E-04	0.89927E-02	0.16898
47.698	957.62	0.18103	0.15105	0.82243E-04	0.86483E-02	0.17290
44.408	953.82	0.17211	0.15224	0.68337E-04	0.82207E-02	0.17777
41.119	948.93	0.16067	0.15354	0.54536E-04	0.76824E-02	0.18395
37.829	942.59	0.14591	0.15485	0.41154E-04	0.69969E-02	0.19185
34.540	934.39	0.12693	0.15590	0.28663E-04	0.61197E-02	0.20201
31.250	923.92	0.10294	0.15611	0.17718E-04	0.50078E-02	0.21496
27.961	911.05	0.74048E-01	0.15422	0.90980E-05	0.36531E-02	0.23084
24.671	896.45	0.42912E-01	0.14788	0.34436E-05	0.21617E-02	0.24857
21.382	882.11	0.16398E-01	0.13344	0.75146E-06	0.85110E-03	0.26473
18.092	870.40	0.26142E-02	0.10789	0.50753E-07	0.14134E-03	0.27479
14.803	860.97	0.66246E-04	0.72974E-01	0.24337E-09	0.37368E-05	0.27905
11.513	851.93	0.42314E-07	0.34929E-01	0.40480E-14	0.22237E-08	0.28204
8.2238	843.81	0.00000E+00	0.00000E+00	0.00000E+00	0.00000E+00	0.28476
4.9343	843.81	0.00000E+00	0.00000E+00	0.00000E+00	0.00000E+00	0.28476
1.6448	843.81	0.00000E+00	0.00000E+00	0.00000E+00	0.00000E+00	0.28476

Bottom Boundary	843.81	0.00000E+00	0.00000E+00	0.00000E+00	0.00000E+00	0.28476

R = 26.670

Z (cm)	Gas Flow (g/s)	H2S (mass fr)	N2 (mass fr)	O2 (mass fr)	NH3 (mass fr)	TAR (mass fr)
Top Boundary	0.00000E+00	0.00000E+00	0.00000E+00	0.00000E+00	0.00000E+00	0.00000E+00
199.02	1084.1	0.54832E-02	0.42698	0.00000E+00	0.40340E-02	0.40759E-01
195.73	1061.3	0.45899E-02	0.43617	0.00000E+00	0.33813E-02	0.32978E-01
192.44	991.29	0.10598E-02	0.46697	0.00000E+00	0.79363E-03	0.44070E-02
189.15	981.21	0.41691E-03	0.47177	0.00000E+00	0.31622E-03	0.72928E-03
185.86	979.54	0.29699E-03	0.47258	0.00000E+00	0.22637E-03	0.24262E-03
182.57	978.96	0.25413E-03	0.47286	0.00000E+00	0.19410E-03	0.10964E-03
179.28	978.69	0.23412E-03	0.47299	0.00000E+00	0.17897E-03	0.61694E-04
175.99	978.53	0.22272E-03	0.47306	0.00000E+00	0.17033E-03	0.41301E-04
172.70	978.42	0.21506E-03	0.47312	0.00000E+00	0.16450E-03	0.31948E-04
169.41	978.32	0.20900E-03	0.47317	0.00000E+00	0.15989E-03	0.26788E-04
166.12	978.23	0.20374E-03	0.47321	0.00000E+00	0.15587E-03	0.23490E-04
162.83	978.15	0.19894E-03	0.47325	0.00000E+00	0.15221E-03	0.21358E-04
159.54	978.06	0.19438E-03	0.47329	0.00000E+00	0.14872E-03	0.19737E-04
156.25	977.97	0.18995E-03	0.47333	0.00000E+00	0.14533E-03	0.18353E-04
152.96	977.88	0.18558E-03	0.47338	0.00000E+00	0.14200E-03	0.16936E-04
149.67	977.79	0.18135E-03	0.47342	0.00000E+00	0.13876E-03	0.15735E-04
146.38	977.68	0.17719E-03	0.47347	0.00000E+00	0.13558E-03	0.14592E-04
143.09	977.58	0.17312E-03	0.47352	0.00000E+00	0.13247E-03	0.13582E-04
139.80	977.47	0.16912E-03	0.47358	0.00000E+00	0.12941E-03	0.12544E-04
136.51	977.35	0.16523E-03	0.47363	0.00000E+00	0.12643E-03	0.11690E-04
133.23	977.23	0.16140E-03	0.47369	0.00000E+00	0.12351E-03	0.10956E-04
129.94	977.10	0.15761E-03	0.47376	0.00000E+00	0.12060E-03	0.10147E-04
126.65	976.95	0.15389E-03	0.47383	0.00000E+00	0.11776E-03	0.94424E-05
123.36	976.80	0.15023E-03	0.47390	0.00000E+00	0.11496E-03	0.87739E-05
120.07	976.64	0.14663E-03	0.47398	0.00000E+00	0.11221E-03	0.81508E-05
116.78	976.46	0.14310E-03	0.47407	0.00000E+00	0.10950E-03	0.75787E-05
113.49	976.27	0.13961E-03	0.47416	0.30242E-35	0.10684E-03	0.70693E-05
110.20	976.06	0.13617E-03	0.47426	0.27319E-31	0.10421E-03	0.66297E-05
106.91	975.83	0.13274E-03	0.47437	0.24685E-27	0.10159E-03	0.61811E-05
103.62	975.58	0.12935E-03	0.47449	0.22310E-23	0.98990E-04	0.57455E-05
100.33	975.31	0.12599E-03	0.47463	0.20169E-19	0.96423E-04	0.53805E-05
97.040	975.01	0.12266E-03	0.47477	0.25153E-09	0.93875E-04	0.52521E-05
93.751	974.67	0.11933E-03	0.47494	0.27817E-06	0.91321E-04	0.65472E-05
90.461	974.31	0.11590E-03	0.47511	0.27419E-05	0.88647E-04	0.18766E-04
87.172	973.95	0.11154E-03	0.47529	0.86781E-05	0.84903E-04	0.12033E-03
83.882	972.21	0.60318E-06	0.47614	0.19353E-04	0.45930E-06	0.60685E-06
80.593	971.70	0.32576E-08	0.47639	0.36715E-04	0.24814E-08	0.30526E-08
77.303	971.13	0.17594E-10	0.47667	0.63783E-04	0.13407E-10	0.15301E-10
74.014	970.47	0.95029E-13	0.47699	0.10500E-03	0.72438E-13	0.76392E-13
70.724	969.70	0.51333E-15	0.47737	0.16687E-03	0.39143E-15	0.37967E-15
67.435	968.80	0.27732E-17	0.47782	0.25898E-03	0.21154E-17	0.18775E-17
64.145	967.72	0.14985E-19	0.47835	0.39536E-03	0.11434E-19	0.92317E-20
60.856	966.44	0.80984E-22	0.47898	0.59625E-03	0.61812E-22	0.45109E-22
57.566	964.88	0.43778E-24	0.47976	0.89149E-03	0.33425E-24	0.21888E-24
54.277	962.97	0.23674E-26	0.48071	0.13249E-02	0.18080E-26	0.10540E-26
50.987	960.60	0.12808E-28	0.48189	0.19610E-02	0.97844E-29	0.50335E-29
47.698	957.62	0.69338E-31	0.48340	0.28948E-02	0.52983E-31	0.23828E-31
44.408	953.82	0.37705E-33	0.48532	0.42664E-02	0.28814E-33	0.11181E-33
41.119	948.93	0.34104E-35	0.48782	0.62825E-02	0.25614E-35	0.94323E-36
37.829	942.59	0.13972E-35	0.49110	0.92458E-02	0.10188E-35	0.15386E-34
34.540	934.39	0.56104E-36	0.49541	0.13594E-01	0.40927E-36	0.69744E-35
31.250	923.92	0.17728E-36	0.50103	0.19946E-01	0.12936E-36	0.31277E-35
27.961	911.05	0.00000E+00	0.50810	0.29121E-01	0.00000E+00	0.13637E-35
24.671	896.45	0.00000E+00	0.51638	0.42098E-01	0.00000E+00	0.55129E-36
21.382	882.11	0.00000E+00	0.52477	0.59805E-01	0.00000E+00	0.17501E-36
18.092	870.40	0.00000E+00	0.53184	0.82737E-01	0.00000E+00	0.00000E+00
14.803	860.97	0.00000E+00	0.53766	0.11025	0.00000E+00	0.00000E+00
11.513	851.93	0.00000E+00	0.54337	0.13966	0.00000E+00	0.00000E+00

8.2238	843.81	0.00000E+00	0.54859	0.16665	0.00000E+00	0.00000E+00
4.9343	843.81	0.00000E+00	0.54859	0.16665	0.00000E+00	0.00000E+00
1.6448	843.81	0.00000E+00	0.54859	0.16665	0.00000E+00	0.00000E+00
Bottom Boundary	843.81	0.00000E+00	0.54859	0.16665	0.00000E+00	0.00000E+00

R = 26.670

Z (cm)	Gas Flow (g/s)	C2H4 (mass fr)	C2H6 (mass fr)	C3H8 (mass fr)	C6H6 (mass fr)
Top Boundary	0.00000E+00	0.00000E+00	0.00000E+00	0.00000E+00	0.00000E+00
199.02	1084.1	0.12670E-02	0.33041E-02	0.19910E-02	0.12260E-02
195.73	1061.3	0.10580E-02	0.28283E-02	0.16625E-02	0.11192E-02
192.44	991.29	0.23700E-03	0.82921E-03	0.37242E-03	0.52001E-03
189.15	981.21	0.90942E-04	0.38135E-03	0.14291E-03	0.28648E-03
185.86	979.54	0.64153E-04	0.28688E-03	0.10081E-03	0.22668E-03
182.57	978.96	0.54671E-04	0.25086E-03	0.85911E-04	0.20197E-03
179.28	978.69	0.50277E-04	0.23325E-03	0.79007E-04	0.18924E-03
175.99	978.53	0.47790E-04	0.22287E-03	0.75098E-04	0.18148E-03
172.70	978.42	0.46126E-04	0.21565E-03	0.72484E-04	0.17590E-03
169.41	978.32	0.44817E-04	0.20982E-03	0.70427E-04	0.17131E-03
166.12	978.23	0.43683E-04	0.20468E-03	0.68645E-04	0.16720E-03
162.83	978.15	0.42653E-04	0.19992E-03	0.67026E-04	0.16335E-03
159.54	978.06	0.41673E-04	0.19537E-03	0.65485E-04	0.15967E-03
156.25	977.97	0.40720E-04	0.19097E-03	0.63988E-04	0.15610E-03
152.96	977.88	0.39782E-04	0.18665E-03	0.62515E-04	0.15261E-03
149.67	977.79	0.38872E-04	0.18242E-03	0.61085E-04	0.14918E-03
146.38	977.68	0.37979E-04	0.17828E-03	0.59682E-04	0.14582E-03
143.09	977.58	0.37107E-04	0.17422E-03	0.58311E-04	0.14252E-03
139.80	977.47	0.36248E-04	0.17022E-03	0.56961E-04	0.13926E-03
136.51	977.35	0.35413E-04	0.16632E-03	0.55649E-04	0.13609E-03
133.23	977.23	0.34592E-04	0.16248E-03	0.54359E-04	0.13295E-03
129.94	977.10	0.33777E-04	0.15871E-03	0.53078E-04	0.12990E-03
126.65	976.95	0.32979E-04	0.15499E-03	0.51825E-04	0.12687E-03
123.36	976.80	0.32195E-04	0.15132E-03	0.50592E-04	0.12388E-03
120.07	976.64	0.31423E-04	0.14771E-03	0.49379E-04	0.12093E-03
116.78	976.46	0.30664E-04	0.14415E-03	0.48187E-04	0.11802E-03
113.49	976.27	0.29918E-04	0.14065E-03	0.47013E-04	0.11517E-03
110.20	976.06	0.29180E-04	0.13720E-03	0.45854E-04	0.11234E-03
106.91	975.83	0.28444E-04	0.13377E-03	0.44698E-04	0.10955E-03
103.62	975.58	0.27715E-04	0.13038E-03	0.43552E-04	0.10680E-03
100.33	975.31	0.26995E-04	0.12702E-03	0.42421E-04	0.10406E-03
97.040	975.01	0.26282E-04	0.12367E-03	0.41300E-04	0.10132E-03
93.751	974.67	0.25571E-04	0.12024E-03	0.40183E-04	0.98465E-04
90.461	974.31	0.24864E-04	0.11611E-03	0.39072E-04	0.94631E-04
87.172	973.95	0.24161E-04	0.10613E-03	0.37967E-04	0.82741E-04
83.882	972.21	0.13056E-06	0.57633E-06	0.20516E-06	0.45101E-06
80.593	971.70	0.70457E-09	0.31249E-08	0.11072E-08	0.24541E-08
77.303	971.13	0.38026E-11	0.16942E-10	0.59755E-11	0.13351E-10
74.014	970.47	0.20525E-13	0.91854E-13	0.32253E-13	0.72621E-13
70.724	969.70	0.11080E-15	0.49799E-15	0.17411E-15	0.39498E-15
67.435	968.80	0.59817E-18	0.26999E-17	0.93999E-18	0.21480E-17
64.145	967.72	0.32301E-20	0.14639E-19	0.50758E-20	0.11681E-19
60.856	966.44	0.17446E-22	0.79376E-22	0.27415E-22	0.63518E-22
57.566	964.88	0.94252E-25	0.43046E-24	0.14811E-24	0.34541E-24
54.277	962.97	0.50939E-27	0.23349E-26	0.80047E-27	0.18784E-26
50.987	960.60	0.27544E-29	0.12669E-28	0.43283E-29	0.10217E-28
47.698	957.62	0.14903E-31	0.68773E-31	0.23419E-31	0.55590E-31
44.408	953.82	0.80899E-34	0.37428E-33	0.12726E-33	0.30286E-33
41.119	948.93	0.62882E-36	0.26990E-35	0.11281E-35	0.18326E-35
37.829	942.59	0.19770E-36	0.64258E-36	0.45167E-36	0.13090E-36
34.540	934.39	0.00000E+00	0.21633E-36	0.14233E-36	0.60296E-37
31.250	923.92	0.00000E+00	0.17876E-37	0.00000E+00	0.24606E-37
27.961	911.05	0.00000E+00	0.54133E-38	0.00000E+00	0.74516E-38
24.671	896.45	0.00000E+00	0.00000E+00	0.00000E+00	0.00000E+00
21.382	882.11	0.00000E+00	0.00000E+00	0.00000E+00	0.00000E+00

18.092	870.40	0.00000E+00	0.00000E+00	0.00000E+00	0.00000E+00
14.803	860.97	0.00000E+00	0.00000E+00	0.00000E+00	0.00000E+00
11.513	851.93	0.00000E+00	0.00000E+00	0.00000E+00	0.00000E+00
8.2238	843.81	0.00000E+00	0.00000E+00	0.00000E+00	0.00000E+00
4.9343	843.81	0.00000E+00	0.00000E+00	0.00000E+00	0.00000E+00
1.6448	843.81	0.00000E+00	0.00000E+00	0.00000E+00	0.00000E+00
Bottom Boundary	843.81	0.00000E+00	0.00000E+00	0.00000E+00	0.00000E+00

R = 26.670

Z (cm)	Solids Flow (g/s)	Carbon (mass fr)	VM (mass fr)	Moisture (mass fr)	Solids Density (g/cm^3)
Top Boundary	284.75	0.51620	0.37200	0.36400E-01	1.1645
199.02	261.90	0.56458	0.33061	0.22824E-01	1.0711
195.73	191.89	0.79221	0.94401E-01	0.15046E-02	0.78475
192.44	181.82	0.84406	0.37838E-01	0.15432E-04	0.74356
189.15	180.14	0.85392	0.26893E-01	0.84016E-07	0.73669
185.86	179.56	0.85745	0.22982E-01	0.45463E-09	0.73433
182.57	179.29	0.85909	0.21157E-01	0.24559E-11	0.73322
179.28	179.13	0.86001	0.20128E-01	0.13259E-13	0.73257
175.99	179.02	0.86063	0.19437E-01	0.71561E-16	0.73211
172.70	178.92	0.86111	0.18897E-01	0.38619E-18	0.73173
169.41	178.84	0.86152	0.18429E-01	0.20841E-20	0.73137
166.12	178.75	0.86189	0.17998E-01	0.11247E-22	0.73102
162.83	178.66	0.86224	0.17588E-01	0.60693E-25	0.73066
159.54	178.58	0.86258	0.17192E-01	0.32753E-27	0.73030
156.25	178.48	0.86290	0.16807E-01	0.17676E-29	0.72992
152.96	178.39	0.86321	0.16430E-01	0.95393E-32	0.72953
149.67	178.29	0.86351	0.16062E-01	0.51486E-34	0.72912
146.38	178.18	0.86380	0.15700E-01	0.27403E-36	0.72869
143.09	178.07	0.86408	0.15346E-01	0.00000E+00	0.72824
139.80	177.95	0.86435	0.14999E-01	0.00000E+00	0.72776
136.51	177.83	0.86461	0.14658E-01	0.00000E+00	0.72725
133.23	177.70	0.86485	0.14323E-01	0.00000E+00	0.72671
129.94	177.56	0.86509	0.13994E-01	0.00000E+00	0.72613
126.65	177.40	0.86531	0.13670E-01	0.00000E+00	0.72551
123.36	177.24	0.86551	0.13352E-01	0.00000E+00	0.72484
120.07	177.06	0.86570	0.13039E-01	0.00000E+00	0.72411
116.78	176.87	0.86588	0.12730E-01	0.00000E+00	0.72333
113.49	176.66	0.86604	0.12426E-01	0.00000E+00	0.72248
110.20	176.43	0.86618	0.12126E-01	0.00000E+00	0.72155
106.91	176.19	0.86631	0.11830E-01	0.00000E+00	0.72053
103.62	175.91	0.86641	0.11538E-01	0.00000E+00	0.71941
100.33	175.61	0.86649	0.11249E-01	0.00000E+00	0.71817
97.040	175.28	0.86654	0.10963E-01	0.00000E+00	0.71681
93.751	174.91	0.86657	0.10680E-01	0.00000E+00	0.71532
90.461	174.55	0.86660	0.10396E-01	0.00000E+00	0.71384
87.172	172.81	0.87570	0.56642E-04	0.00000E+00	0.70672
83.882	172.30	0.87539	0.30641E-06	0.00000E+00	0.70465
80.593	171.73	0.87498	0.16583E-08	0.00000E+00	0.70232
77.303	171.07	0.87450	0.89790E-11	0.00000E+00	0.69961
74.014	170.30	0.87393	0.48651E-13	0.00000E+00	0.69647
70.724	169.40	0.87326	0.26382E-15	0.00000E+00	0.69277
67.435	168.33	0.87245	0.14321E-17	0.00000E+00	0.68838
64.145	167.04	0.87147	0.77838E-20	0.00000E+00	0.68313
60.856	165.48	0.87026	0.42380E-22	0.00000E+00	0.67676
57.566	163.57	0.86874	0.23126E-24	0.00000E+00	0.66895
54.277	161.20	0.86681	0.12657E-26	0.00000E+00	0.65925
50.987	158.22	0.86430	0.69560E-29	0.00000E+00	0.64705
47.698	154.42	0.86096	0.38443E-31	0.00000E+00	0.63151
44.408	149.53	0.85641	0.21414E-33	0.00000E+00	0.61151
41.119	143.19	0.85006	0.11991E-35	0.00000E+00	0.58560
37.829	134.99	0.84095	0.00000E+00	0.00000E+00	0.55206
34.540	124.52	0.82758	0.00000E+00	0.00000E+00	0.50924
31.250	111.65	0.80770	0.00000E+00	0.00000E+00	0.45660
27.961	97.055	0.77878	0.00000E+00	0.00000E+00	0.39691

24.671	82.716	0.74043	0.00000E+00	0.00000E+00	0.33827
21.382	70.997	0.69759	0.00000E+00	0.00000E+00	0.29035
18.092	61.572	0.65130	0.00000E+00	0.00000E+00	0.25180
14.803	52.528	0.59126	0.00000E+00	0.00000E+00	0.21482
11.513	44.412	0.51657	0.57011E-37	0.00000E+00	0.18163
8.2238	44.412	0.51657	0.00000E+00	0.00000E+00	0.18163
4.9343	44.412	0.51657	0.00000E+00	0.00000E+00	0.18163
1.6448	44.412	0.51657	0.00000E+00	0.00000E+00	0.18163
Bottom Boundary	0.00000E+00	0.00000E+00	0.00000E+00	0.00000E+00	0.00000E+00

R = 26.670

Z Drop (cm)	TG (K)	TS (K)	VG (cm/s)	VS (cm/s)	Void fr	Pressure (dyne/cm^2)
Top Boundary	835.57	310.93	0.00000E+00	0.00000E+00	0.40000	0.00000E+00
199.02	835.57	658.77	60.287	-0.45618E-01	0.40000	78.000
195.73	936.65	826.72	66.121	-0.45618E-01	0.40000	140.00
192.44	1002.7	947.34	66.082	-0.45618E-01	0.40000	195.00
189.15	1034.8	1007.9	67.427	-0.45618E-01	0.40000	251.00
185.86	1051.9	1038.4	68.402	-0.45618E-01	0.40000	307.00
182.57	1062.3	1055.0	69.025	-0.45618E-01	0.40000	364.00
179.28	1069.6	1065.1	69.476	-0.45618E-01	0.40000	421.00
175.99	1075.6	1072.4	69.845	-0.45618E-01	0.40000	478.00
172.70	1080.9	1078.2	70.178	-0.45618E-01	0.40000	535.00
169.41	1085.9	1083.5	70.496	-0.45618E-01	0.40000	593.00
166.12	1090.9	1088.5	70.807	-0.45618E-01	0.40000	651.00
162.83	1095.8	1093.4	71.117	-0.45618E-01	0.40000	709.00
159.54	1100.7	1098.3	71.428	-0.45618E-01	0.40000	767.00
156.25	1105.7	1103.2	71.740	-0.45618E-01	0.40000	826.00
152.96	1110.7	1108.2	72.055	-0.45618E-01	0.40000	885.00
149.67	1115.8	1113.1	72.372	-0.45618E-01	0.40000	944.00
146.38	1120.9	1118.2	72.693	-0.45618E-01	0.40000	1003.0
143.09	1126.1	1123.2	73.017	-0.45618E-01	0.40000	1063.0
139.80	1131.4	1128.4	73.345	-0.45618E-01	0.40000	1123.0
136.51	1136.7	1133.6	73.676	-0.45618E-01	0.40000	1183.0
133.23	1142.2	1138.8	74.012	-0.45618E-01	0.40000	1243.0
129.94	1147.7	1144.2	74.353	-0.45618E-01	0.40000	1304.0
126.65	1153.3	1149.6	74.698	-0.45618E-01	0.40000	1365.0
123.36	1159.1	1155.1	75.049	-0.45618E-01	0.40000	1426.0
120.07	1164.9	1160.7	75.405	-0.45618E-01	0.40000	1487.0
116.78	1170.9	1166.4	75.768	-0.45618E-01	0.40000	1548.0
113.49	1177.1	1172.2	76.138	-0.45618E-01	0.40000	1610.0
110.20	1183.4	1178.1	76.516	-0.45618E-01	0.40000	1672.0
106.91	1189.9	1184.2	76.903	-0.45618E-01	0.40000	1734.0
103.62	1196.6	1190.4	77.299	-0.45618E-01	0.40000	1796.0
100.33	1203.5	1196.7	77.706	-0.45618E-01	0.40000	1859.0
97.040	1210.7	1203.3	78.124	-0.45618E-01	0.40000	1922.0
93.751	1218.2	1210.0	78.556	-0.45618E-01	0.40000	1985.0
90.461	1226.0	1217.0	79.002	-0.45618E-01	0.40000	2048.0
87.172	1234.1	1224.2	79.461	-0.45618E-01	0.40000	2111.0
83.882	1242.7	1231.7	79.790	-0.45618E-01	0.40000	2174.0
80.593	1251.8	1239.4	80.290	-0.45618E-01	0.40000	2237.0
77.303	1261.3	1247.3	80.812	-0.45618E-01	0.40000	2300.0
74.014	1271.5	1255.6	81.358	-0.45618E-01	0.40000	2364.0
70.724	1282.4	1264.2	81.928	-0.45618E-01	0.40000	2428.0
67.435	1294.0	1273.1	82.525	-0.45618E-01	0.40000	2492.0
64.145	1306.5	1282.2	83.152	-0.45618E-01	0.40000	2556.0
60.856	1320.1	1291.6	83.807	-0.45618E-01	0.40000	2619.0
57.566	1334.8	1301.1	84.490	-0.45618E-01	0.40000	2682.0
54.277	1350.9	1310.6	85.197	-0.45618E-01	0.40000	2745.0
50.987	1368.5	1319.8	85.920	-0.45618E-01	0.40000	2807.0
47.698	1387.6	1328.2	86.644	-0.45618E-01	0.40000	2868.0
44.408	1408.6	1335.2	87.341	-0.45618E-01	0.40000	2927.0
41.119	1431.4	1340.0	87.968	-0.45618E-01	0.40000	2984.0
37.829	1455.8	1341.8	88.454	-0.45618E-01	0.40000	3038.0

34.540	1481.1	1341.1	88.685	-0.45618E-01	0.40000	3087.0
31.250	1505.2	1341.6	88.474	-0.45618E-01	0.40000	3131.0
27.961	1522.4	1355.9	87.516	-0.45618E-01	0.40000	3168.0
24.671	1520.0	1404.7	85.290	-0.45618E-01	0.40000	3198.0
21.382	1472.0	1481.8	80.912	-0.45618E-01	0.40000	3222.0
18.092	1344.0	1484.2	73.077	-0.45618E-01	0.40000	3241.0
14.803	1122.0	1311.7	60.884	-0.45618E-01	0.40000	3254.0
11.513	834.07	1003.1	45.256	-0.45618E-01	0.40000	3262.0
8.2238	525.79	563.98	28.529	-0.45618E-01	0.40000	3267.0
4.9343	501.10	505.33	27.189	-0.45618E-01	0.40000	3272.0
1.6448	499.46	499.81	27.100	-0.45618E-01	0.40000	3277.0
Bottom Boundary	500.92	500.92	10.874	-0.45618E-01	1.0000	0.00000E+00

```
---------------------------
|                         |
|  MGAS SIMULATION REPORT |
|                         |
---------------------------
```

INPUT DATA: METC experiment R-106 Baseline

```
 COAL= 1          PAFC=0.51620   PAVM=0.37200   PAM=0.03640    PAA=0.07540
 UAC=0.74930      UAH=0.04800    UAO=0.05550    UAN=0.01420    UAS=0.02120
 DP(in)=0.78740                  ROS(g/cc)=1.16451

 FTC=0.88000      FTH=0.08000    FTO=0.02000    FTN=0.01000    FTS=0.01000

 RLEN(ft)= 6.58 RDIA(ft)= 3.50 HXZONE(in)=  3.937
 PI(atm)= 14.5  EPMIN=0.400     TI(°F)= 699.98
 TWALL(°F)= 179.31              HLFAC=  2.631

 Port No: 1       R1(ft)= 0.00   R2(ft)= 1.75   Z1(ft)= 0.00   Z2(ft)= 0.00
 FSTEAM(lb/h)=  1907.0           TSTEAM(°F)= 741.97
 FAIR(lb/h)=  4790.0             TAIR(°F)= 209.98

 Port No: 2       R1(ft)= 0.00   R2(ft)= 1.75   Z1(ft)= 6.58   Z2(ft)= 6.58
 FCOAL(lb/h)=  2260.0            TCOAL(°F)=  99.99
```

RESULTS: METC experiment R-106 Baseline

Inflow and Outflow Streams:

```
 Gas inflow to port no.   1
 Flow Rates (lb/h) :
   Dry, tar-free, gas =   4790.0
                Steam =   1907.0
                  Tar =  0.00000E+00
            Total Gas =   6697.0
```

```
 Tar-free, Gas Composition (mole %) :
          Wet Basis      Dry Basis
   CO  =   0.000000       0.000000
   CO2 =   0.000000       0.000000
   CH4 =   0.000000       0.000000
   C2H4=   0.000000       0.000000
   C2H6=   0.000000       0.000000
   C3H8=   0.000000       0.000000
   C6H6=   0.000000       0.000000
   H2  =   0.000000       0.000000
   H2O =  38.945572        ---
```

H2O =	38.945572	---
H2S =	0.000000	0.000000
N2 =	48.233543	79.000900
NH3 =	0.000000	0.000000
O2 =	12.820879	20.999102

Temperature of Gas Stream (°F) = 441.97

Gas outflow from port no. 2

Flow Rates (lb/h) :

Dry, tar-free, gas =	6972.3
Steam =	1281.5
Tar =	350.71
Total Gas =	8604.5

Tar-free, Gas Composition (mole %) :

	Wet Basis	Dry Basis
CO =	17.067757	21.283367
CO2 =	7.667929	9.561851
CH4 =	1.852286	2.309787
C2H4=	0.108320	0.135074
C2H6=	0.263642	0.328760
C3H8=	0.108320	0.135074
C6H6=	0.037627	0.046921
H2 =	15.629408	19.489756
H2O =	19.807062	---
H2S =	0.386052	0.481404
N2 =	36.503563	45.519672
NH3 =	0.568033	0.708333
O2 =	0.000000	0.000000

Temperature of Gas Stream (°F) = 1044.3

Heating Value of Tar-free, Product Gas (Btu/ft^3) = 139.60

Coal inflow (lb/h) = 2260.0

Coal Temperature (°F) = 310.93

Maximum Char Temperature (°F) = 2211.9

Carbon Conversion (%) = 89.247

Heat Loss from the Gasifier (Btu/h) = 0.12215E+07

--- ELEMENTAL BALANCES ---

The following tables give the kg/s of each element flowing in and out as a particular species, the total in and out flow rates, the difference between the total flow rates, and the % error compared with the inflow rate. The % error need not be small for nonsteady-state conditions. A steady-state in the computations is indicated by the number of iterations (NIT) being equal to 1.

Number of iterations for the last time step (NIT) = 0

CARBON

	IN (g/s)	OUT (g/s)
CO	0.0000000E+00	92.75948
CO2	0.0000000E+00	41.67350
CH4	0.0000000E+00	10.06677
C2H4	0.0000000E+00	1.177388
C2H6	0.0000000E+00	2.865673
C3H8	0.0000000E+00	1.766082
C6H6	0.0000000E+00	1.226972
TAR	0.0000000E+00	38.88579
FC	146.9879	22.94223
VM	66.37523	0.0000000E+00
Total	213.3632	213.3639
Difference	-0.7171631E-03	
Error (%)	-0.3361232E-03	

HYDROGEN

	IN (g/s)	OUT (g/s)
H2	0.0000000E+00	14.15706
CH4	0.0000000E+00	3.355588
C2H4	0.0000000E+00	0.1962314
C2H6	0.0000000E+00	0.7164183
C3H8	0.0000000E+00	0.3924628
C6H6	0.0000000E+00	0.1022477
NH3	0.0000000E+00	0.7717840
H2S	0.0000000E+00	0.3496847
TAR	0.0000000E+00	3.535072
H2O	26.69778	17.94117
VM	13.66800	0.0000000E+00
M	1.151656	0.0000000E+00
Total	41.51743	41.51772
Difference	-0.2899170E-03	
Error (%)	-0.6983018E-03	

	(g/s)	(g/s)
CO	0.0000000E+00	123.6793
CO2	0.0000000E+00	111.1293
TAR	0.0000000E+00	0.8837680
H2O	213.5822	143.5293
O2	140.6225	0.0000000E+00
VM	15.80362	0.0000000E+00
M	9.213245	0.0000000E+00
Total	379.2216	379.2218
Difference	-0.1831055E-03	
Error (%)	-0.4828456E-04	

NITROGEN

	IN (g/s)	OUT (g/s)
NH3	0.0000000E+00	3.601659
N2	462.9075	462.9072
TAR	0.0000000E+00	0.4418840
VM	4.043450	0.0000000E+00
Total	466.9510	466.9507
Difference	0.2441406E-03	
Error (%)	0.5228399E-04	

SULFUR

	IN (g/s)	OUT (g/s)
H2S	0.0000000E+00	5.594956
TAR	0.0000000E+00	0.4418840
VM	6.036700	0.0000000E+00
Total	6.036700	6.036840
Difference	-0.1401901E-03	
Error (%)	-0.2322297E-02	

```
|----------------- CPU TIME -------------------------|
|                                                    |
| CPU time =   0.5099983     s                       |
| Number of computational cells =   189              |
| Number of phases =     2                           |
| Number of cycles =     0                           |
| CPU time/cell/phase/cycle =   0.0000000E+00 s      |
|----------------------------------------------------|
```

920765

END DATE
4-16-92